C.P. No. 590

C.P. No. 590

MINISTRY OF AVIATION

AERONAUTICAL RESEARCH COUNCIL

CURRENT PAPERS

The 7in. x 7in. Hypersonic Wind Tunnel at R.A.E. Farnborough

Parts I, II & III

by

J. F. W. Crane and L. F. Crabtree

LONDON: HER MAJESTY'S STATIONERY OFFICE

1962

TWELVE SHILLINGS NET

U.D.C. No. 533.6.071 : 533.6.011.35

C.P. No.590

August, 1961

THE 7 IN. × 7 IN. HYPERSONIC WIND TUNNEL AT R.A.E. FARNBOROUGH

PARTS I, II AND III

by

J.F.W. Crane and L.F. Crabtree

SUMMARY

Part I gives some details of the design and lay-out of the plant, together with the calculated performance figures, and the major components of the facility are briefly described. The instrumentation provided for the wind tunnel is described in some detail, including the optical and other methods of flow visualisation used.

Part II describes tests on the storage heater, which is cylindrical in form and mounted horizontally, and shows that its performance is adequate for operation at M = 6.8 and probably adequate for flows at M = 8.2 with the existing nozzles. In its present state, the maximum design temperature of 680°C for operation at M = 9 cannot be realised in the tunnel because of heat loss to the outlet attachment of the heater and quick-acting valve which form, in effect, a large heat sink. Because of this heat loss there is rather poor response of stagnation temperature in the working section at the start of a run. It is hoped to cure this by preheating the heater outlet cone and the quick-acting valve.

At pressures greater than about 100 psig free convection through the fibrous insulation surrounding the heated core causes the top of the heater shell to become somewhat hotter than the bottom, which results in "hogging" distortion of the shell. This free convection cools the heater core and a vertical temperature gradient is set up across it after only a few minutes at high pressure.

Modifications to be incorporated in the heater to improve its performance are described.

Part III shows that the fused silica nozzle designed to give M = 7 in the wind tunnel produces a flow field with an average Mach number of 6.85 along the centreline of the working section. The Mach number gradually decreases towards the boundary layer, but over a core of approximately four inches there is a decrease of only two per cent below the centreline Mach number.

The nozzle heats up during a run but this has little effect on the Mach number distribution. At one station the Mach number was one third per cent greater after a run of one minute than after a run of ten seconds.

The temperature field in the inviscid flow has an average variation of two degrees centigrade at four hundred degrees centigrade, but there is some increase in temperature with time throughout a run.

Part IV, to be published at a later date, gives some measurements of diffuser performance, model blockage, starting loads and humidity.

THE 7 IN. × 7 IN. HYPERSONIC WIND TUNNEL AT FARNBOROUGH

PART I

DESIGN, INSTRUMENTATION AND FLOW VISUALIZATION TECHNIQUES

by

L. F. Crabtree,
and
J. F. W. Crane

Previously issued as R.A.E. Tech. Note No. Aero 2716 - A.R.C. 22,486

LIST OF CONTENTS

LIST OF ILLUSTRATIONS

1 INTRODUCTION

The R.A.E. hypersonic wind tunnel is on intermittent blow-down tunnel designed to operate at Mach numbers of 5 to 9. The working section is 7 in. square and the maximum running time (at M = 7) is about 3 minutes. An electrical storage heater is provided which can give stagnation temperatures of up to 680°C.

Some details of the design and layout of the plant, together with performance figures are given in para.2, and the major components of the facility are briefly described.

Para.3 describes the instrumentation provided for the measurement of pressures, temperatures and forces and para.4 contains a description of the optical and other methods of flow visualization used in the tunnel.

The calibration of the flow in the working section is described in Part III of this report[1]. Stagnation temperature measurements in the settling chamber and working section are also given. These are used in a discussion of the performance of the heater (Part II).

Part IV of the report[2] describes an investigation of the pressure ratios required for starting and running the tunnel, and measurements of blockage factors, starting loads, and humidity of the air flow.

2 PLANT DESIGN AND PERFORMANCE

A simple line diagram of the tunnel circuit is given in Fig.1 and a cutaway view of part of the circuit in Fig.2. A general view of the tunnel is shown in Fig.3. The design stagnation conditions are given in Table 1, together with the corresponding conditions in the working section. The stagnation pressure varies from 20 atmospheres at M = 5 to 50 atmospheres at M = 7 and above, in order to reduce the mass flow required at the lower Mach numbers*.

2.1 Pressure supply and outline of circuit (Fig.1)

There are two Fullerton, Hodgart and Barclay compressors, each capable of delivering 128 cu ft of free air per min at pressures up to 4000 p.s.i. This air is passed into 24 large storage bottles with a total capacity of 260 cu ft. The pressure in the bottles is kept at about 3000 p.s.i. thus giving a capacity of 3,300 lb of air.

When the tunnel runs, the air leaves the bottles (located outside the building for reasons of safety) and returns to the tunnel room to pass through a reducing valve. After flowing through on electrically heated storage heater, the air passes through a quick-acting stop valve, used for starting and stopping the flow. From here the air passes into a settling chamber, through the nozzle and working section, through a diffuser incorporating a variable second throat, and into the vacuum vessels. (The region of the working section is shown in more detail in Fig.2.)

2.2 Main reducing valve

This pressure reducing valve accepts air from the storage bottles, at a pressure which necessarily varies during a run and delivers it to the heater at a constant pressure (usually 50 atmos.) The valve and its control gear

---

* This reduction in stagnation pressure at the lower Mach numbers was dictated by considerations of economy in heater design.

were built by Messrs. James Gordon, and, after some development proved to be capable of holding the pressure constant to within ±0.5 p.s.i. at 750 p.s.i.

2.3 Electrical storage heater

This was designed and built by the Incandescent Heat Co. Ltd., in association with Metalectric Co. Ltd. A sketch of the heater is shown in Fig.4. There is an outer mild steel shell, 3 ft in diameter, capable of withstanding the pressure loads and an inner coaxial cylinder of $1\frac{1}{2}$ ft diam, made of heat resistant steel. This is vented to the annular space, which is filled with fibrous aluminium silicate, an insulating material, to cut down heat losses. Spaced along the centre of the inner cylinder are 15 heat storage matrices, made up of alternate layers of flat and corrugated heat resistant steel sheet with a total weight of 2 tons. The matrices are heated by 8 Brightray strip heating elements which radiate onto the edges of the sheet material, as is the best annealing practice for sheet metal, to prevent warping.

Correct functioning of the heater depends on the matrix material all being at a uniform temperature before the tunnel starts. During a run, the air quickly reaches the correct temperature as it flows through the heater, at the same time cooling each matrix in turn, starting at the inlet end. However, immediately the last matrix temperature starts to drop, then so will the outlet air temperature. This then determines the maximum time of a run which is about 3 minutes at M = 7. (Stagnation temperature 410°C, stagnation pressure 50 atmospheres.)

In practice the heater insulation is not good enough at 50 atmosphere pressure, and temperature gradients arise within the matrices due to convection when the heater is standing-by in a hot, pressurised condition. This leads to temperature gradients in the air flow at the exit from the heater. However this difficulty is partly overcome by bringing the heater up to temperature at atmospheric pressure (at which the insulation is quite sufficient) and pressurising the heater as quickly as possible (7-10 minutes) immediately before a run.

2.4 Quick acting valve (seen in Fig.2)

After the heater the air passes through a quick-acting valve which is used for starting and stopping the flow. This valve has to operate hot and consists of a central bullet which moves downstream into a circular seat to shut off the flow, and is retracted upstream to open. When the valve is open, the air flows symmetrically round the bullet and is only impeded by the small webs which support the bullet housing. In practice, the valve has been shown to be a very good mixer in smoothing out temperature gradients across the flow. Movement is controlled by adjusting the pressure on the rear face of the bullet.

The valve was built by Messrs. James Gordon; considerable later development has taken place in conjunction with the firm and several modifications have been incorporated by the R.A.E. workshops.

2.5 Nozzle

The nozzle in current use is two dimensional, with two vertical sides and profiled top and bottom surfaces. It was designed for M = 7 by the source flow method, and a simple boundary layer correction was applied to the calculated ordinates. These ordinates are tabulated in Ref.1, and a photograph of the built-up nozzle is shown in Fig.5 of the present report.

The material chosen for the nozzle was fused silica, supplied by Messrs. Thermal Syndicate Ltd. and Messrs. Quartzglass Ltd. The two main properties of fused silica which influenced this decision are, first, that it has an extremely small coefficient of thermal expansion, and secondly, that its thermal conductivity is extremely small, as shown by the comparisons in the following table:-

	Coefficient of Expansion in./in./°C	Thermal Conductivity C.H.U./ft^2/°C/ft/sec
Silica	0.5×10^{-6}	0.024×10^{-2}
Copper	16×10^{-6}	6×10^{-2}
Tungsten	4×10^{-6}	2.4×10^{-2}

Thus at the throat the surface temperature of the silica rises very quickly to near the air temperature, and extracts very little heat from the airstream. At the same time the large temperature gradient produced in the material causes negligible distortion.

The disadvantages of silica as a constructional material are its poor handling qualities and its low tensile strength; nevertheless a successful design was produced whereby tensile and shear stresses in the silica when assembled were minimized. Considerable production problems were overcome by the R.A.E. workshops in their manufacture[3].

A two-dimensional nozzle was chosen because of the time it was believed that axisymmetric nozzles would be subject to a strong focussing effect, on the centre line, of any disturbances arising from the throat region. This worry has been reduced by recent experience in the U.S.A. and accordingly two axisymmetric nozzles have been designed for M = 6.85 and 8.24 using heat resistant steel (E.N.25). In the throat region of these axisymmetric nozzles, the material is 0.050 in. thick to minimise thermal shock, and the ordinates are compensated for expansion. Thus, on starting the throat temperature will rise rapdily (less than 1 second) to recovery temperature and hence heat transfer at the throat will be negligibly small during a run.

The calibration of the silica nozzle is fully described in Part III of this report[1].

2.6 Working section

The 30 in. long working section is built up from heat resistant steel plate and is provided with two pairs of schlieren quality quartz windows of 5.3 in. aperture diameter, as shown in Fig.2.

There are three separate means of mounting models in the working-section:-

(1) A longitudinal-traverse sting, fixed at zero incidence. It has a motor driven longitudinal traverse of 10 in. and extension pieces are available which extend the range up into the nozzle if required.

A photograph of the working-section with one side wall removed is shown in Fig.6. The traverse sting, on which is mounted a pitot-tube rake, can be seen clearly.

(2) A single-strut or pedestal mount from the floor of the tunnel with an incidence range (of model) of -5° to +25°. The incidence can be adjusted manually from outside the tunnel.

This support rig is used for the investigation of flow fields around the base of a model.

(3) A support system with an incidence range of 0° to $+30^{\circ}$ operated by pneumatic jacks with preset incidence stops. This rig was designed principally for the measurement of aerodynamic forces, using models with strain gauge balances.

The working section is being redesigned to incorporate a balance gear which can be pitched from -1° to +35° incidence and incorporating digitised read-out of the angle to an accuracy of $1/10^{\circ}$ or less.

Possible distortion of the model and sting under load will, of course, have to be checked.

2.7 Diffuser

The diffuser consists of three main sections; first a rectangular section incorporating the variable second throat, separated from a conical divergent section of 6° total angle by a combined expansion joint and transition piece (rectangular to circular). The third section is a straight-through cylindrical pipe leading directly to the vacuum vessels and incorporating an atmospheric blow-off valve. This safeguards the working section in case the tunnel is started with the main vacuum valve closed.

The second throat is made of flexible steel plates top and bottom with fixed side-walls (see Fig.2). The flexible plates are operated by pneumatic jacks to give a throat area predetermined by setting mechanical stops before a run. The maximum possible angle of each flexible plate is 5°. The optimum second throat setting was found from tests of starting pressure ratios as described in Part IV[2].

The pneumatic jacks can be seen on the left-hand edge of Fig.6, and also in Figs.2 and 3.

2.8 Vacuum system

The vacuum system is part of the R.A.E. Intermittent Supersonic Wind Tunnel Plant and as such has been described by Winter[4]. Fig.2 of Ref.4 also shows a general view of the plant including the hypersonic wind tunnel.

There are two cylindrical vacuum vessels of 30,000 cu ft total capacity. They are evacuated by reciprocating double-acting twin-cylinder Pearn pumps, the two cylinders of each being used in parallel. There are twenty one pumps, each driven by an electric motor of nominally 15 H.P., and twenty of these are in use at any one time, so that continuous maintenance is possible. A pressure of less than 0·5 in. Hg abs. can be reached from atmospheric in something under 20 minutes.

one stagnation, static or pitot pressure to either of the remaining two. In a supersonic flow with M > 1·4 or so, the best accuracy in the determination of M is obtained from the ratio of stagnation pressure to pitot pressure (see Ref.5); practical difficulties in the measurement of the tunnel static pressure (about 0·2 p.s.i. for M = 7 and 50 atmospheres stagnation pressure) are thus avoided. Moreover at the high stagnation pressures used, viscous effects on the pitot pressure (about 12 p.s.i. for the same conditions) become negligible.

It was estimated that an accuracy of ±0·1% was required in the measurement of stagnation pressure in order to get the same accuracy in Mach number. The system now in use for this purpose was developed by Holbeche and Vandome. In its operation, the pressure in the settling chamber P_s is continuously compared with a known reference pressure (made nominally equal to P_s), which has been measured previously with a dead weight tester. Any departures of P_s from the reference value, over a maximum range of approximately ±30 p.s.i., cause corresponding changes in the inductance of an inductance-type differential pressure transducer (Southern Instruments Type G.255-2) which is incorporated in the tuned circuit of a high-frequency oscillator. This circuit is designed to work with either a variable inductance or a variable capacitance transducer, and, in fact, the latter was originally used. However it was found to be essentially non-linear and was replaced by the inductance-type transducer. This has more sensitivity and a better linearity (either positive or negative w.r.t. the reference pressure) than the capacitance-type.

The resulting changes in the oscillator frequency are detected by a conventional frequency-modulated amplifier (Southern Instruments Type E7A) which has an output voltage of up to ±10 volts D.C. This, in turn, is fed to a recording voltmeter (Elliott Bros.) of the centre-zero type with a 6 in. chart. The chart drive may be run at speeds of 1 in., 3 in., 6 in., or 12 in. per minute, so that it is possible to select a suitable speed for monitoring the pressure variations, i.e., a slow speed for routine pressure recording, but a fast speed for checking the behaviour of the main reducing valve (Section 2.2).

As the pressure range of the transducer before damage may occur is only about 70 p.s.i., and the settling chamber is at a low pressure before a run starts, an automatic pneumatically-operated change-over valve has been developed. This switches the "measuring" side of the transducer from the heater to the settling chamber at the instant when the pressure in the latter has increased (due to opening the quick-acting valve, Section 2.4) to a valve within the working range of the transducer, i.e., at about 49 atmospheres absolute. Conversely when pressure falls in the settling chamber after closing the quick-acting valve, the change-over valve automatically switches to the heater pressure line.

3.2 Stagnation temperature measurement

The measurement of stagnation temperature is by means of a Chromel-Alumel thermocouple mounted on a probe in the settling chamber. Calibration of the temperature field has shown it to be very uniform[1], and hence measurement by a single thermocouple is justified. The trace of temperature is obtained from the measurement of the E.M.F.-output of the thermocouple by a Speedomax chart recorder, which runs at a speed of ½ in./sec. The response time of the thermocouple is shorter than the response time of the Speedomax recorder (the latter has full scale deflection in under one second). A more detailed description of the probe is given in Ref.1.

3.3 Model surface temperature measurement

Normal practice so far has been to use thin skinned models (0•050 in. or less) and to spot-weld thermocouples to the inside surface. Chromel-Alumel wires are usually favoured, and the outputs are recorded on Speedomax machines as described in Section 3.2. A more complete description of the technique is given in Ref.8.

3.4 Model surface pressure measurement

Since the static pressure of the flow in the working-section is so low (see Table 1) a sensitive means of measuring surface pressure on models is required (particularly for slender bodies, base pressures etc.)

The system used is the Electromanometer Type 37-103 manufactured by the Consolidated Engineering Corporation, Pasadena, California. It is a null-balance type of instrument employing two pressure-sensitive bellows, one of which contains a reference pressure and is separated by a diaphragm from the other bellows which is fed with the pressure to be measured. Movement of the diaphragm operates a differential transformer and null-balance is obtained by means of a force balancing system (an Alnico V magnet and driving coil, similar to a permanent magnet loud-speaker). A servo-amplifier is also incorporated. These components are arranged to provide a closed-loop, self balancing servo-system. Visual read-out is by means of a Honeywell-Brown recording voltmeter. Two pressure heads are available, one for the range up to 1•5 p.s.i. and the other up to 15 p.s.i.

To enable pressure distributions on models to be measured, a Scanivalve, made by General Design Co., San Diego, California, (a rotary 48-channel pressure switch) is currently incorporated in the system. However, rather long pressure lags occur, since a long piece of small-bore tubing has to re-adjust to the new pressure each time the switch is operated, and it is felt that a simple system of stop-cocks replacing the Scanivalve would be more satisfactory, since larger bore tubing could then be used which would reduce pressure lag effects.

Additionally we propose to develop a liquid manometer system using di-butyl phthalate (an oil with a low vapour pressure), which will be able to measure pressure differences between a large number of points on a model. Thus by reference of a single point to an absolute instrument, such as the Electromanometer, pressure distributions can be obtained in a much shorter time than at present.

It should be mentioned that pitot pressures can be measured using the 15 p.s.i. C.E.C. head, or on a mercury manometer, or on the di-butyl manometer, depending on the range required for any particular test conditions.

3.5 Measurement of aerodynamic forces on models

The wind tunnel operates with high stagnation temperatures, so that, if a strain gauge balance is to be used for measuring aerodynamic forces and moments, then care must be taken to isolate the strain gauges from any temperature rise. There are two possible methods:-

(a) By cooling the complete strain gauge balance.

(b) By restricting the length of a run so that no appreciable temperature rise is experienced by the strain gauges.

Water cooled balances have been investigated, but method (b) is currently in use. It has been found that a run of 10 seconds is adequate

for measuring normal force and pitching moment with the Elliott Bros. recording system. The latter has been described by Anderson[6]. In 10 seconds there is no temperature rise at the strain gauge locations, and there is sufficient time for the Elliott gear to balance out after the model has moved to the particular incidence of the test, on the pneumatically-operated incidence gear. (The incidence required for any test is set by mechanical stops before the run.) The operation of moving the model from zero incidence (for starting the tunnel) to the test incidence takes about 2 seconds.

4 FLOW VISUALIZATION TECHNIQUES

4.1 Schlieren and shadowgraph

A conventional Z-type schlieren system with two spherical, surface-reflecting mirrors of 8 in. diam. and 20 ft focal length is provided. It has two light sources, using a common adjustable condenser lens system. One is a flash tube mounted on the optical axis and of microsecond duration (which is commonly used for photography), and the other is a high pressure mercury vapour lamp, 250 watts, for continuous viewing. The latter is offset from the optical axis and at 90° to it, so that a small mirror is required to turn the beam along the axis. When the flash tube is used, the mirror is rotated out of position by a solenoid.

The objective employs either (a) a 35 mm cine camera with synchronized flash contacts operated continuously at 3 frames per second or by manual selection, or (b) a photographic plate of size 6" × 4" mounted in a plateholder/viewing screen. The lens system for either format is selected manually.

The cut-off normally in use is a graded filter, but an adjustable knife edge is also provided. Quite good results can also be obtained with an optical filter used as a cut off.

For unequal magnification of boundary layers, useful for transition study, an anamorphous lens system is available.

The whole system is enclosed in two lightproof boxes suspended from a rigid boxed beam, and mounted on tripod stands: the connection to the tunnel windows is by way of telescopic tubes. The system is thus light-tight, free from external convection currents and is easily moved.

By use of the light source box of this system, direct shadow pictures of the flow may be taken with a 6" × 4" photographic plate mounted on the exit window of the working-section. This is of most use for pictures of shock waves, since the shadowgraph system measures the second differential of density whereas the schlieren system measures the density gradient. Some typical photographs are shown in Figs.7 and 8.

4.2 Schlieren-interferometer

The schlieren-interferometer is obtained through a simple modification of the standard schlieren system. A Wollaston prism and polaroid filter is inserted at the focus of each spherical mirror, and suitably orientated. By this means, a double image of the flow field is obtained with an overlap proportional to the angle of the prism. (In our case, the overlap is $\frac{1}{8}$ in. for a 2° angle). The small difference in impedence of optical path of 2 rays separated by the overlap distance, and caused by density variation, results in colour changes or fringe shifts according to the system set up. Knowledge of the geometry of the flow field enables a direct measurement of density increment, and hence density, to be calculated from the picture by use of the Gladstone-Dale law relating density to refractive index. A full description of this technique is given in Ref.7.

This system is also useful for qualitative studies of flow fields and is, therefore, complementary to the standard schlieren technique. A typical picture is shown in Fig.9.

4.3 Surface oil flow studies

The technique of coating a model with oil and observing the pattern of the surface flow under air friction is well known, and used extensively at lower Mach numbers. Generally, a run of several minutes is made, the oil pattern is formed and the tunnel is stopped; after which the model is photographed.

In our case a picture is required to form in a few seconds both because of the short running time available, and because of the high heat transfer to the model. If an oil of too high a viscosity is used it will not flow until its temperature is increased, and hence, the viscosity reduced. The oil flow picture is then temperature sensitive. On the other hand if an oil of too low a viscosity is used the force of gravity becomes influential. Some time was therefore spent in trying out various mixtures in order to obtain a suitable one. The photograph must also be taken during the run, since the mechanism of flow breakdown completely destroys the picture. Hence, a cine camera is used which continuously photographs the model surface throughout the run.

A number of oils and mixtures were tried, and the following mixture was chosen as being most suitable.

Ingredient	Use
Engineers blue marking grease (trace)	Dye
High vacuum silicone grease (trace) Di-butyl phthalate oil (20-30 drops)	mixed to give desired viscosity
Oleic acid - (2-3 drops)	helps mixture to flow uniformly
The above paste is dissolved in a copious amount of tri-chlorethylene and is sprayed onto the model from a distance of 3 to 4 feet to obtain a thin uniform coating.	

Some pictures obtained on a series of arrowhead wings are shown in Fig.10.

LIST OF REFERENCES

Ref.No.	Author	Title, etc.
1	Crane, J.F.W.	The 7 in. × 7 in. hypersonic wind tunnel at R.A.E. Farnborough. Part III. Calibration of the flow in the working section. Part III of this Current Paper.
2		Blockage tests, starting loads, pressure ratios etc. (Part IV.) To be published.
3	Marchant, J.E.	The machining of wind tunnel liners (fused silica). Unpublished M.O.A. Report.
4	Winter, K.G.	Brief description of the R.A.E. intermittent supersonic wind tunnel plant. CP.336 June 1956.
5	Hill, J. et al	Mach number measurements in high speed wind tunnels. NATO Agardograph No.22 October 1956.
6	Anderson, J.R.	A note on the use of strain gauges in the wind tunnel balances. Unpublished M.O.A. Report.
7	Renet, C.	Quantitative schlieren interferometry in wind tunnels. R.A.E. Library Translation 874. February 1960.
8	Woodley, J.G.	Measurements of heat transfer to a 15° total angle cone at a Mach number of 6.8. Unpublished M.O.A. Report.

TABLE 1

Hypersonic wind tunnel calculated air flows

M	Stagnation Conditions	Throat Height (width = 7")	Working Section Conditions (A = 0.34 ft^2)
5	p = 294 p.s.i. T = 413°K ρ = 1.067 lb/ft^3 a = 1339 f.p.s.	0.28"	p = 0.555 p.s.i. T = 68.8°C ρ = 0.0121 lb/ft^3 a = 546 f.p.s. V = 2730 f.p.s. m = 11.23 lb/sec
6	p = 588 p.s.i. T = 543°K ρ = 1.622 lb/ft^3 a = 1533 f.p.s.	0.1315"	p = 0.3725 p.s.i. T = 66.3°K ρ = 0.00842 lb/ft^3 a = 535 f.p.s. V = 3210 f.p.s. m = 9.2 lb/sec
7	p = 735 p.s.i. T = 683°K ρ = 1.611 lb/ft^3 a = 1720 f.p.s.	0.0672"	p = 0.1774 p.s.i. T = 63.3°K ρ = 0.00421 lb/ft^3 a = 523 f.p.s. V = 3660 f.p.s. m = 5.23 lb/sec
8	p = 735 p.s.i. T = 813°K ρ = 1.354 lb/ft^3 a = 1875 f.p.s.	0.0368"	p = 0.0753 p.s.i. T = 58.9°K ρ = 0.001912 lb/ft^3 a = 505 f.p.s. V = 4040 f.p.s. m = 2.625 lb/sec
9	p = 735 p.s.i. T = 953°K ρ = 1.156 lb/ft^3 a = 2030 f.p.s.	0.0214"	p = 0.0348 p.s.i. T = 55.4°K ρ = 0.000943 lb/ft^3 a = 489 f.p.s. V = 4,400 f.p.s. m = 1.411 lb/sec

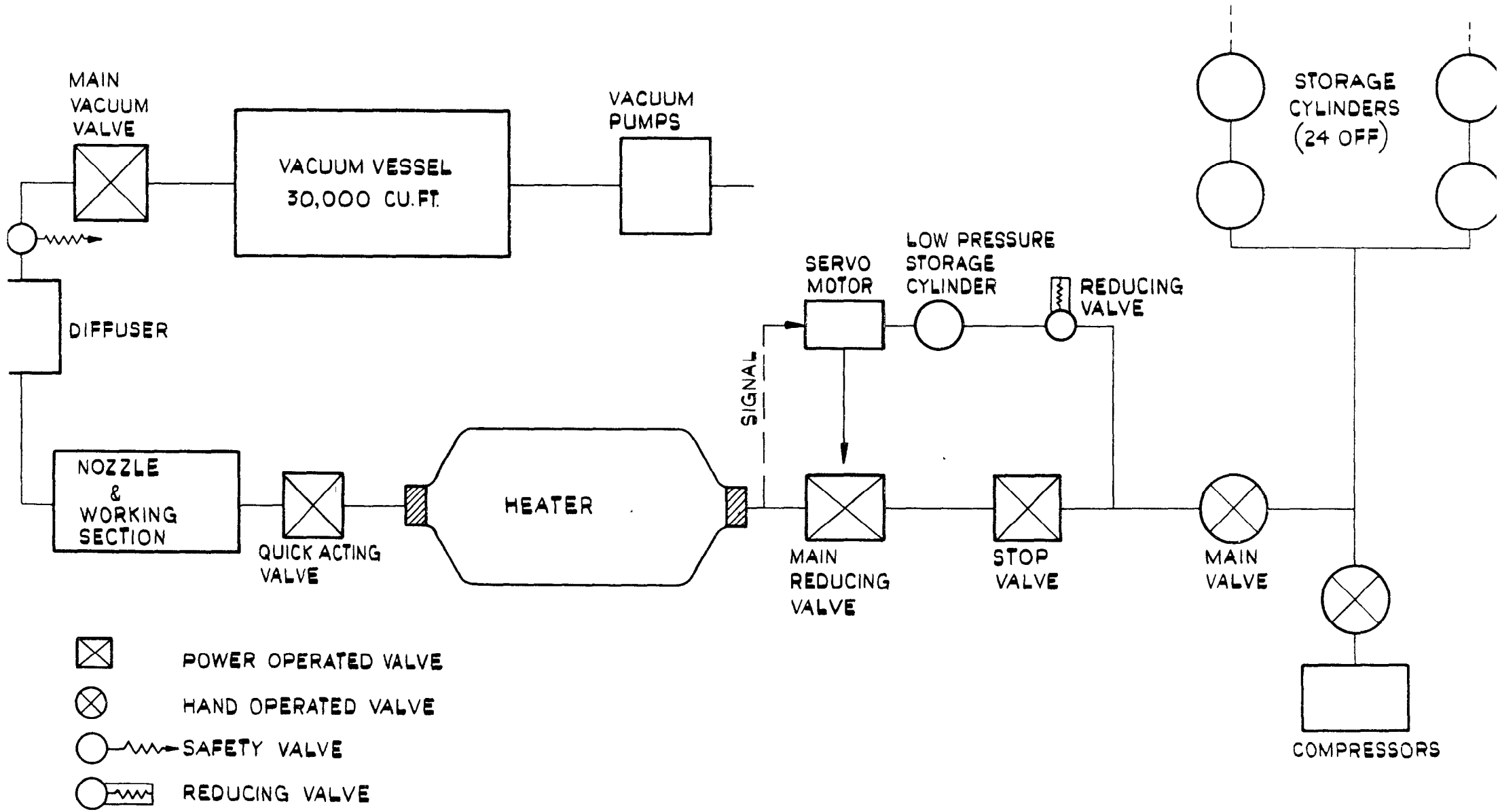

FIG.1. LINE DIAGRAM OF TUNNEL CIRCUIT.

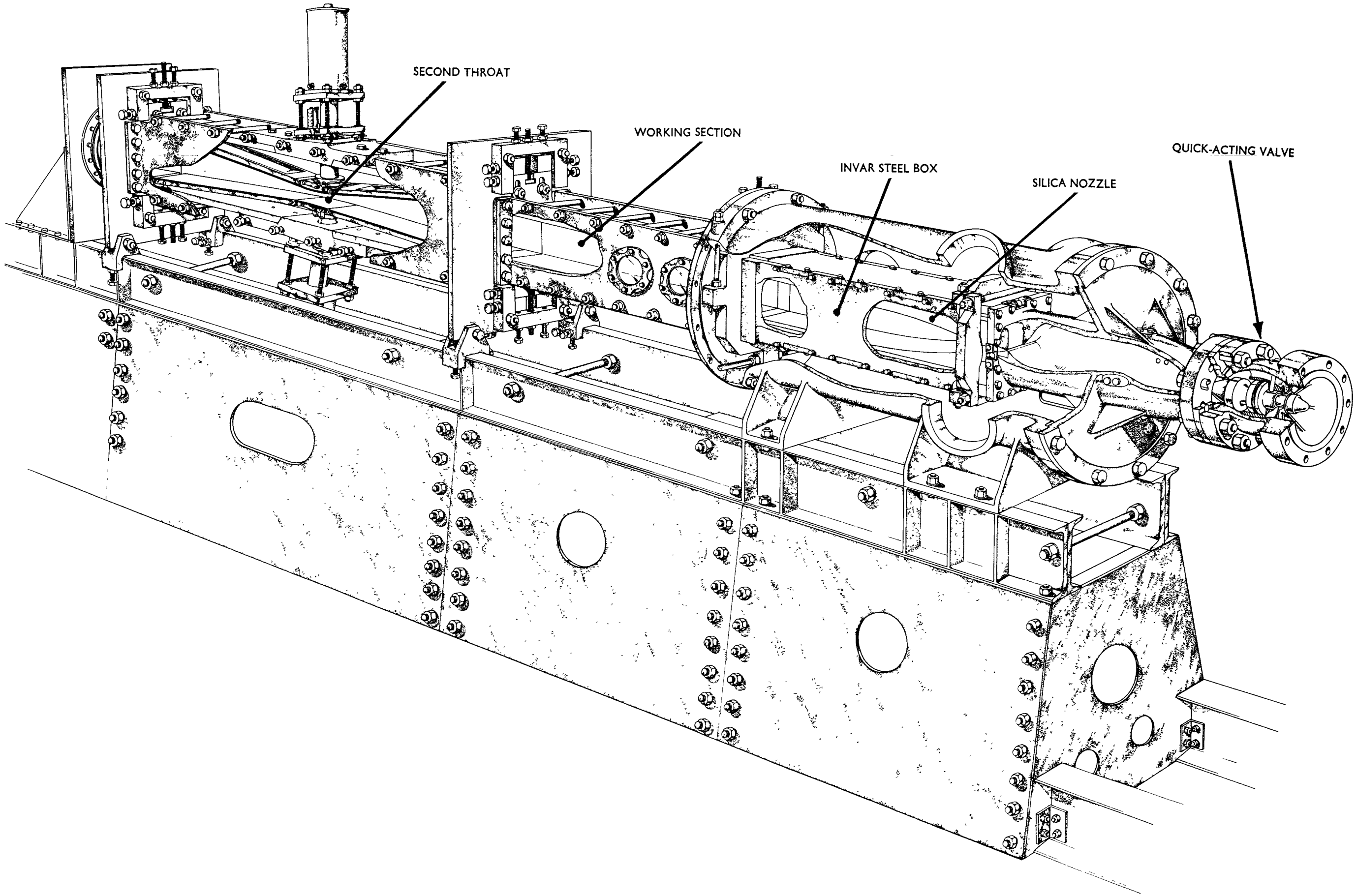

FIG. 2. CUT-AWAY VIEW OF PART OF TUNNEL

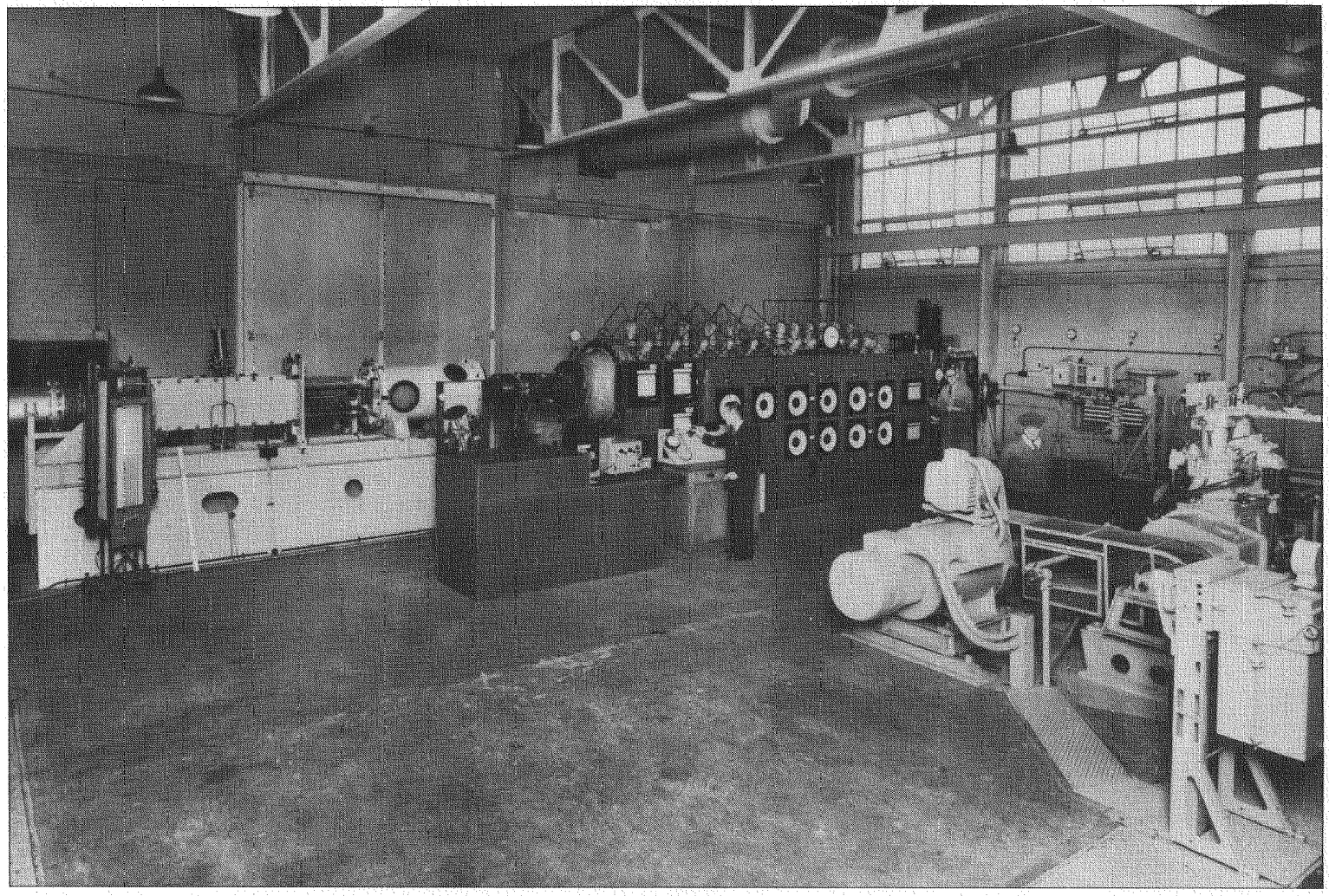

FIG. 3. GENERAL VIEW OF TUNNEL

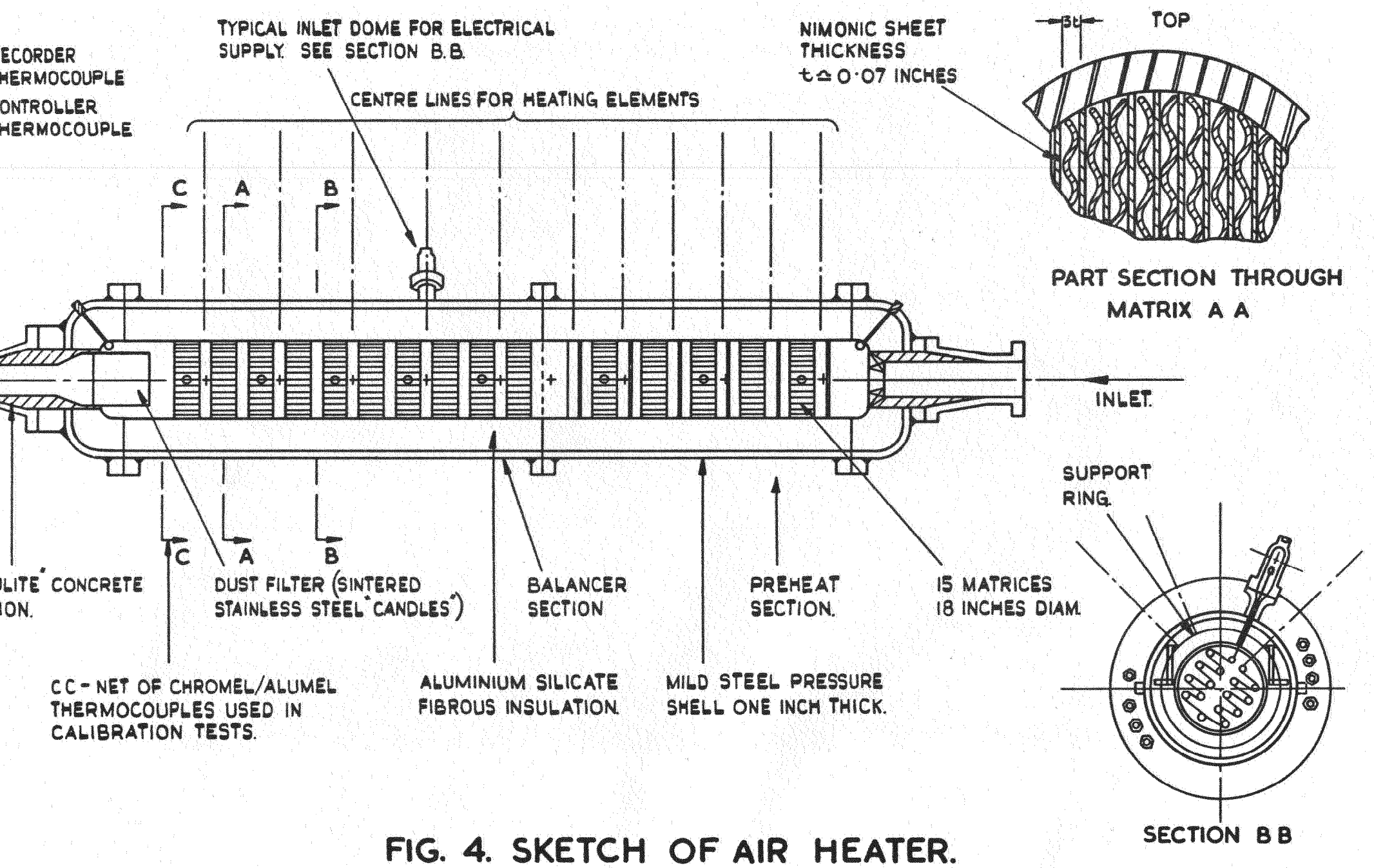

FIG. 4. SKETCH OF AIR HEATER.

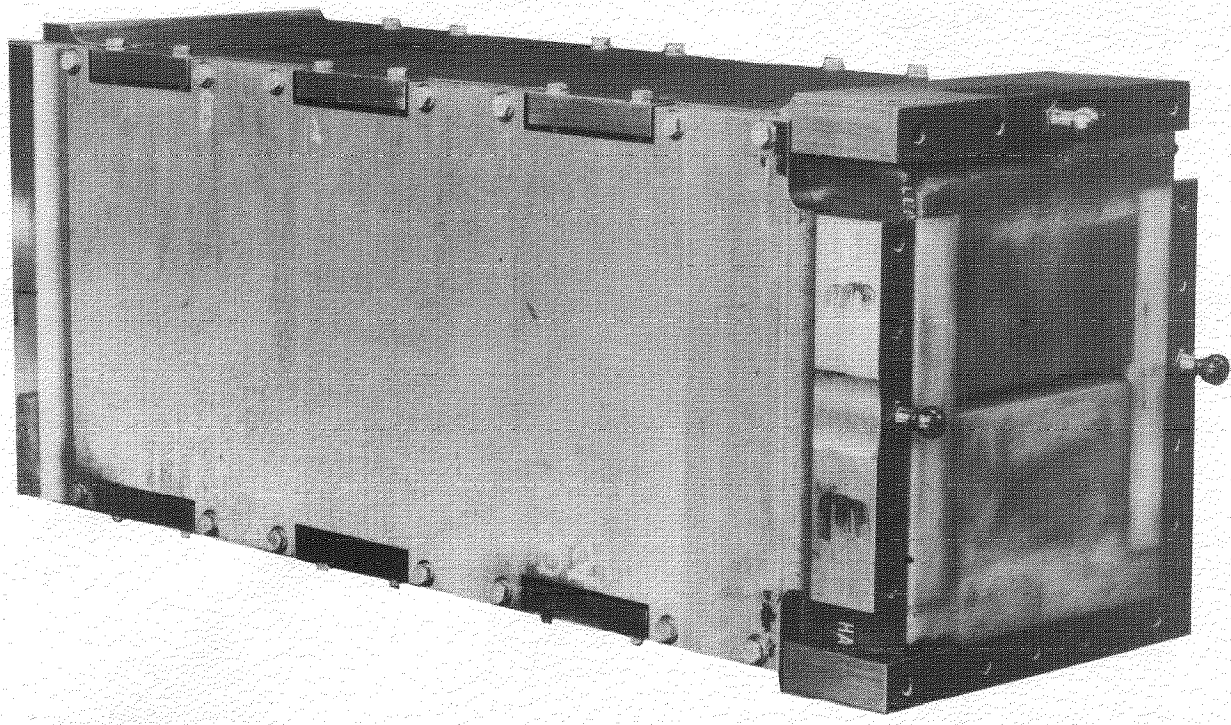

FIG. 5. BUILT UP FUSED-SILICA NOZZLE, M = 7

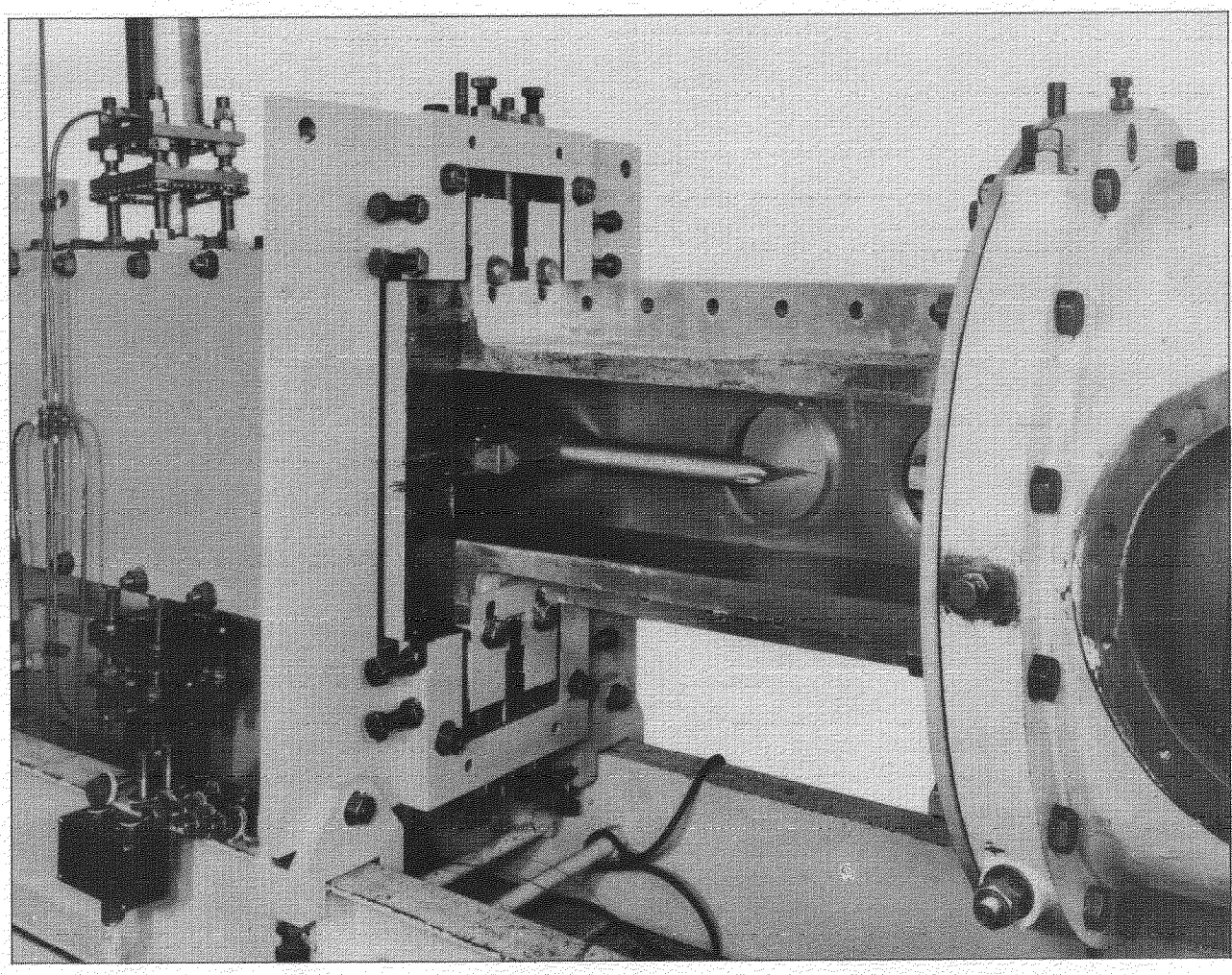

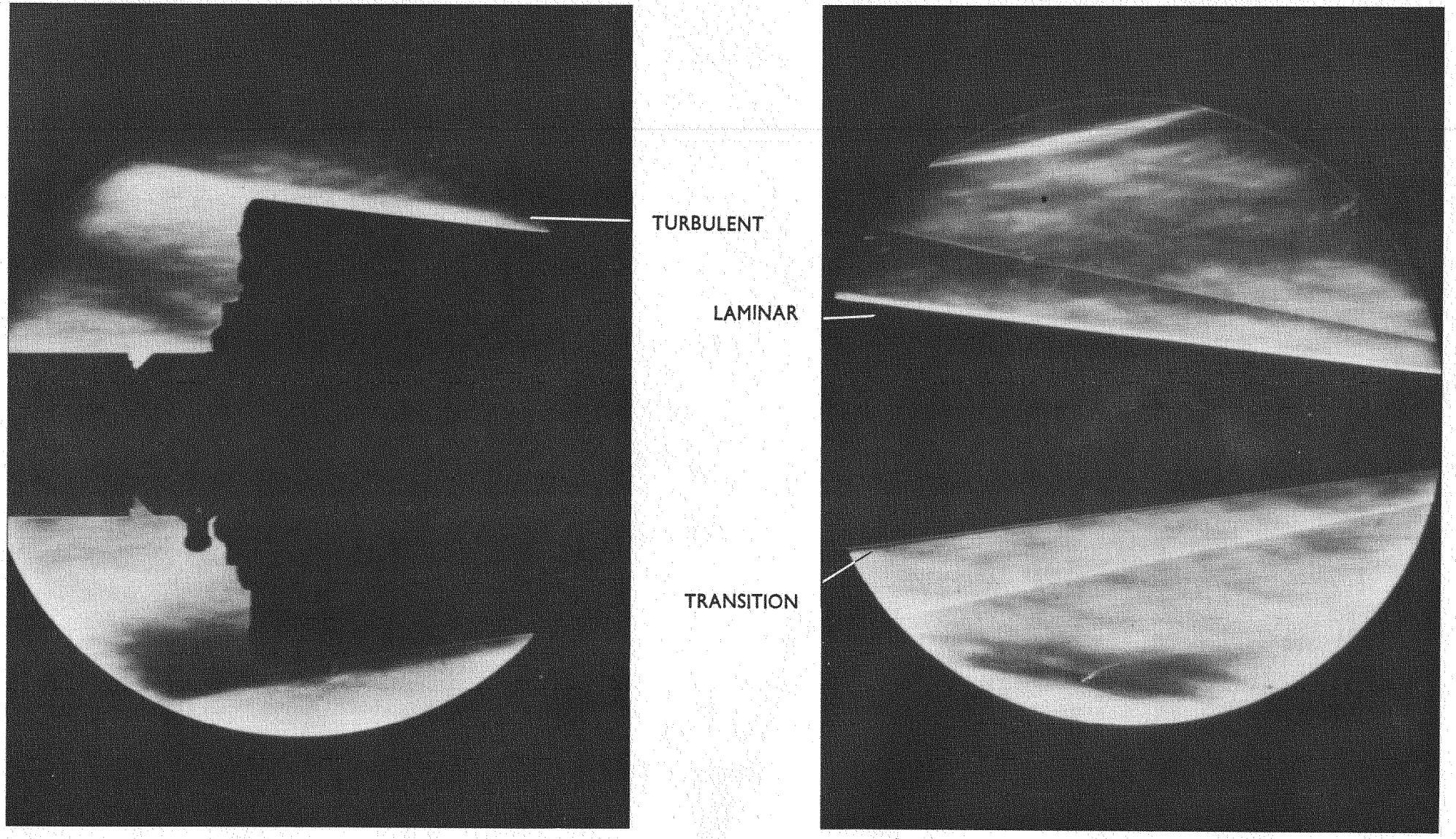

FIG. 7. TYPICAL SCHLIEREN PICTURE (15° CONE AT ZERO INCIDENCE - $M_\infty = 6{\cdot}8$)

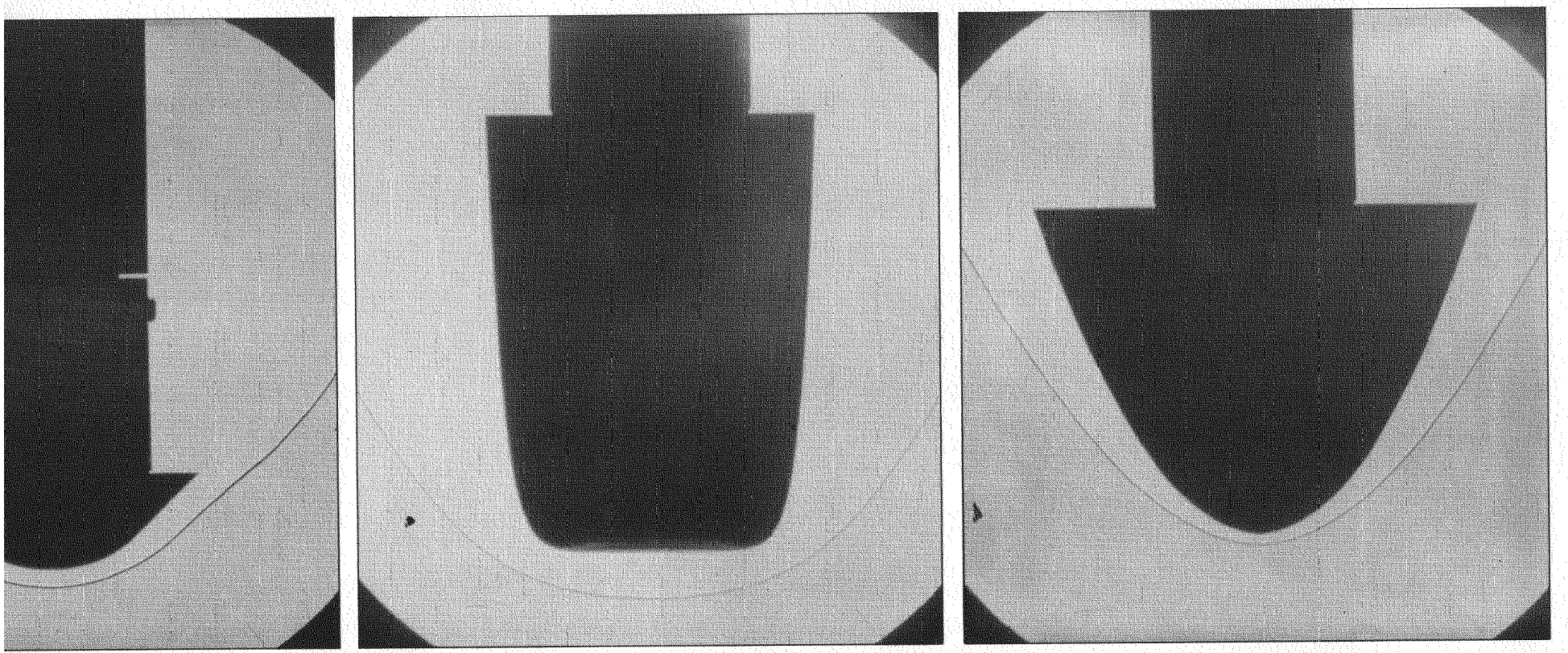

FIG. 8. SOME TYPICAL SHADOWGRAPH PICTURES (AXISYMMETRIC BLUNT BODIES - $M_\infty = 7$)

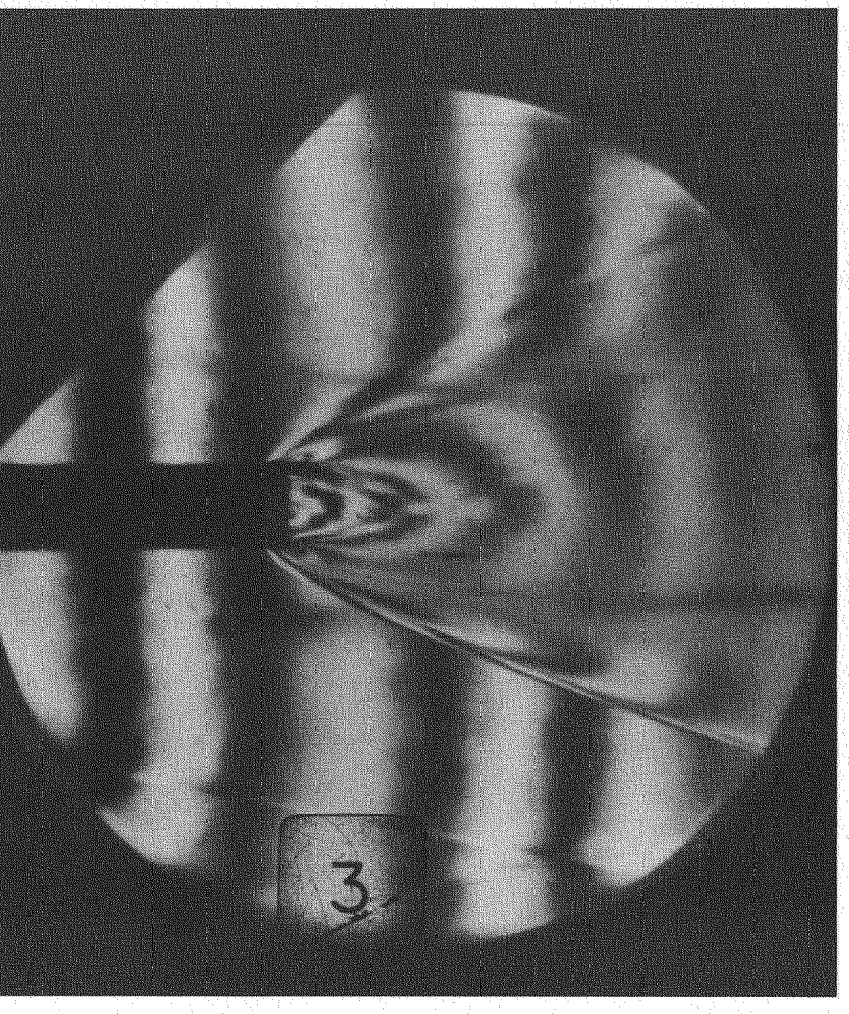

FRINGE SHIFT METHOD

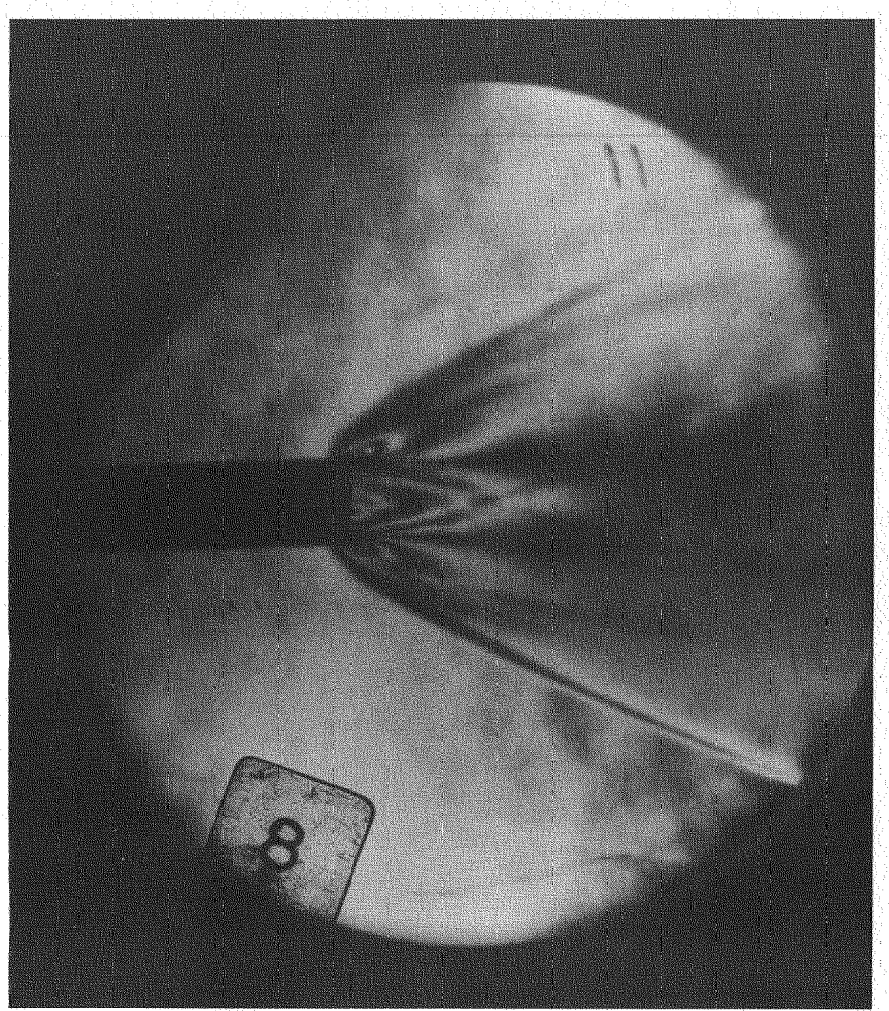

TINT METHOD

FIG. 9. TYPICAL SCHLIEREN INTERFEROMETER PICTURES (UNDER-EXPANDED JET EXHAUSTING INTO WORKING-SECTION)

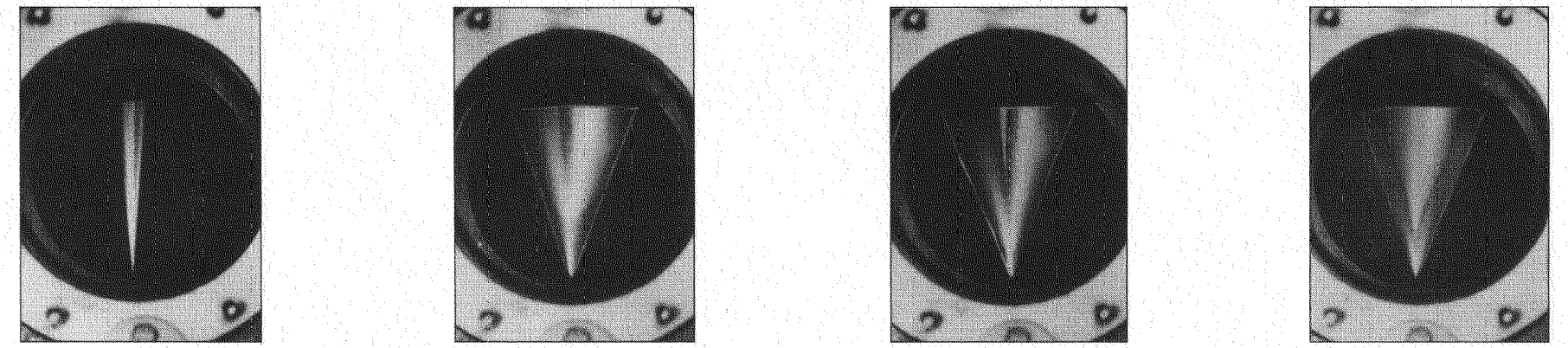

1 sec. 10 sec. 5 sec. 1 sec.

FIG. 10. TYPICAL SURFACE OIL FLOW PICTURES ON 70° AND 85° CAMBERED DELTA WINGS

THE 7 IN. × 7 IN. HYPERSONIC WIND TUNNEL AT R.A.E. FARNBOROUGH

PART II. HEATER PERFORMANCE

by

J. F. W. Crane

Previously issued as R.A.E. Tech Note No. Aero 2717 - A.R.C. 23,435

LIST OF CONTENTS

LIST OF ILLUSTRATIONS

LIST OF ILLUSTRATIONS (Contd)

1 INTRODUCTION

The R.A.E. 7 in. x 7 in. hypersonic tunnel employs a storage heater to heat the air supply and thus avoid liquefaction in the working section. This heater was designed as a cylindrical vessel mounted horizontally. A concentric core houses the storage material which is electrically heated. The heater is rated at 100 KW.

In the first design the thermal insulation surrounding the hot core was a brick material which dusted severely through abrasion, and some breakage of bricks occurred. Because of this the bricks were removed and the heater was modified slightly to allow the use of a fibrous insulation, namely, aluminium silicate which it was thought would be less prone to dusting.

Subsequent use of this heater since 1958 has shown that the dusting problem has been solved by the use of this fibrous insulation but the performance of the heater has been affected by free convection in the insulation at high pressure. This phenomenon is manifested by an increase in temperature of the upper surface of the cylindrical outer shell.

A way of avoiding this adverse effect is to limit the time during which the heater is held at high pressure, but this imposes a severe limitation on tunnel usage.

The selected heater temperature is not realised in the settling chamber and there is a gradual rise in stagnation temperature during a tunnel run because of heat loss to the relatively cool dust-filter section, outlet cone and quick acting valve. Its performance, however, is adequate for the M = 6.8 nozzle and probably adequate for the M = 8.2 nozzle.

Modifications in hand to improve the heater performance are described.

Temperature distributions in the heater and settling chamber are discussed herein whilst Part III of the tunnel report contains a discussion on the temperature distributions in the settling chamber and working section.

2 DESCRIPTION OF HEATER

Fig.1 is a sketch of the heater which shows the main details of its construction. The storage material is in the form of matrices (which consists of alternate flat and corrugated Nimonic sheets mounted edgeways to the flow) and has a heat capacity of 450 C.H.U./deg.C. This capacity allows a tunnel run of at least 3 minutes at M = 7 flow conditions[1].

The heater has been designed for operation at a maximum temperature of 680 deg.C (corresponding to the theoretical temperature required to avoid liquefaction in the working section at M = 9 flow conditions) but the heating elements can withstand a temperature of 1100 deg.C.

The maximum operating pressure is 750 p.s.i.g. and the pressure vessel has been hydraulically tested to $1\frac{1}{2}$ times this value.

The heater is mounted horizontally on rollers and is fixed rigidly at the outlet end only, via the quick acting valve, to the tunnel strong point, which is the nozzle drum and mounting frame. Thus all axial movement due to starting shock and thermal expansion is in a direction away from this point.

The heater core, which houses the matrices and heating elements, is suspended from tie rods attached to hoops which are expanded into the pressure shell, and sufficient clearance between each section is allowed for thermal expansion.

At the centre and at each end, near to the flanged joints of the pressure shell, the core is ventilated to the surrounding fibrous insulation through a number of 3 inch diameter holes (12 at each station). This ventilation should accommodate fairly rapid pressure changes without detriment to the packing of the insulation. (The density of packing is 10 lb/ft^3.) In normal operation rapid changes in pressure are avoided.

The 24 volt electrical connections to the heating elements are made in the four rows of electrical coupling domes mounted on top of the pressure shell. Each dome is supplied with cold air from an external manifold at a pressure 5 p.s.i. greater than that in the heater, in order to assist the air seal on the element lead and to ensure that any leakage will be of cold air into the heater rather than vice versa.

It is important to maintain the pressure tightness of the manifold and domes in order to avoid leakage of hot air from inside the heater. In the tests analysed in this report leakage of hot air from the heater via the dome seals did occur. Later, overhaul of the dome seals and enlargement of the supply line to the manifold has eliminated this source of hot air leakage.

The heater core is divided into eight zones (No.1 is at the inlet end) and thermocouples are inserted from one side of the pressure shell to monitor temperatures on the centreline. For each zone there are two thermocouples; one buried in the matrix is used to record the zone temperature on a chart potentiometer, and the other mounted on a heating element supplies the signal to the zone controller and dial indicator. Thermocouples are also installed to show on dial indicators the air temperatures at the heater inlet and outlet and in the centre section, Fig.4a.

3 DESCRIPTION OF ADDITIONAL THERMOCOUPLE INSTRUMENTATION

Preliminary trials of the heater showed that under high pressure the pressure shell became much hotter at the top than at the bottom. Accordingly, additional thermocouple instrumentation was fitted, as follows.

At the heater outlet at station CC, Figs.1 and 2, nine welded chromel/alumel thermocouples were arranged to cover the vertical and horizontal centrelines at 0, 3 and 6 inches radii of the 18 inch diameter duct. The outputs of these thermocouples were recorded on a Speedomax potentiometer during a tunnel run and cross-sectional temperature distributions were obtained. (The test method is described in Part III of the tunnel report[2].)

At the heater mid-section (station DD, Fig.2) four thermocouples, each with its own gauge, were mounted half an inch from the top and bottom of the heater core so as to measure matrix and air temperatures at the top and bottom of the core and so obtain the overall vertical temperature gradients across the matrix and air at this station.

In order to measure the temperature distributions along the top and bottom surfaces of the heater 24 copper/constantan thermocouples were strapped to the shell in the arrangement shown in Fig.2. A portable pyrometer box was used to measure the outputs of these thermocouples. Because of the method of attachment and the large size of the sensitive junctions it is probable that the measured temperatures were slightly below the true values.

4 RESULTS

4.1 Skin temperature distributions (Pressure shell)

Fig.2 shows a sketch of the heater and its attachments together with the positions of the thermocouples strapped to the top and bottom surfaces. Plots of skin temperature at equilibrium conditions (soaked at pressure for

2 and 3 hours) with the heater controllers set at 680 deg.C are given for pressures of 20 and 750 p.s.i.g. At the lower pressure the skin temperature was reasonably uniform at 35 deg.C which indicates an absence of free convection in the insulation at this pressure level.

At the higher pressure the effect of free convection in the insulation was shown by a rise of 100 deg.C in the temperature of the upper surface of the cylindrical shell. (Warming up of the top surface of the shell is first noticed at pressures around 100 p.s.i.g.) The highest shell temperature of 180 deg.C was recorded near the outlet end. Further downstream the maximum temperature of 200 deg.C was measured for the top of the quick acting valve.

The temperature distribution along the bottom of the pressure shell was affected by the internal free convection occurring at high pressure at two points; near the outlet where an increase of 35 deg.C was measured, and in the middle (12.6 ft on the length scale) where the temperature increased by 20 deg.C.

At the higher pressure the inlet was much cooler than the outlet because of cooling by convection currents inside the heater which were augmented by the influx of cold topping-up air required to compensate leakages at the electrical coupling domes, flanges and quick acting valve seat.

Because of these temperature differences between the upper and lower surfaces of the heater at high pressure, differential thermal expansion takes place which results in 'hogging' distortion of the shell. This distortion causes (a) bending of the pipework at the inlet end and (b) flexing of the joints of the quick acting valve. The latter joints are made specially flexible to suit this condition.

Fig.3 compares the skin temperature distributions after soaking at two levels of core temperature, namely 680 deg.C and 500 deg.C at a pressure of 750 p.s.i.g. As would be expected a reduction of core temperature reduces the amount of heat transferred to the upper surface of the shell by internal free convection, which is indicated by the lower level of temperature recorded, about 15 deg.C in this case.

To obtain a much larger relief from this adverse effect of internal free convection at high pressure the heater must be pressurised for only short periods. This entails depressurisation of the heater to around atmospheric pressure soon after a tunnel run. Fig.5b compares the results of short cycle and long cycle pressurisation namely, quick pressurisation and soaked conditions and shows the large amount of relief which can be obtained by the use of the quick pressurisation technique.

4.2 Core temperature distributions

4.2.1 Effect of pressure on temperatures along the centreline

Fig.4a shows the longitudinal temperature distributions along the centreline of the core at pressures of 20 and 750 p.s.i.g. with the heater controllers set at 680 deg.C.

At the lower pressure the temperatures were roughly at the controller

At high pressure the centreline temperature distribution was much less uniform than in the low pressure case and the controller setting was not reached. The heat transferred to the quick acting valve and heater outlet attachments by the internal convection is greater because of the increased density and hence heat content of the fluid. Probably because of the "guard ring effect" of the higher temperature of the outlet attachments when soaked at high pressure the outlet temperature at $4\frac{1}{2}$ ft distance from AA was somewhat greater for this condition.

There was a large drop in temperature of about 200 deg.C from the middle of the heater to its inlet which did not occur at low pressure. This cooling-off can be attributed to the more complex and more vigorous convection currents inside the heater which were augmented by the large amount of topping-up air required to compensate for leakage. At this time the overall leakage of air from the tunnel, a large part of which was from the heater joints, was slightly greater than the output of one air compressor (9.64 lb per min.). Leakage from the heater has been considerably reduced since then but no measure of the present leakage rate has been made.

4.2.2 Effect of pressure on temperatures at the top and bottom of the core. (Station DD)

Fig.4b shows the histories of the air and matrix temperatures at the top and bottom of the heater core at station DD (Fig.2) measured in the above test (section 4.2.1). The heater was soaked at 20 p.s.i.g. and 680 deg.C for approximately 2 hours and was then pressurised to 750 p.s.i.g. and soaked at this pressure for a further $3\frac{1}{2}$ hours.

At the low pressure there were negligible differences between the air and matrix temperatures which indicated a uniform temperature distribution across the core.

After raising the pressure to 750 p.s.i.g. the temperatures at the bottom of the core began to fall - slowly during the first hour, rapidly during the second hour - and finally reached equilibrium values during the third hour. At this stage there were vertical temperature gradients of 240 deg.C across the matrix and 160 deg.C across the air, the bottom being cooler than the top. The temperature at the top of the core dropped by only 30 deg.C during this period.

The tunnel was then operated for about one minute. The greater drop in temperature at the bottom of the core due to the tunnel run suggests greater heat transfer to the base of the flowing stream. The bottom of the matrix has dropped in temperature by 190 deg.C but the top has dropped by only 45 deg.C. This is due to 'waterfall effect' because at this flow rate (M = 7 conditions) the average velocity of the inlet air is only 0.8 ft/sec and of the same order of magnitude as the free convection velocities produced by the mixing with the warmer residual air. Hence the resultant velocity of the inlet air has a component due to gravity and the inlet air tends to flow along the lower half of the heater core.

4.2.3 Replenishment of storage heat at high pressure

Fig.5a shows the temperature history at station DD when recovering at high pressure. For the first hour of this test the heater was soaked at a pressure of 50 p.s.i.g. and the core temperature at this station was reasonably uniform at about 450 deg.C (i.e. 50 deg.C below the controller setting of 500 deg.C). The heater was then quickly pressurised to 750 p.s.i.g. and the tunnel operated for 100 seconds. Immediately after this run measurements showed that the temperature at the bottom of the core had dropped by about 250 deg.C, whilst that at the top remained unchanged.

The heater was then held at this high pressure for several hours. Measurements of core temperature made at hourly intervals showed that the replenishment of storage heat was very slow at this high pressure, (most of the electrical energy being dissipated in heat losses, see Appendix 1) and there was little reduction of the vertical gradient, even after 5 hours. (There was sufficient heat remaining in the downstream section of the heater for further tunnel running if required.)

Because of the vertical temperature gradient and the centreline position of the controller thermocouple it is possible to obtain temperatures greater than the controller setting at the top of the core. (Note that at the end of the test the matrix (top) temperature was 25 deg.C greater than the controller setting.)

4.3 Temperature distributions at the heater outlet

Because of the effect of internal convection on the temperature distributions in the heater core it is of interest to measure the cross sectional temperature distribution at the heater outlet during a tunnel run. Fig.6 shows typical profiles of outlet temperature at station CC, Fig.2, for both soaked and quick pressurisation conditions at time 40 seconds during a tunnel run.

The heater was pressurised to 750 p.s.i.g. and the controllers set at 500 deg.C.

For the soaked condition the heater was held at high pressure for 3 hours before running. The centreline temperature, Tc, was 450 deg.C and a large vertical temperature gradient of 180 deg.C with temperature decreasing downwards existed. This was very similar to the gradient measured at station DD in the middle of the heater. On the horizontal centreline the temperature profile was symmetrical, with the centre slightly cooler than the edges.

For the quick pressurisation condition (in which the heater was brought up to temperature at atmospheric pressure, and then pressurised and the tunnel operated in 7 mins. and 10 mins.) the distributions were almost uniform. The centreline temperature was 500 deg.C, the controller setting. In the horizontal plane the temperatures were uniform. In the vertical plane there were slight temperature gradients with the temperature decreasing downwards. This was more marked in the 10 min. test than in the 7 min. test, which shows that internal free convection has some effect for even these short periods of time.

The outlet temperature distribution is, therefore, much more uniform for the quick pressurisation condition than for the soaked condition.

4.4 Temperature measurements in the settling chamber

4.4.1 Cross sectional distribution

From the heater outlet the air passes through the dust filter section, outlet cone and quick acting valve and then enters the settling chamber. At this station it is important that the temperature distribution should be uniform in order to produce a uniform flow field of temperature and velocity in the working section which is just downstream of it.

Fig.7 shows that despite the large vertical temperature gradient which can exist at the heater outlet and also, incidentally, at the entrance to the quick acting valve, the cross sectional temperature distribution in the settling chamber is effectively uniform. In the 7 inch diameter section there is a 5 inch diameter core in which the average temperature variation from the centreline value of 400 deg.C is only 2 deg.C. Outside this core there is a

cooler thermal layer and temperatures at a $\frac{1}{4}$ inch from the wall are about 10 deg.C lower than the centreline temperature. (A description of the thermocouples and testing technique is given in Part III of this report[2].)

When vertical temperature gradients were first measured in the flow from the heater a mixing vane was installed at the most convenient point upstream of the settling chamber namely, at the entrance to the quick acting valve. Subsequent measurements of temperature both with and without the mixing vane, Fig.7, showed that the vane was not required because the quick acting valve is itself a very good mixer. The mixing vane has, therefore, been removed.

4.4.2 Temperature rise during a run

Because of heat loss to the outlet attachments there is a rise in temperature of the air in the settling chamber during a tunnel run. Fig.8 shows a typical history for M = 6.8 conditions with the heater controllers set at 500 deg.C. There was a sharp rise in temperature over the first 2 seconds from 60 deg.C to 330 deg.C. This was followed by a more gradual rise as the outlet attachments warmed up and at 30 secs a temperature of 400 deg.C was reached. From this point the rate of rise was constant at $\frac{1}{2}$ deg.C per sec. This trace was from a typical heat transfer test on a model with the heater condition nearer to the quick pressurisation than soaked states. (Also shown are uncorrected curves for soaked and quick pressurisation conditions, to illustrate the slight gain in temperature level obtained by the use of the quick pressurisation technique.)

This variation of settling chamber temperature with time imposes an undesirable variable on heat transfer tests on wind tunnel models when the heat pulse technique is used. Therefore, modifications to the heater, described in the next section, are to be incorporated to remedy this defect.

5 DESCRIPTION OF MODIFICATIONS TO IMPROVE THE HEATER PERFORMANCE

In order to obtain the design maximum temperature of 680 deg.C in the settling chamber at the design maximum pressure of 750 p.s.i.g. for the most favourable condition of quick pressurisation, heat loss to the outlet attachments must be minimised. It will not be possible to attain 680 deg.C for the soaked condition because of the non-uniformity of core temperature set up by internal free convection, but a considerable improvement should be achieved by the elimination of heat loss to the outlet attachments.

Accordingly, a modified outlet cone incorporating a guard heater which will preheat the outlet passage to the required temperature is being made. Also, the quick-acting valve will be preheated through a jacket.

To eliminate 'hogging' distortion the underbody of the heater is to be heated by jacket heaters so that the temperature distribution along the bottom is similar to that along the top. This will therefore help to avoid leaks at the heater flanges. This application of heat should, incidentally, produce some reduction of the free convection through the thermal insulation inside the heater and hence reduce the temperature gradient across the heater core.

6 CONCLUSIONS

The following conclusions may be drawn from tests of the storage heater of the R.A.E. 7 in. x 7 in. hypersonic wind tunnel, described in this note.

(a) In the heater's present form the design maximum temperature of 680 deg.C cannot be obtained in the settling chamber because of heat loss to the relatively cool outlet attachments (the dust filter section, the outlet cone and the quick-acting valve). Its performance is adequate for the M = 6.8 nozzle and probably for the M = 8.2 nozzle but will not be adequate for nozzles of higher Mach number when higher stagnation temperatures are necessary. With the incorporation of guard heating of the outlet attachments the heat loss from the outlet air should be eliminated.

(b) At high pressure (greater than about 100 p.s.i.g.) a phenomenon of free convection in the fibrous insulation, packed in the annulus surrounding the matrix core, transports heat from the core to the upper surface of the heater where it is dissipated by external convection and radiation (see Appendix 1). Because of the horizontal disposition of the cylindrical heater a vertical temperature gradient is set up across the core such that the bottom is cooler than the top. This gradient appears after only a few minutes at high pressure and becomes very large after 2 hours, and results in an average outlet temperature lower than that selected.

(c) By use of the 'quick pressurisation' technique, in which the heater is kept at high pressure for only a short time, the vertical temperature gradient across the core (see (b) above) may be considerably reduced. This technique seriously limits the flexibility of use of the tunnel and is wasteful of pressurised air, because depressurisation of the heater to near atmospheric pressure after a run is imposed by its use.

(d) At equilibrium temperature, when the heater is soaked at high pressure for 2 or 3 hours, the top of the heater becomes hotter than the bottom by about 100 deg.C. This temperature differential results in 'hogging' distortion of the assembly. With the incorporation of underbody heating jackets the 'hogging' distortion should be greatly reduced and some relief of vertical temperature gradients across the core (see (b) above) may be obtained.

(e) In the soaked condition, at the maximum conditions of 750 p.s.i.g. and 680 deg.C, there is a pronounced cooling off along the core from about the middle to the inlet end.

ACKNOWLEDGMENTS

Thanks are due to the staff of Incandescent Heat Co. who designed and built the air heater and gave valuable assistance in its development, and also to the staff at R.A.E., in particular Mr. W.W. Bland.

Grateful acknowledgment is due to Mr. L.R. Vandome, who played a major part in the development of this facility. The results quoted for the heater in this note were derived in the main from measurements made by him.

LIST OF REFERENCES

No.	Author	Title, etc.
1	Crabtree, L.F., Crane, J.F.W.	The 7 in. x 7 in. hypersonic wind tunnel at R.A.E. Farnborough. Part 1 Design, Instrumentation and flow visualization techniques. Part I of this Current Paper.
2	Crane, J.F.W.	The 7 in. x 7 in. hypersonic wind tunnel at R.A.E. Farnborough. Part III Calibration of flow in the working section. Part III of this Current Paper.
3	Brown, A.I., Marco, S.M.	Introduction to heat transfer. McGraw-Hill Book Co. Inc.

APPENDIX 1

APPROXIMATE ANALYSIS OF HEAT LOSSES FROM THE HEATER AT HIGH PRESSURE AND HIGH TEMPERATURE. (BASED ON SKIN TEMPERATURE MEASUREMENTS MADE ON 24TH SEPT. 1958)

Using standard formulae and tables[3], the heat losses from the heater, for the conditions of 750 p.s.i.g. and 680 deg.C, by the modes of free convection and radiation were computed. Table 1 lists these results which are based on skin temperatures given in Fig.2. The heater was considered as a number of cylindrical sections each at a temperature equal to the arithmetic mean of the measured temperatures of top and bottom surfaces. These assumptions facilitate the calculation and produce an error of only a few per cent and, in view of the limited and the approximate nature of the analysis, are considered reasonable. In the case of the electrical coupling domes the temperature was assumed to be equal to the average temperature of the top surface of the heater.

The table shows that the heat lost by free convection was 13.5 KW, about half that lost by radiation (black body). The measured power consumption during this period of thermal equilibrium was 68 KW. The balance of 28.3 KW must be accounted for by (a) leakage of hot air from the heater, (b) external forced convection, (c) the approximate nature of the analysis.

One significant feature of this analysis is the large heat loss from the electrical coupling domes, which accounts for about 50 per cent of the total calculated loss and 29 per cent of the overall loss.

Also significant is the large heat loss unaccounted for by free convection and radiation namely 41 per cent of the overall loss. A large portion of this was due to leakage of hot air from the heater, especially from the electrical coupling domes.

TABLE 1

APPROXIMATE ANALYSIS OF HEAT LOSSES FROM THE HEATER AT HIGH PRESSURE AND HIGH TEMPERATURE
(FOR TEST ON 24TH SEPT. 1958, FIG. 2)

Section	Area (ft^2)	Mean Temp. (deg.C)	Heat losses (per cent)	
			Free convection	Radiation
Inlet cone	4.5	47	0.33	0.3
Inlet dome	10	52	0.90	0.8
Inlet flange	16.2	70	2.62	2.1
Centre flange	16.2	75	2.95	2.4
Outlet flange	16.2	100	4.70	4.0
Cyl. shell	104	82	22.58	18.1
Cyl. shell	38	110	12.75	11.0
Outlet dome	10	95	2.66	2.2
Outlet cone	8	87	1.56	1.5
Elect. coupling domes	130	135	45.75	53.7
Quick acting valve	6	170	3.2	3.9
Totals per cent			100	100
Equivalent power (KW)			13.5	26.2
Measured power input (KW)			68	
Balance (KW) Accounted for by (a) leakage of hot air (b) external forced convection (c) approximate nature of the analysis			28.3	

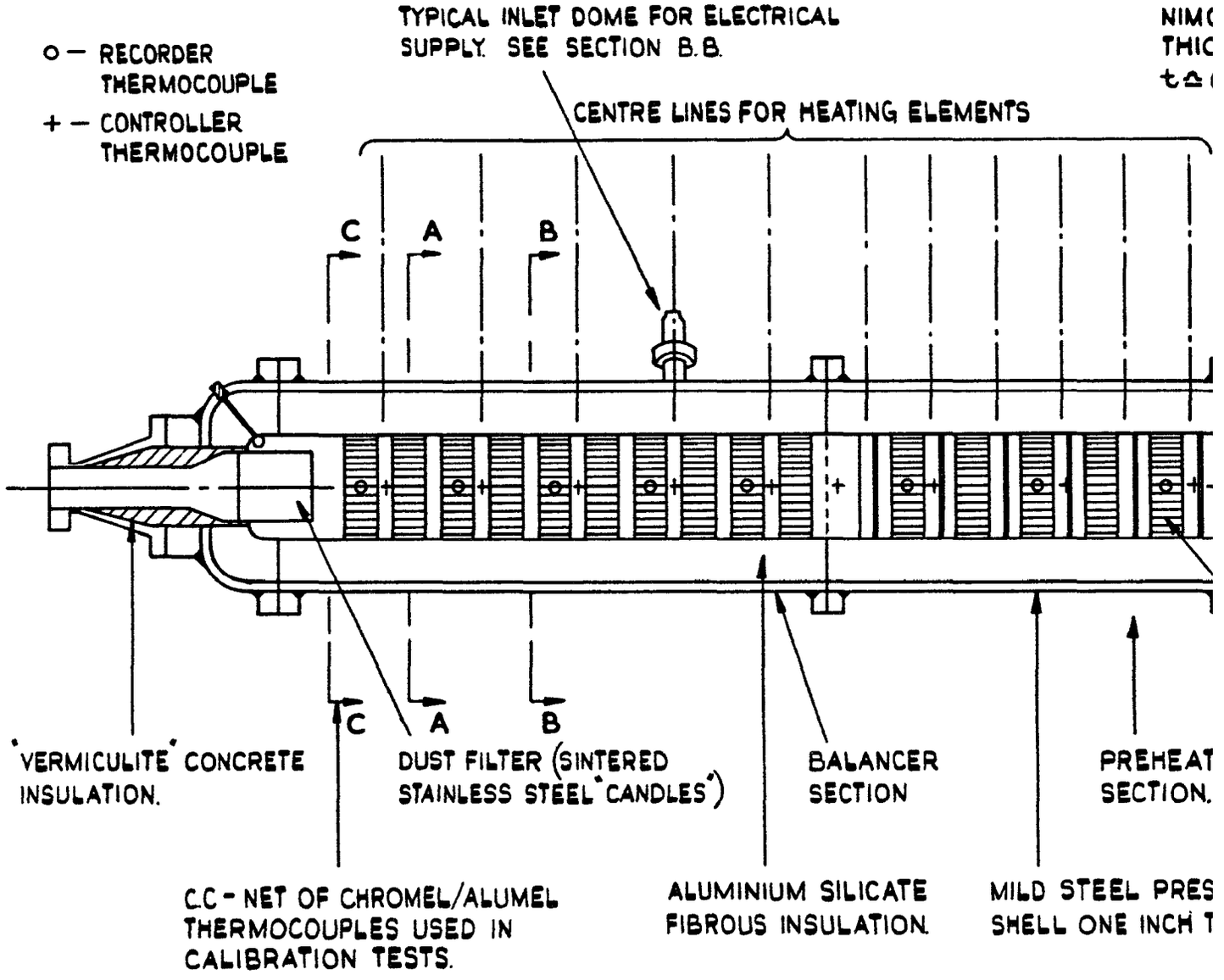

FIG. 1 SKETCH OF AIR H

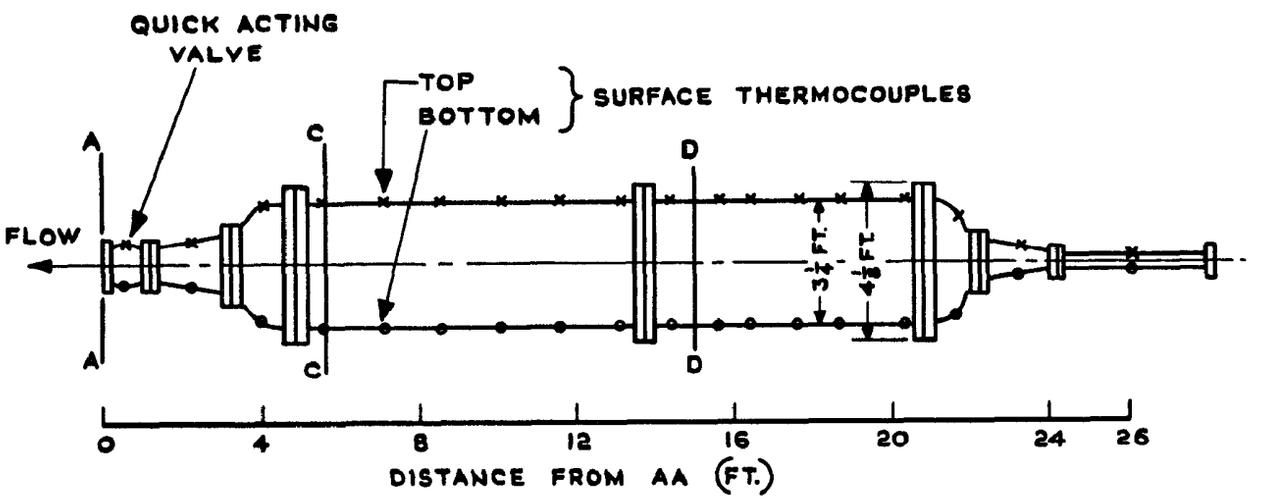

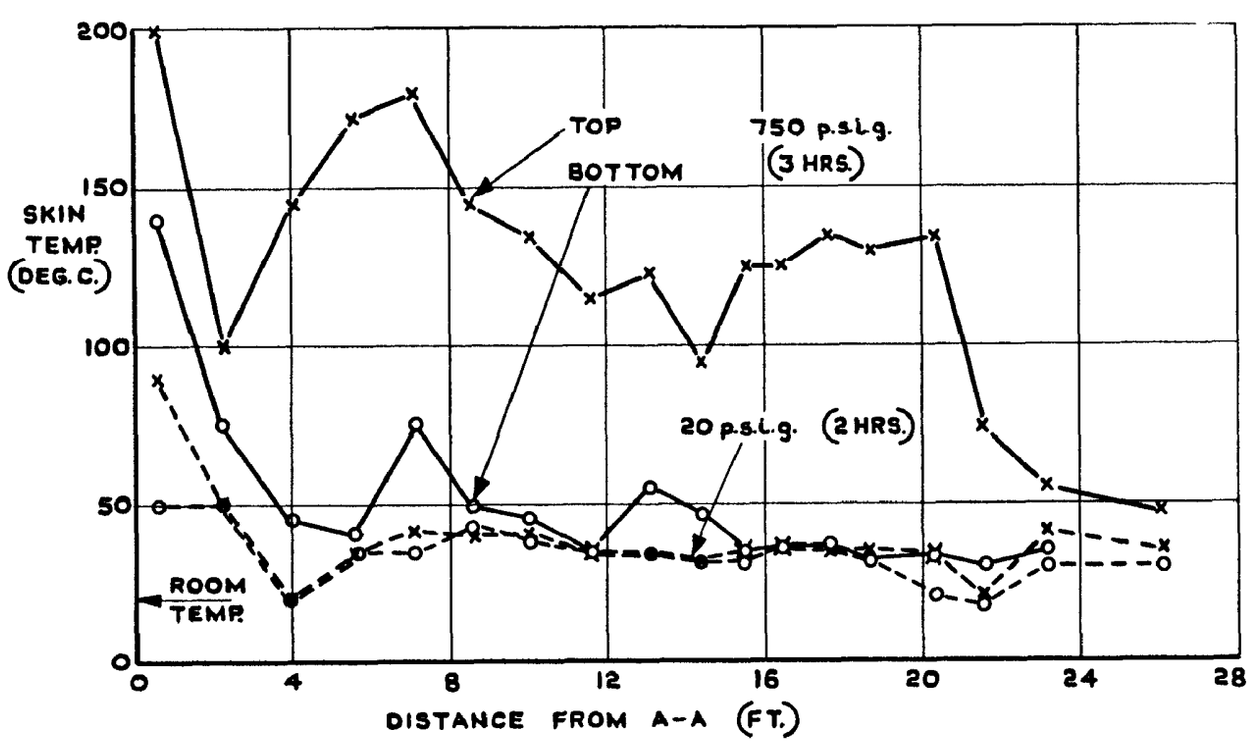

FIG. 2. EQUILIBRIUM SKIN TEMPERATURE DISTRIBUTIONS ON THE TOP AND BOTTOM OF THE HEATER AT HIGH AND LOW AIR PRESSURES.

(FOR CORE TEMPERATURES SEE FIG. 4(a))

(24 SEPT. 1958)

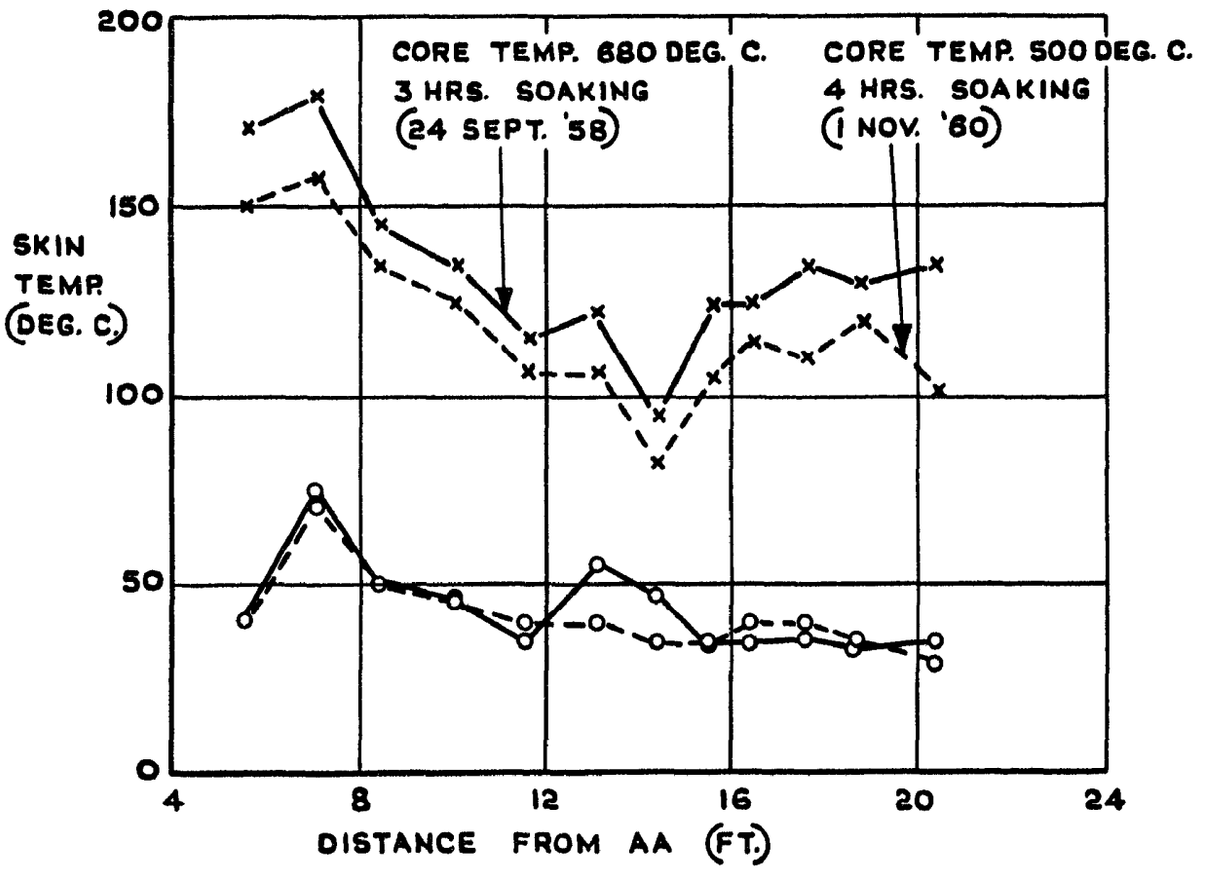

FIG. 3. THE EFFECT OF CORE TEMPERATURE ON EQUILIBRIUM SKIN TEMPERATURES AT HIGH PRESSURE, 750 p.s.i.g.

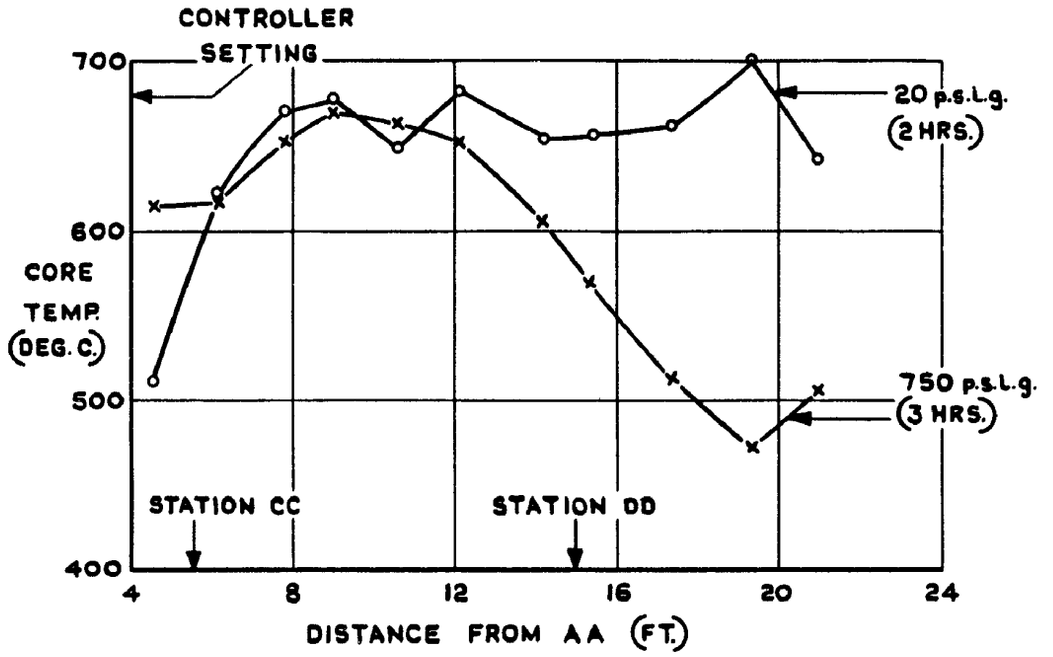

FIG. 4(a). TEMPERATURE DISTRIBUTIONS ON THE CORE CENTRELINE AT HIGH AND LOW PRESSURES.
(24 SEPT. 1958)

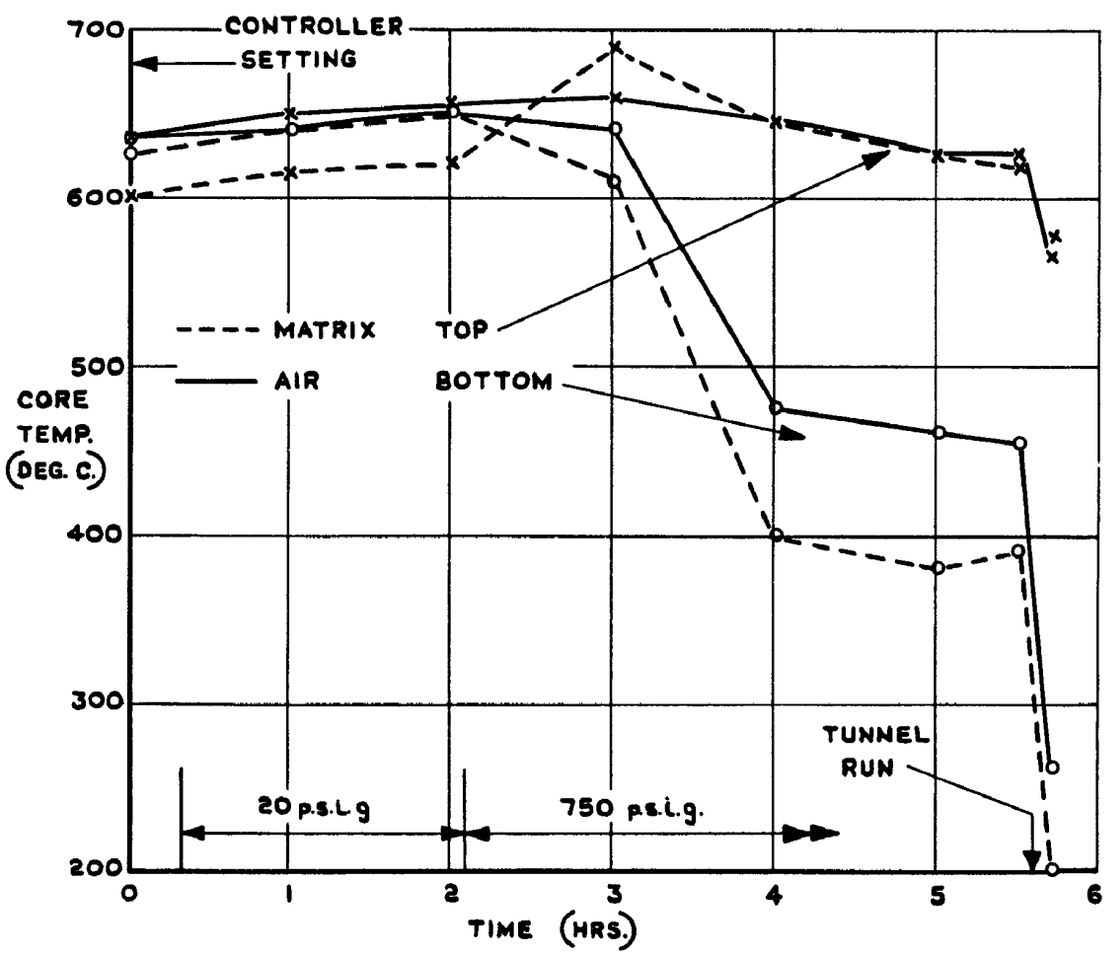

FIG. 4(b). HISTORY OF TEMPERATURES AT THE TOP AND BOTTOM OF THE HEATER CORE AT STATION DD.
(24 SEPT. 1958)

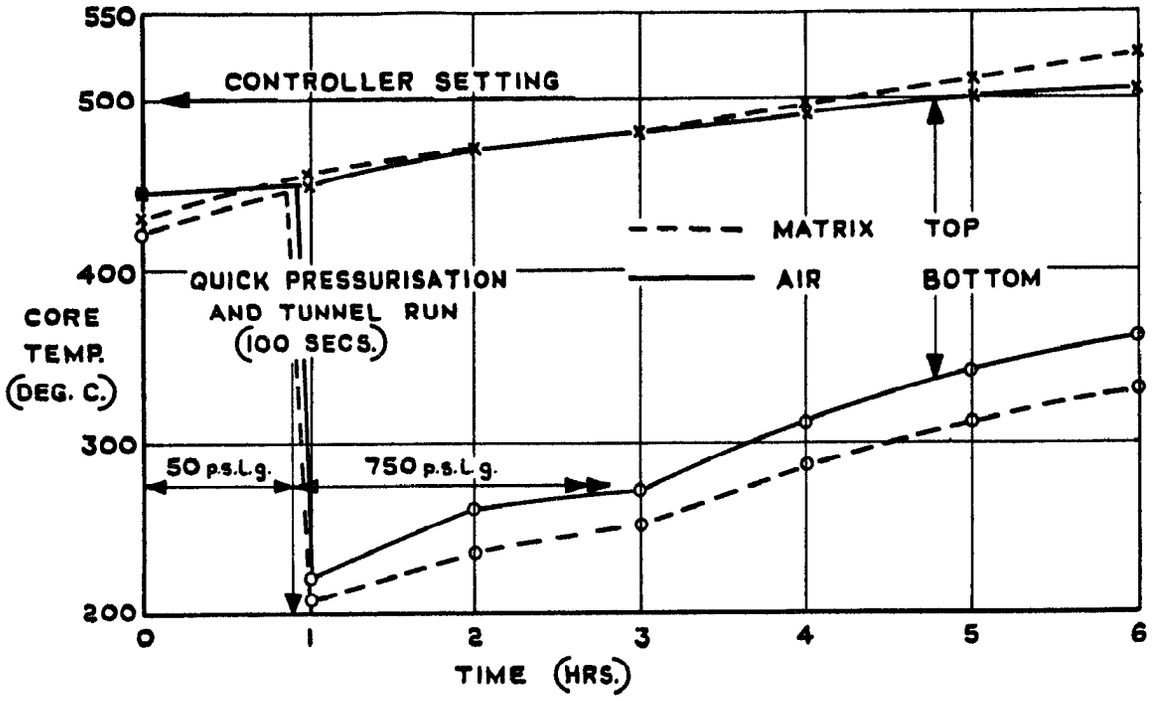

FIG. 5(a). HISTORY OF TEMPERATURES AT TOP AND BOTTOM OF THE HEATER CORE, AT STATION DD, SHOWING LARGE VERTICAL GRADIENTS AFTER A TUNNEL RUN FOLLOWING QUICK PRESSURISATION, AND POOR RECOVERY AT HIGH PRESSURE.
(5 MAY 1959)

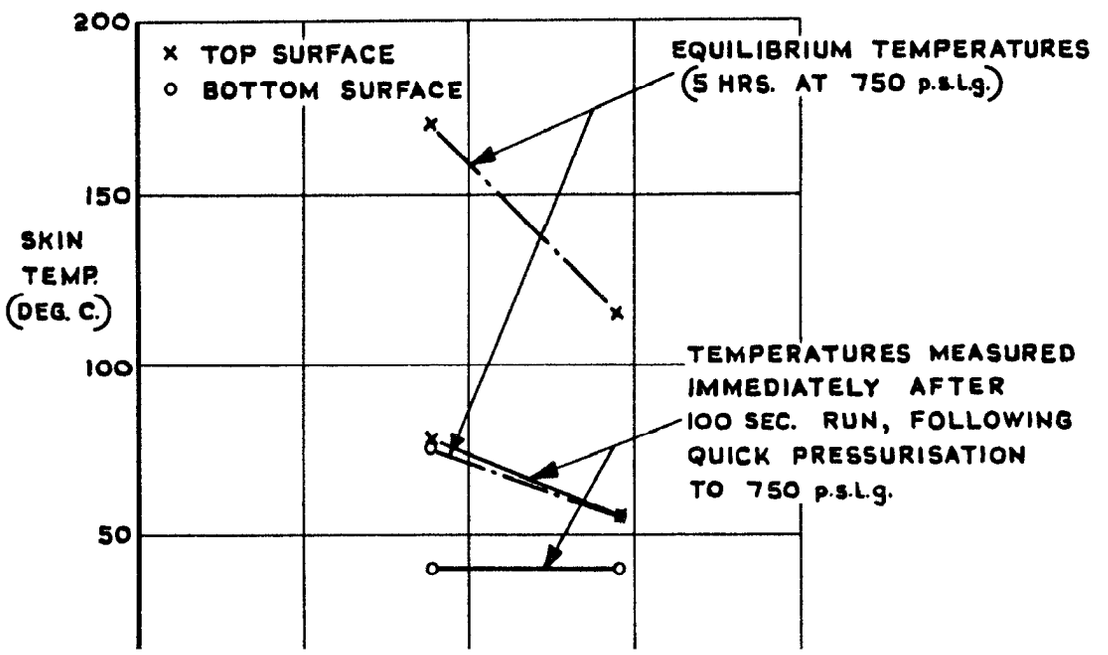

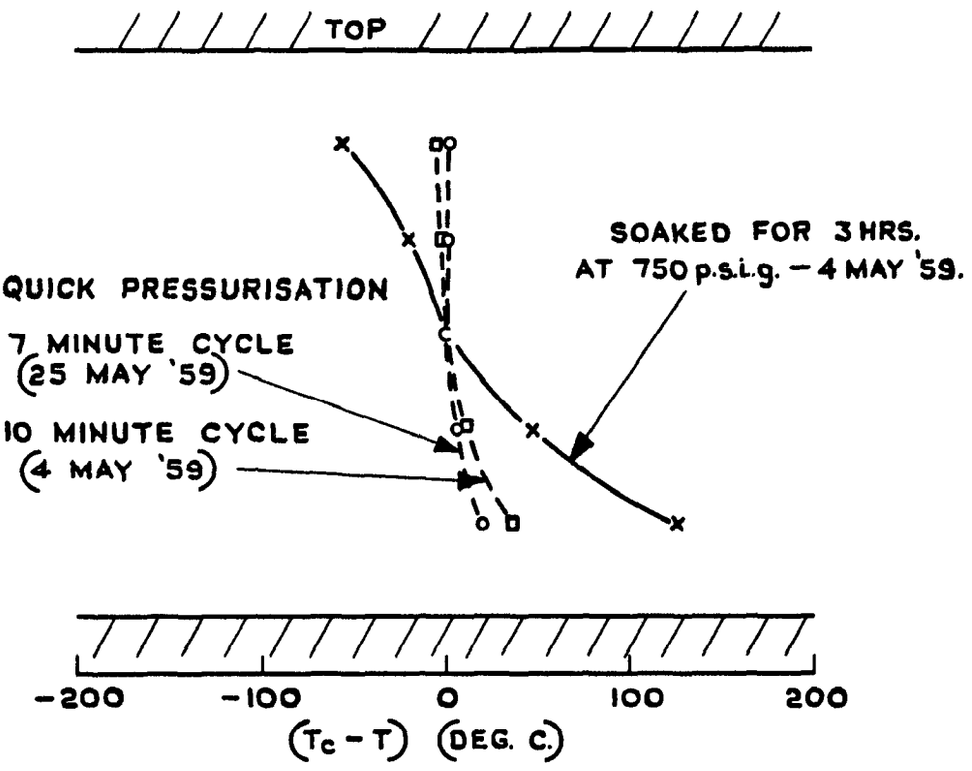

(a) VERTICAL CENTRELINE

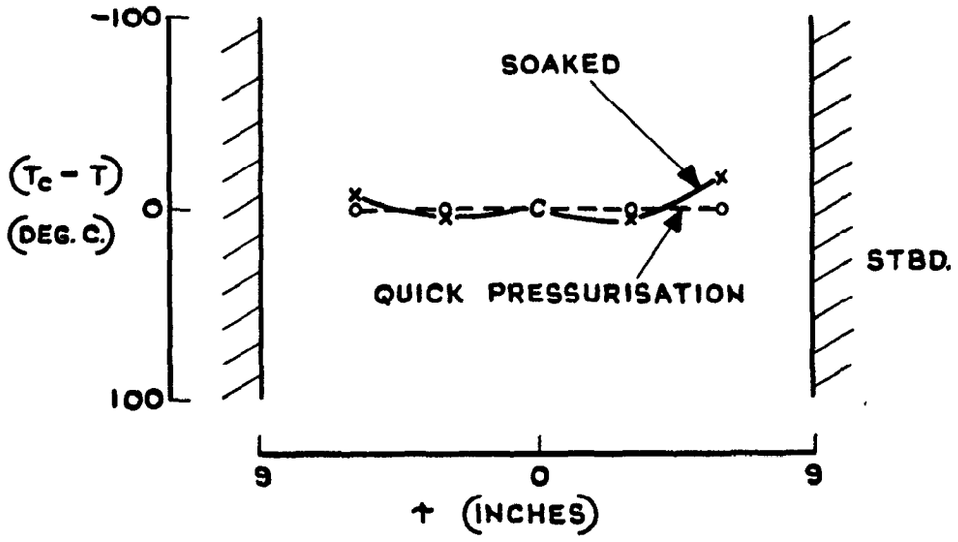

(b) HORIZONTAL CENTRELINE

FIG. 6. HEATER OUTLET TEMPERATURES.

(STATION CC) (T_c = 450 TO 500 DEG. C., TIME 40 SECS.)

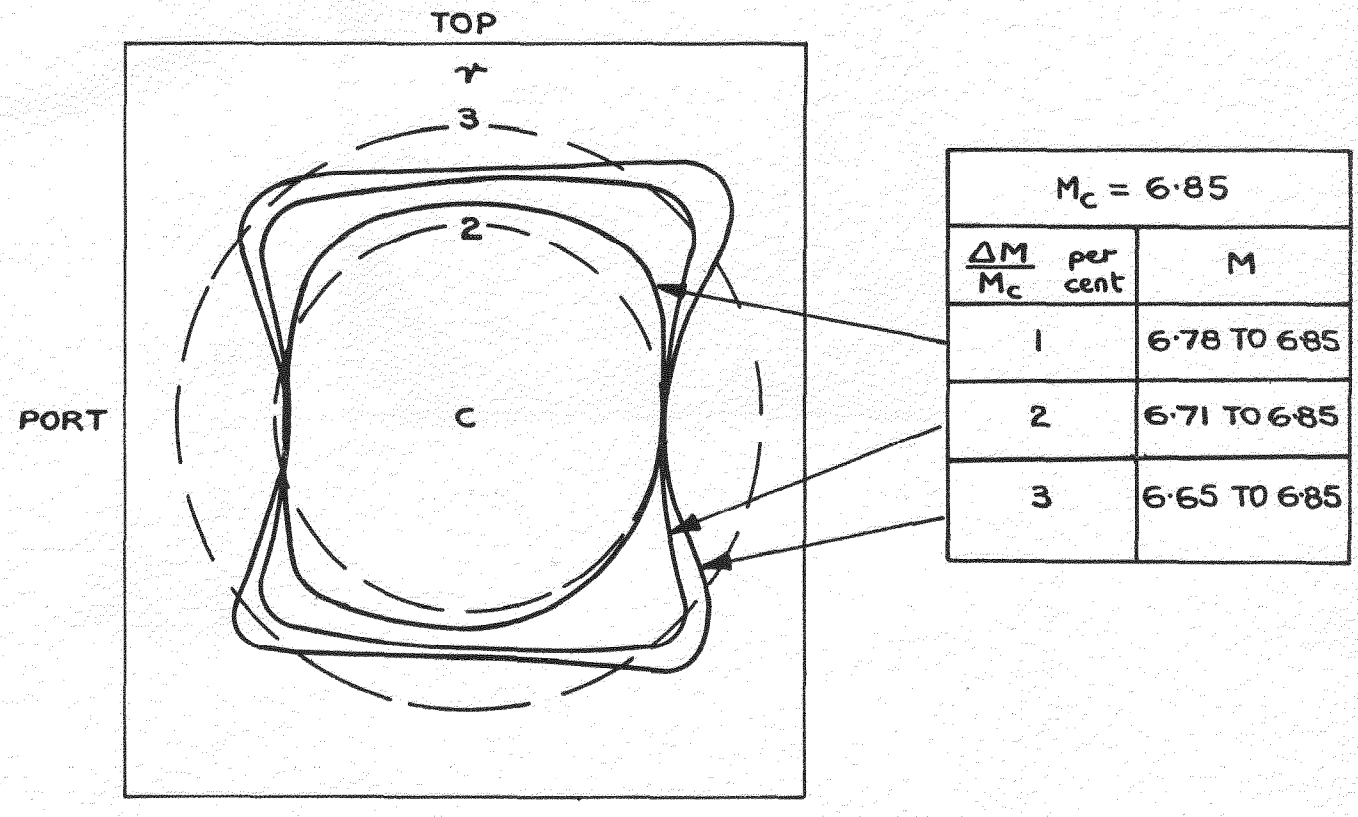

(c) STATION X=16. AT 10 TO 15 SECONDS

FIG. 6. CROSS SECTIONS OF MACH NUMBER

DISTURBANCES FROM JOINTS AT X = 22 AND 24·75

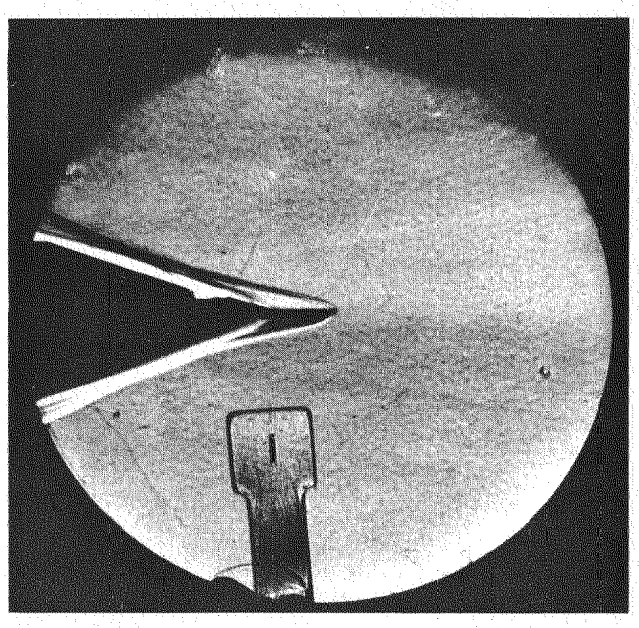

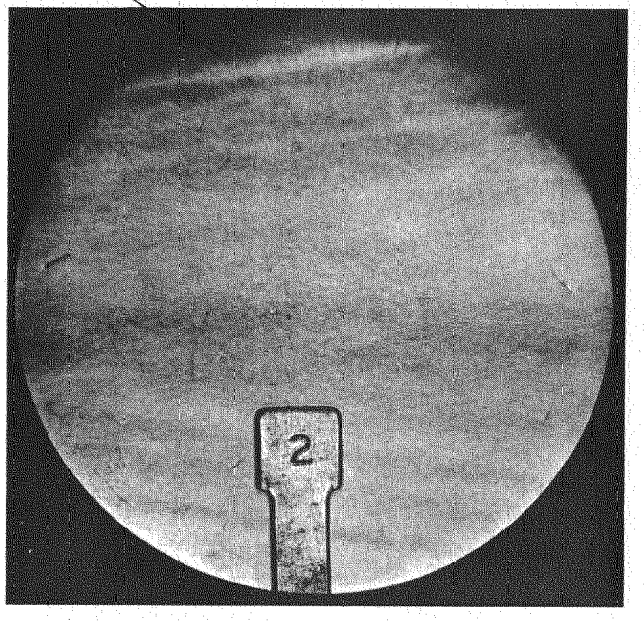

DENSITY GRADIENT ABOUT THE HORIZONTAL CENTRE LINE DUE TO HEATING UP OF WINDOWS OVER A LONG RUN

FIG.7. SCHLIEREN PICTURES OF FLOW IN THE WORKING SECTION

($M = 6.8$, $T_o \simeq 400$ deg C, $p_o = 50$ atmos.)

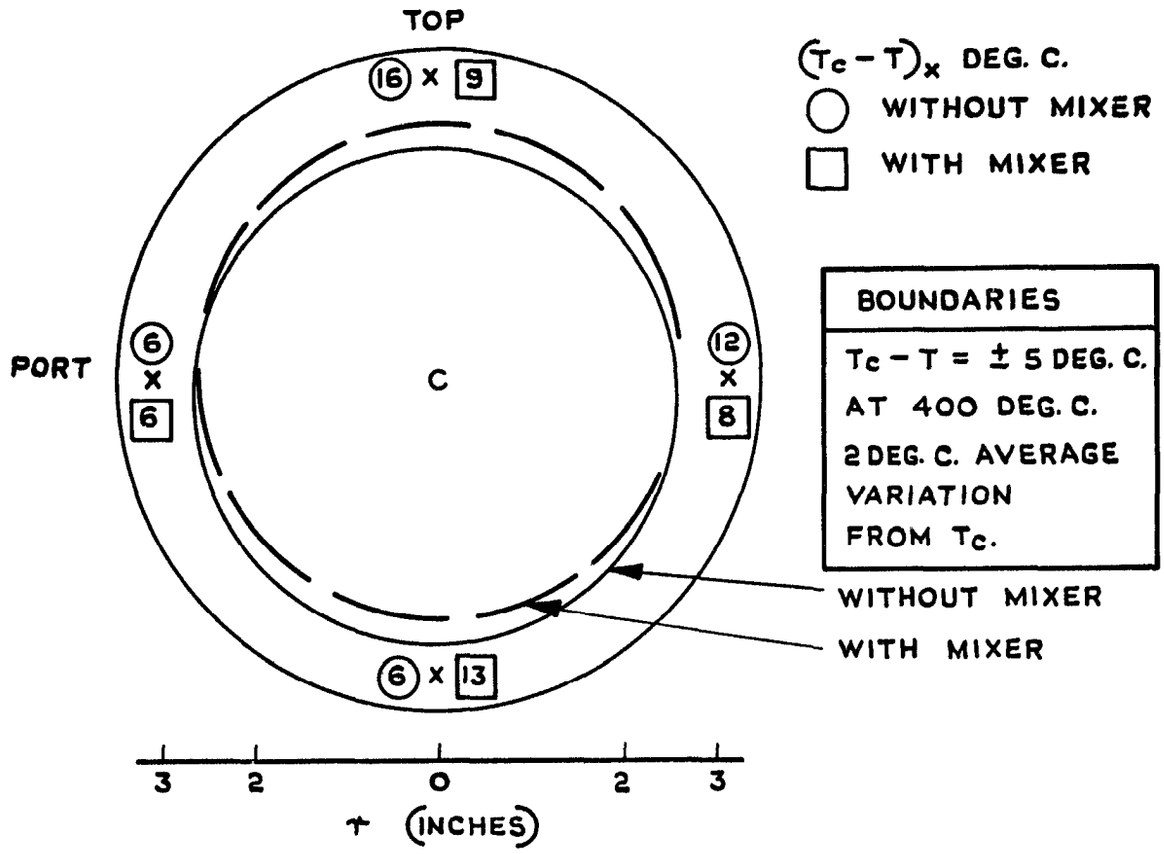

FIG. 7. TEMPERATURE DISTRIBUTIONS IN THE SETTLING CHAMBER (TIME 40 SECS.)

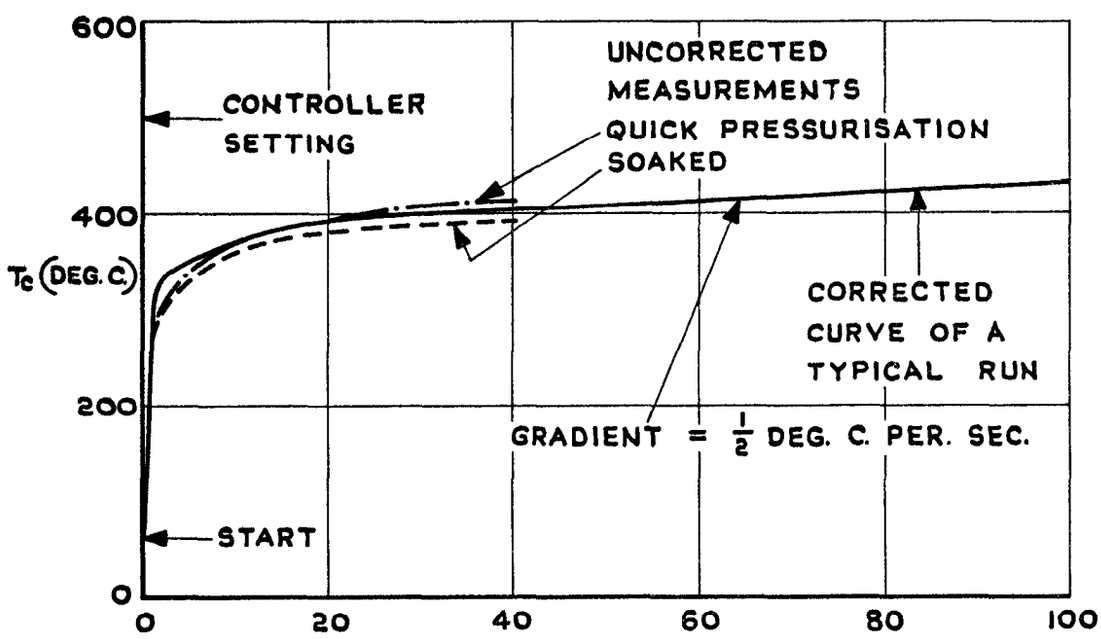

THE 7 IN. × 7 IN. HYPERSONIC WIND TUNNEL AT R.A.E., FARNBOROUGH

PART III - CALIBRATION OF THE FLOW IN THE WORKING SECTION

by

J. F. W. Crane

Previously issued as R.A.E. Tech.Note No. Aero 2718 - A.R.C. 23,436

LIST OF CONTENTS

LIST OF CONTENTS (CONTD.)

1 INTRODUCTION

This note describes the calibration of the flow in the working section of the R.A.E. 7 in. × 7 in. hypersonic wind tunnel.

A unique feature of this tunnel is the fused silica two-dimensional nozzle[1] for M = 7. This material was chosen because it has a very small co-efficient of thermal expansion. Thus the thermal distortion of the nozzle throat section due to the high heating rate in this region is quite small, and produces a negligible change of Mach number in the working section during a run. This is shown in the calibration results described.

Unfortunately, the first nozzle made of this material was damaged in fitting and one of the profiled liners had to be replaced. Whilst the repair of the silica nozzle was proceeding some calibration work was performed with a steel nozzle of simple wedge shape. The flow produced by this nozzle was quite adequate and the calibration of the Mach number along the centreline is given herein.

A large number of runs were made with the repaired nozzle, designated 1st fused silica nozzle, before failure of the remaining original profiled block by the loss of a chip from the throat region.

After replacement of the chipped block, the nozzle, designated 2nd fused silica nozzle, was then installed and has been in use continuously since September, 1959. Calibration shows that the Mach number of the flow produced by this nozzle is around 6.8, with the highest value at the tunnel centreline. In a working core $4\frac{1}{2}$ in. high by $3\frac{3}{4}$ in. wide there is a Mach number decrement of 2 per cent from the centreline to the boundary. There is very little variation in Mach number with time or along a streamline in the working core.

Temperature measurements show that the working core has a very uniform temperature distribution but there is an increase in stagnation temperature with time. This latter is explained by the loss of heat to the outlet attachments of the heater[2].

2 DESCRIPTION OF THE WORKING SECTION AND CALIBRATION NOTATION

Some details of the working section which are relevant to the argument of this note are given in Fig.1. The fused silica nozzle is two-dimensional and has a simple boundary layer correction applied only to the profiled liners; the ordinates are given in Table 1. The width of the working section is thus a constant 7 in. but the height varies from 7.66 in. at the nozzle exit to 8.12 in. at the calibration datum plane.

There is a steel transition section which protects the fragile end of the fused silica nozzle, and a small gap separates it from the steel working section to accommodate movement due to differential thermal expansion. For the tests on the 1st fused silica nozzle this gap was 0.1 in. and disturbances from it and from the silica joint can be seen in Fig.7. Reduction of the gap to 0.05 in. for the tests on the 2nd fused silica nozzle produced no noticeable weakening of this disturbance.

For reference purposes, the datum plane was taken to be normal to the airflow and 57.75 in. downstream from the throat (24.75 in. downstream from

3 PITOT PRESSURE CALIBRATION

3.1 Description of test apparatus and testing technique

Two pitot rakes shown in Fig.2 were used to calibrate the flow in the working section. (No effect of their different ratios of tube and orifice diameters was measured.) They were mounted on a sting which could be traversed in the stream direction, and a range X = 0 to X = 20 was covered.

Pressures were fed to a 7 tube mercury manometer, one tube of which was referred to a Midwood absolute manometer. A clamping device was used to isolate the manometers towards the end of a run and readings were made between runs. The interval between runs was made sufficiently long to allow the probe and support to cool and thus avoid overheating the rubber connectors in the traverse gear.

For a fixed angle of roll, θ, measurements of pitot pressure, p_o', were made at one in. intervals in X.

The stagnation pressure, p_o, was measured at the settling chamber and was approximately 750 p.s.i.g. for the tabulated results. A trace of the stagnation pressure was made for each run and the results showed a high order of control of this pressure, namely, $\pm\frac{1}{2}$ p.s.i., or 0.0006 p_o.

3.2 Results of pitot pressure measurements

3.2.1 Mach number along the centreline

Calibration of the 1st fused silica nozzle was made with the rake of Fig.2a, and covered a 4 in. diameter core from X = 0 to X = 20. The results are given in Table 2. Fig.3a shows a plot of the four traverses of M_c, the Mach number at the centreline of the working section, and shows that the upstream region, from X = 20 to X = 10, had an almost uniform flow with $M_c = 6.96$. Downstream of X = 10 the flow deteriorated and at X = 4 and X = 7 disturbances from the top and bottom walls were encountered. These disturbances originated at the joints on the transition section at the nozzle exit and are shown in the flow picture, Fig.7.

The overall repeatability of the results may be estimated from the standard deviation of the samples, Fig.3b. In the region X > 12 the standard deviation is less than 0.1 per cent of the average Mach number. Further downstream the standard deviation is greater, especially in the region of the disturbances.

Calibration of the 2nd fused silica nozzle, the results of which are given in Table 3, show that this nozzle produces a flow of slightly lower Mach number, $M_c = 6.85$, but the centreline distribution is of similar shape to that of the 1st fused silica nozzle. The reason for this lower level of Mach number has not been determined.

Fig.4 compares the Mach number distributions along the centreline of the two silica nozzles with that of an uncooled steel nozzle of similar Mach number, reported some years ago from the Langley 11 in. tunnel[3]. The plot is made dimensionless by dividing x, the distance from the throat by y^x, the throat height.

The fused silica nozzle has a superior flow quality up to the region of the disturbances from the wall joints. In terms of Mach number gradient per in. however, the steel nozzle compares less unfavourably with the fused silica nozzle.

Fig.4 also shows the distribution for the steel wedge nozzle. The flow produced by this nozzle was reasonably uniform in a plane normal to the flow but, as would be expected from this "source flow" nozzle, a Mach number gradient existed in the stream direction.

3.2.2 Profiles of pitot pressure at station X = 10 (2nd fused silica nozzle)

Fig.5 shows profiles of pitot pressure divided by stagnation pressure at station X = 10 from the results listed in Table 4. The offset rake, Fig.2b, was used in order to obtain measurements of pitot pressure through the boundary layer and, by interpolation, to obtain the limits of the inviscid field.

In the diagonal planes, Fig.5, the boundary layer was not encountered and the inviscid field spanned 7 in.

In the horizontal plane the boundary layer was about $1\frac{1}{2}$ in. thick on the port wall and about $1\frac{3}{4}$ in. thick on the starboard wall, resulting in a width of the inviscid flow equal to about $3\frac{3}{4}$ in. The kink in the boundary layer profile in this plane[3] is probably caused by transverse flow in the boundary layer, towards the horizontal centreline, produced by the transverse pressure gradients in the expansion region of a two-dimensional nozzle, which are particularly large at hypersonic Mach numbers. There was some variation in the boundary layer profile on the starboard wall between short and long runs but elsewhere there was very little variation in the pitot pressure profiles.

In the vertical plane, Fig.5c, the inviscid field was 5 in. across and the profiles through the boundary layer did not exhibit a kink.

3.2.3 Contours of Mach number in the inviscid flow at stations X = 10 and X = 16 (2nd fused silica nozzle)

From the results in Table 4 plots are drawn in Fig.6 of the cross sectional Mach number, showing regions where $\Delta M/M_c$, the Mach number decrement divided by the Mach number at the centre, is equal to 1, 2 and 3 per cent. A more detailed analysis was not attempted because of the effect of experimental error. Note that the standard deviation of the centreline results increases as X decreases, Fig.3, as the disturbances from the top and bottom walls, shown in Fig.7 are encountered. By analogy, the standard deviation, which is quite low at the centre, should increase within increase in r, as the disturbances are encountered.

At station X = 16 the Mach number distribution is slightly superior in degree of uniformity to that at station X = 10. The 1 per cent region is quite large, covering a rectangle 4 in. high by $3\frac{3}{4}$ in. wide. The 2 per cent region covers much of the flow in the corners, and the 3 per cent region accounts for most of the remainder up to the edge of the boundary layer. At this station $M_c = 6.85$ for runs of 10 to 15 seconds duration.

Heating up of the silica nozzle walls over a long run can affect the flow pattern in the working section because of (a) the increase in displacement thickness of the boundary layer and (b) the probable variation in throat height due to thermal expansion of the silica. Accordingly, runs of 10 to 15 seconds and of 60 seconds were made at station X = 10 to measure the variation of Mach number with length of run. There is a very small increase in M_c of $^1/_3$ per cent over 1 minute at this station. This is negligible compared with the transverse and longitudinal variations in Mach number which are themselves quite small. By comparison, an uncooled steel nozzle[3] produces an increase in Mach number of 3 per cent for similar conditions.

3.3 Calibration of the flow at low stagnation pressure

A short series of tests was recently made to determine the range of stagnation pressure for which the foregoing calibration at 750 p.s.i.g. stagnation pressure is applicable. Accordingly pitot pressure measurements were made at low stagnation pressures.

Fig.8a compares the pitot pressure profiles in the vertical and horizontal planes at low stagnation pressures with those at 750 p.s.i.g. There was very little increase in boundary layer thickness but, at stagnation pressures around 100 p.s.i.g., there was an increase in the ratio p_o'/p_o and hence a decrease in Mach number.

Fig.8b shows the variation of p_o'/p_o with p_o and it appears that the flow is unchanged until the stagnation pressure drops to about 200 p.s.i.g. Below this figure the flow deteriorates in quality, for example, at a pressure of 90 p.s.i.g. the Mach number distribution along the tunnel centre-line is very poor compared with that at high pressure, Fig.8c.

4 TOTAL TEMPERATURE CALIBRATION

4.1 Description of temperature probes

4.1.1 Settling chamber probe

A detailed sketch of the settling chamber probe, of which there were four covering the horizontal and vertical centrelines, is given in Fig.9a. Its construction is sufficiently robust to withstand the load produced by the tunnel starting shock, which is quite strong in the settling chamber, and it can operate up to a temperature of about 600°C on the probe body brazed joints. For higher temperatures of the brazed joints a brazing material of higher melting point will be required, for example, a eutectic brazing alloy which has a melting temperature of 778°C.

The thermocouple wires are chromel and alumel and are housed in a stainless steel tube and insulated with aluminium oxide powder. The sensitive junction was formed by nickel plating across the square-cut end of the tube and wires.

For these tests, M = 7 conditions, the time constant of this probe was 0.72 seconds (see Appendix 1).

4.1.2 Working section probe

Fig.9b shows details of the working section probe which was used for calibrating the inviscid flow field and was designed for maximum recovery. This probe should read local stagnation temperature quite accurately since there is no loss of total temperature through a shock wave and the thermo-couple junction is in a low Mach number subsonic stream. (For M < 0.2 the error should be less than 1/3 per cent or 2°C at 400°C, from results collected in Ref.5. This low Mach number condition is obtained at the nose of a blunt body in hypersonic flow in a region from the body surface to about 1/3 the distance to the bow shock.)

The calculated radiation loss is negligible, and the loss due to conduction into the Sindanyo backing will be small since it provides an insulated surface from which the thermocouple junction stands proud.

The time constant for this probe was $\frac{1}{2}$ second. Another probe using chromel/alumel wire of 0.005 in. diameter had a time constant of 0.16 seconds.

4.2 Test methods

Speedomax recording potentiometers were used to record the voltage outputs of the thermocouples during a tunnel run. Cold junction temperatures, at room temperature, were measured with calibrated mercury thermometers. Two main methods of testing were used, as follows.

(a) Switching method

In this method ten thermocouple outputs were fed to a single Speedomax recorder and by means of a very accurate electronic switch each thermocouple was surveyed in turn for 2 seconds every 20 seconds. Thus, for runs of 100 seconds duration five measurements of voltage output and hence temperature, for each thermocouple were obtained at accurately known times. Interpolation of the resultant temperature/time plots was made to obtain the temperature distribution of the thermocouple array at a fixed instant, namely, at 40 seconds from the start.

(b) Continuous monitoring method

In this method each thermocouple output was measured on a single Speedomax recorder and a complete temperature/time curve obtained. This method was used for measurements in the boundary layer where large temperature gradients exist and fluctuations occur.

It was also used to record the fluctuations and differences between two similar thermocouples at the same level of temperature. The outputs were opposed to one another and the resultant difference was measured. A very sensitive Speedomax was used for this job. In Fig.11a a scale sensitivity of 5°C per in. deflection with a resolution of about 0.1°C was used. In Fig.11b a scale sensitivity of about 13°C per in. deflection with a resolution of about 0.25°C was used.

4.3 Results of temperature calibration

4.3.1 Stagnation temperature history

Fig.10 gives typical results for the total temperature histories in the settling chamber and working section. The heater was set at 500°C but the temperatures measured in the settling chamber did not reach this figure because of heat loss[2] to the heater outlet attachments.

The full line shows the temperature measured by the settling chamber probe, T_{sp}, and the dashed line that by the working section probe, T_{wp}. The corrected temperature in the settling chamber, T_{sc}, is denoted by a chain dotted line (derived from Fig.11b, Appendix 1).

From an initially fast rise of 240°C in the first second there follows a rapid reduction in the rate of temperature increase and at 30 seconds the rate of increase is steady at $\frac{1}{2}$°C per second at a level of 400°C. At the end of the run, after 100 seconds, the temperature was 65°C below the heater temperature and still rising at a constant rate.

of the heater. Therefore, for runs of less than about 200 seconds at these conditions, because of heat loss to the walls, there is a cooler thermal boundary layer in the settling chamber, Fig.13a, which is probably mixed with the hotter core in the contraction section of the nozzle resulting in a temperature drop in the main stream in the working section.

To account for this drop the stagnation temperature in the working section for these conditions is given by the following empirical equation, derived in Appendix 1.

$$T_o = T_{sc} - 10 + \frac{t}{20} \ ^oC \ . \qquad (2)$$

It is of interest to note from Fig.11a that with two fast response thermocouples mounted $\frac{1}{2}$ in. apart in the working section the temperature difference, and the fluctuation of this difference, $\pm\frac{1}{8}^oC$ is extremely small after about 2 seconds. On the other hand from Fig.11b with two thermocouples of widely different response times, one being mounted in the settling chamber and the other in the working section, the fluctuation of the temperature difference is much larger, $\pm 1\frac{1}{2}^oC$ at 3 cycles per second. Because of its large time constant the settling chamber probe is relatively insensitive to this frequency of oscillation, therefore, the fluctuation must have been sensed by the fast response working section thermocouple.

4.3.2 Cross sectional temperature distributions

Fig.12 shows profiles in the working section of total temperature difference from temperature at the centre, T_c, for horizontal and vertical planes, at a level of 400^oC and at a time 40 seconds during a tunnel run. The distribution is very good across the inviscid flow. The edge of the thermal boundary layer is denoted by the sharp increase in $(T_c - T)$.

Fig.13 shows complete cross sections of temperature distribution for the working section and the settling chamber. Both have very uniform cores with an average variation from T_c of 2^oC at 400^oC.

Because early calibration measurements, using probes of a different design, indicated the existence of large vertical temperature gradients in the settling chamber, a mixing vane was positioned just upstream of the quick acting valve (the most convenient location) in an attempt to eliminate them. The probes were proved to be faulty, and in fact were severely damaged by the tunnel starting shock, and the present probes were made. Measurements with the present probes, both with and without the mixing vane, show that the vane is not required as sufficient mixing is performed by the quick acting valve. (Temperature measurements at the quick acting valve inlet show that large vertical gradients exist at this point.)

5 CONCLUSIONS

The calibration shows that the two-dimensional fused silica nozzle designed for M = 7 produces a very uniform flow, by present standards for this type of tunnel, in the direction of the stream and with time. The highest Mach number, 6.85, occurs on the centreline and there is a gradual decrease in Mach number towards the boundary layer. For a 2 per cent decrease the cross section is $3\frac{3}{4}$ in. wide by $4\frac{1}{2}$ in. high. It is recommended that model testing be confined to the region of the upstream window where the disturbances from the nozzle exit (section 3.2.3) should not be encountered.

The temperature distribution in the inviscid core is very good; for example, there is an average variation of 2°C at a level of 400°C, but the level increases with time due to heat loss[2] at the heater outlet attachments.

LIST OF SYMBOLS

M = Mach number

p = pressure

p' = pressure behind a normal shock wave

r = radius from centreline (in.)

t = time (seconds)

T = temperature

x = distance downstream from throat (in.)

X = distance upstream from datum plane (in.)

y = nozzle ordinate

y^x = throat height for a two dimensional nozzle

θ = roll angle (measured from starboard horizontal looking upstream)

λ = loss co-efficient $\left(1 - \frac{\text{indicated temperature change}}{\text{true temperature change}}\right)$

Suffixes

c = centreline of stream

o = stagnation conditions

sp = settling chamber probe

wp = working section probe

LIST OF REFERENCES

Ref. No.	Author	Title, etc.
1	Crabtree, L.F. Crane, J.F.W.	The 7 in. × 7 in. hypersonic wind tunnel at R.A.E., Farnborough, Part I. Design, instrumentation and flow visualization techniques. Part I of this Current Paper.
2	Crane, J.F.W.	The 7 in. × 7 in. hypersonic wind tunnel at R.A.E., Farnborough, Part II. Heater performance. Part II of this Current Paper.
3	McLellan, C.H. Williams, T.W. Beckwith, I.E.	Investigation of the flow through a single stage two dimensional nozzle in the Langley 11 in. hypersonic tunnel. N.A.C.A. T.N. No. 2223 December, 1950
4	Schurmeier, H.M.	Design and operation of a continuous flow hypersonic wind tunnel using a two dimensional nozzle. Agardograph 38 May, 1959
5	Scadron, M.D. Warshawsky, I.	Experimental determination of time constants and Nusselt numbers for bare wire thermocouples in high velocity airstreams and analytic approximation of conduction and radiation errors. N.A.C.A. T.N. No. 2599 January, 1952

APPENDIX 1

DESCRIPTION OF THE EVALUATION OF TIME CONSTANTS AND ERROR EQUATIONS FOR THERMOCOUPLE PROBES USED IN THE TUNNEL CALIBRATION

An exhaustive analysis of bare wire thermocouples is given in Ref.5 and with the aid of nomograms supplied the time constants for the thermocouple probes were calculated.

By definition the time constant of a thermocouple is the time taken for it to reach a value $(1 - \frac{1}{e})$ of a step change in temperature of the surrounding medium. To a first approximation the time constant is inversely proportional to the square root of the Reynolds number, hence, with other conditions constant its value will decrease with decrease in temperature or with increase in pressure.

For the working section probe, of which there were two, the subsonic flow conditions at the position of the thermocouple were used to calculate the time constant. Providing that this junction is located at the nose of a blunt body, and within the region from the body surface to 1/3 the distance to the shock wave, the Mach number of the flow around the junction is less than 0.2 and the temperature recovery should be better than 99.6 per cent[5]. The insulated body acts as a radiation shield since it warms up quickly, however, the heat transmitted by radiation is insignificant in comparison with the rate of heat input by forced convection at these conditions. Hence, the assumption of 100 per cent recovery for this probe is reasonable.

In the case of the settling chamber probe an approximate time constant was calculated assuming a wire diameter of 0.04 in. and no heat losses. However, calibration of this probe was made as follows.

Using the technique described in section 4.2(b) the output of a thermocouple junction at the centre of the settling chamber (calculated time constant = 0.72 seconds) was balanced against one of similar wire and faster response (time constant = 0.16 seconds) mounted in the centre of the working section. The voltage generated by the temperature difference between the two junctions was measured on a sensitive Speedomax recorder. The trace of this voltage, shown as a temperature difference in Fig.11b, shows that the settling chamber probe does not measure true temperature until 20 seconds from the start of a run at M = 7 conditions. This is probably due to heat loss from the junction to the cooler probe body. Using this trace the error curve for the settling chamber probe was obtained as follows.

Assuming that (a) the very fast response thermocouple in the working section was raised to the stream temperature in a second or two, and (b) the temperature drop across the throat, shown by the negative value of $T_{wp} - T_{sp}$, varied linearly from t = 2 to t = 20 in the same way as it varied from t = 20 to t = 80, a base line was drawn on the trace, Fig.11b, and the temperature error of the settling chamber probe obtained by differencing from the trace to this base line. From these measurements the error curve for the settling chamber probe at M = 7 conditions is given by the following equation.

Appendix 1

The stagnation temperature in the working section for M = 7 conditions is given by the following equation, which accounts for the temperature drop across the throat.

$$T_o = T_{sc} - 10 + \frac{t}{20} \ ^oC \qquad \ldots (2)$$

where

$$T_{sc} = T_{sp}/(1 - \lambda) \ . \qquad \ldots (3)$$

There is a good agreement, section 4.3.1, between the time calculated for the attainment of heater temperature in the settling chamber by extrapolating the curve of Fig.10, and the time calculated for the elimination of the temperature drop across the throat using the rate of reduction derived from Fig.11b.

TABLE 1

DESIGN CO-ORDINATES OF M = 7 FUSED SILICA NOZZLE
(DIMENSIONS IN IN.)

x	$y/2$	x	$y/2$	x	$y/2$	x	$y/2$	x	$y/2$
-0.75	0.2562	0.14	0.0423	0.88	0.2656	2.10	0.7488	10.00	2.4155
-0.70	0.2275	0.16	0.0447	0.90	0.2741	2.20	0.7827	11	2.5486
-0.65	0.2007	0.18	0.0474	0.92	0.2827	2.30	0.8159	12	2.6717
-0.60	0.1760	0.20	0.0503	0.94	0.2913	2.40	0.8484	13	2.7858
-0.55	0.1532	0.22	0.0535	0.96	0.2999	2.50	0.8803	14	2.8915
-0.50	0.1325	0.24	0.0570	0.98	0.3086	2.60	0.9117	15	2.9894
-0.48	0.1247	0.26	0.0607	1.00	0.3173	2.70	0.9425	16	3.0800
-0.46	0.1173	0.28	0.0647	1.02	0.3260	2.80	0.9728	17	3.1638
-0.44	0.1102	0.30	0.0689	1.04	0.3347	2.90	1.0026	18	3.2412
-0.42	0.1034	0.32	0.0733	1.06	0.3435	3.00	1.0319	19	3.3126
-0.40	0.0969	0.34	0.0779	1.08	0.3523	3.10	1.0607	20	3.3784
-0.38	0.0907	0.36	0.0827	1.10	0.3611	3.20	1.0890	21	3.4387
-0.36	0.0848	0.38	0.0878	1.12	0.3698	3.30	1.1169	22	3.4939
-0.34	0.0793	0.40	0.0931	1.14	0.3785	3.40	1.1445	23	3.5443
-0.32	0.0741	0.42	0.0986	1.16	0.3872	3.50	1.1717	24	3.5901
-0.30	0.0692	0.44	0.1043	1.18	0.3959	3.60	1.1985	25	3.6314
-0.28	0.0646	0.46	0.1102	1.20	0.4046	3.70	1.2249	26	3.6685
-0.26	0.0603	0.48	0.1162	1.22	0.4132	3.80	1.2509	27	3.7018
-0.24	0.0563	0.50	0.1224	1.24	0.4217	3.90	1.2765	28	3.7315
-0.22	0.0527	0.52	0.1287	1.26	0.4302	4.00	1.3018	29	3.7577
-0.20	0.0494	0.54	0.1351	1.28	0.4387	4.25	1.3637	30	3.7805
-0.18	0.0464	0.56	0.1417	1.30	0.4471	4.50	1.4236	31	3.8000
-0.16	0.0437	0.58	0.1485	1.32	0.4555	4.75	1.4818	32	3.8164
-0.14	0.0413	0.60	0.1555	1.34	0.4638	5.00	1.5383	33	3.8300
-0.12	0.0392	0.62	0.1626	1.36	0.4721	5.25	1.5933		
-0.10	0.0374	0.64	0.1698	1.38	0.4803	5.50	1.6467		
-0.08	0.0360	0.66	0.1772	1.40	0.4885	5.75	1.6986		
-0.06	0.0349	0.68	0.1847	1.42	0.4966	6.00	1.7492		
-0.04	0.0341	0.70	0.1923	1.44	0.5047	6.25	1.7985		
-0.02	0.0337	0.72	0.2001	1.46	0.5127	6.50	1.8466		
0	0.0336	0.74	0.2080	1.48	0.5207	6.75	1.8936		
0.02	0.0339	0.76	0.2160	1.50	0.5286	7.00	1.9395		
0.04	0.0345	0.78	0.2241	1.60	0.5676	7.50	2.0282		
0.06	0.0354	0.80	0.2323	1.70	0.6056	8.00	2.1129		
0.08	0.0367	0.82	0.2405	1.80	0.6426	8.50	2.1937		
0.10	0.0383	0.84	0.2488	1.90	0.6788	9.00	2.2709		
0.12	0.0402	0.86	0.2572	2.00	0.7142	9.50	2.3448		

TABLE 2 - SHEET 1

1ST FUSED SILICA NOZZLE PITOT PRESSURE AND MACH NUMBER DISTRIBUTIONS (AT 10 TO 15 SECONDS)

$(p_o'/p_o) \times 10$						M				
θ	180			0		180		0		
r	2	1	0	1	2	2	1	0	1	2
X										
0	0.0747	0.1686	0.1868	0.1825	0.0944	-	6.85	6.69	6.73	-
1	0.0737	0.1772	0.1889	0.1860	0.1028	-	6.77	6.67	6.70	-
2	0.0744	0.1834	0.1959	0.1877	0.1113	-	6.72	6.62	6.68	-
3	0.0766	0.1804	0.1958	0.1862	0.1156	-	6.74	6.62	6.70	-
4	0.0750	0.1673	0.1691	0.1680	0.1106	-	6.86	6.85	6.86	-
5	0.0830	0.1564	0.1469	0.1606	0.1327	-	6.97	7.07	6.93	-
6	0.0869	0.1587	0.1458	0.1612	0.1393	-	6.95	7.08	6.92	-
7	0.0907	0.1568	0.1451	0.1615	0.1403	-	6.97	7.09	6.92	-
8	0.0948	0.1589	0.1498	0.1644	0.1457	-	6.95	7.04	6.89	-
9	0.0993	0.1611	0.1560	0.1610	0.1564	-	6.92	6.97	6.92	-
10	0.1065	0.1592	0.1596	0.1581	0.1617	-	6.94	6.94	6.95	-
10	0.1054	0.1654	0.1590	0.1579	0.1604	-	6.88	6.94	6.96	-
11	0.1125	0.1538	0.1544	0.1538	0.1580	-	6.99	6.99	7.00	-
12	0.1207	0.1560	0.1567	0.1590	0.1661	-	6.97	6.97	6.95	6.88
13	0.1266	0.1553	0.1583	0.1544	0.1665	-	6.98	6.95	6.99	6.87
14	0.1306	0.1533	0.1562	0.1512	0.1682	-	7.00	6.97	7.02	6.86
15	0.1335	0.1560	0.1581	0.1535	0.1665	-	6.97	6.95	7.00	6.87
16	0.1350	0.1562	0.1580	0.1542	0.1584	-	6.97	6.95	6.99	-
17	0.1310	0.1589	0.1599	0.1578	0.1583	-	6.95	6.94	6.96	-
18	0.1305	0.1609	0.1594	0.1575	0.1546	-	6.93	6.94	6.96	-
19	0.1400	0.1582	0.1567	0.1564	0.1528	-	6.95	6.97	6.97	-
20	0.1452	0.1578	0.1553	0.1581	0.1542	-	6.96	6.98	6.95	-

TABLE 2 - SHEET 2

$(p_o'/p_o) \times 10$						M				
θ	225			45		225			45	
r	2	1	0	1	2	2	1	0	1	2
X										
0	0.1690	0.1616	0.1825	0.1660	0.1716	6.85	6.92	6.73	6.88	6.82
1	0.1677	0.1613	0.1883	0.1708	0.1726	6.86	6.92	6.68	6.83	6.81
2	0.1648	0.1614	0.1945	0.1759	0.1696	6.89	6.92	6.63	6.78	6.84
3	0.1642	0.1618	0.1972	0.1772	0.1742	6.85	6.90	6.61	6.77	6.80
4	0.1633	0.1653	0.1646	0.1780	0.1762	6.90	6.88	6.89	6.77	6.78
5										
6	0.1688	0.1678	0.1454	0.1795	0.1813	6.85	6.86	7.09	6.75	6.74
7	0.1701	0.1642	0.1446	0.1738	0.1885	6.84	6.89	7.10	6.80	6.68
8	0.1682	0.1590	0.1469	0.1638	0.1977	6.85	6.94	7.07	6.90	6.60
9	0.1648	0.1559	0.1527	0.1529	0.1676	6.89	6.98	7.01	7.01	6.86
10	0.1609	0.1533	0.1581	0.1535	0.1690	6.93	7.00	6.95	7.00	6.85
10	0.1631	0.1529	0.1579	0.1533	0.1692	6.90	7.01	6.96	7.00	6.85
11	0.1728	0.1522	0.1559	0.1514	0.1718	6.81	7.01	6.98	7.02	6.82
12	0.1607	0.1518	0.1568	0.1512	0.1680	6.93	7.02	6.97	7.02	6.86
13	0.1604	0.1533	0.1576	0.1615	0.1615	6.93	7.00	6.96	6.92	6.92
14	0.1578	0.1566	0.1566	0.1575	0.1602	6.96	6.97	6.97	6.96	6.93
15	0.1577	0.1567	0.1574	0.1566	0.1557	6.96	6.97	6.96	6.97	6.98
16	0.1597	0.1573	0.1565	0.1576	0.1580	6.94	6.96	6.97	6.96	6.95
17	0.1601	0.1598	0.1581	0.1591	0.1582	6.93	6.94	6.95	6.94	6.95
18	0.1639	0.1605	0.1587	0.1598	0.1576	6.90	6.93	6.95	6.94	6.96
19	0.1640	0.1595	0.1568	0.1582	0.1609	6.89	6.94	6.97	6.95	6.93

TABLE 2 - SHEET 3

$(p_o'/p_o) \times 10$						M				
θ	270			90		270			90	
r	2	1	0	1	2	2	1	0	1	2
X										
0	0.1549	0.1727	0.1843	0.1779	0.1641	6.99	6.81	6.71	6.77	6.89
1										
2										
3										
4										
5	0.1621	0.1612	0.1471	0.1653	0.1678	6.91	6.92	7.07	6.88	6.86
6										
7	0.1662	0.1637	0.1473	0.1679	0.1716	6.87	6.90	7.07	6.86	6.82
8	0.1679	0.1645	0.1520	0.1704	0.1733	6.86	6.89	7.02	6.83	6.81
9	0.1665	0.1654	0.1589	0.1690	0.1731	6.87	6.88	6.95	6.85	6.81
10										
10	0.1665	0.1598	0.1589	0.1610	0.1726	6.87	6.94	6.95	6.92	6.81
11	0.1672	0.1572	0.1566	0.1570	0.1735	6.86	6.96	6.97	6.96	6.81
12	0.1657	0.1544	0.1571	0.1556	0.1718	6.88	6.99	6.96	6.98	6.82
13	0.1685	0.1544	0.1586	0.1549	0.1731	6.85	6.99	6.95	6.99	6.81
14	0.1690	0.1539	0.1567	0.1532	0.1756	6.85	7.00	6.97	7.00	6.79
15	0.1710	0.1554	0.1579	0.1558	0.1778	6.83	6.98	6.96	6.98	6.77
16	0.1648	0.1583	0.1574	0.1581	0.1780	6.89	6.95	6.96	6.95	6.76
17	0.1614	0.1599	0.1590	0.1609	0.1706	6.92	6.94	6.94	6.93	6.83
18	0.1588	0.1587	0.1585	0.1610	0.1644	6.95	6.95	6.95	6.93	6.89
19	0.1619	0.1596	0.1563	0.1622	0.1630	6.92	6.94	6.97	6.91	6.90
20	0.1645	0.1605	0.1558	0.1633	0.1638	6.89	6.93	6.98	6.90	6.90

TABLE 2 - SHEET 4

$(p_o'/p_o) \times 10$						M				
θ	135			315		135			315	
r	2	1	0	1	2	2	1	0	1	2
X										
0	0.1733	0.1709	0.1843	0.1608	0.1746	6.81	6.83	6.71	6.93	6.80
1	0.1731	0.1680	0.1919	0.1671	0.1666	6.81	6.86	6.65	6.87	6.87
2	0.1694	0.1691	0.1945	0.1665	0.1680	6.84	6.85	6.63	6.87	6.86
3	0.1689	0.1683	0.1956	0.1680	0.1713	6.85	6.85	6.62	6.86	6.83
4	0.1704	0.1694	0.1521	0.1731	0.1701	6.83	6.84	7.01	6.81	6.84
5										
6	0.1768	0.1739	0.1460	0.1719	0.1734	6.78	6.80	7.08	6.82	6.81
7	0.1763	0.1698	0.1452	0.1672	0.1765	6.78	6.84	7.09	6.86	6.78
8										
9	0.1712	0.1539	0.1553	0.1541	0.1604	6.83	7.00	6.98	6.99	6.93
10										
10	0.1721	0.1532	0.1583	0.1537	0.1649	6.82	7.00	6.95	7.00	6.89
11	0.1665	0.1528	0.1590	0.1521	0.1659	6.87	7.01	6.94	7.02	6.88
12	0.1627	0.1550	0.1585	0.1513	0.1698	6.91	6.99	6.95	7.02	6.84
13	0.1610	0.1577	0.1593	0.1537	0.1649	6.92	6.96	6.94	7.00	6.89
14	0.1566	0.1585	0.1585	0.1546	0.1615	6.97	6.95	6.95	6.99	6.92
15	0.1567	0.1576	0.1576	0.1568	0.1585	6.97	6.96	6.96	6.97	6.95
16	0.1569	0.1577	0.1573	0.1583	0.1604	6.97	6.96	6.96	6.95	6.93
17	0.1592	0.1592	0.1582	0.1581	0.1611	6.94	6.94	6.95	6.95	6.92
18	0.1624	0.1601	0.1582	0.1596	0.1613	6.91	6.93	6.95	6.94	6.92
19	0.1621	0.1612	0.1569	0.1596	0.1657	6.91	6.92	6.97	6.94	6.88
20	0.1605	0.1591	0.1564	0.1612	0.1635	6.93	6.94	6.97	6.92	6.90

TABLE 3

2ND FUSED SILICA NOZZLE PITOT PRESSURE AND MACH NUMBER DISTRIBUTIONS (AT 10 TO 15 SECONDS)

	$(p_o'/p_o) \times 10$					M				
θ	180		0			180		0		
r	2	1	0	1	2	2	1	0	1	2
X										
1.0	0.1200	0.2003	0.1978	0.1966	0.1063	-	6.58	6.60	6.61	-
3.3	0.1347	0.1964	0.1892	0.2005	0.1138	-	6.61	6.67	6.58	-
5.6	0.1505	0.1652	0.1563	0.1634	0.1317	-	6.88	6.97	6.90	-
7.9	0.1557	0.1674	0.1567	0.1657	0.1365	-	6.86	6.96	6.88	-
9.0	0.1612	0.1654	0.1620	0.1669	0.1351	-	6.88	6.91	6.87	-
10.3	0.1728	0.1635	0.1665	0.1690	0.1539	6.81	6.90	6.87	6.85	-
10.9	0.1713	0.1640	0.1650	0.1669	0.1454	6.83	6.89	6.89	6.87	-
13.1	0.1750	0.1674	0.1697	0.1674	0.1615	6.79	6.86	6.84	6.86	-
15.3	0.1581	0.1681	0.1692	0.1681	0.1652	-	6.86	6.85	6.86	6.88
17.7	0.1680	0.1705	0.1719	0.1713	0.1739	6.86	6.83	6.82	6.83	6.80
19.9	0.1694	0.1701	0.1676	0.1711	0.1723	6.85	6.84	6.86	6.83	6.82

TABLE 4 - SHEET 1

2ND FUSED SILICA NOZZLE CROSS SECTIONAL PITOT PRESSURE AND MACH NUM
(STATION X = 10)

	$(p_o'/p_o) \times 10$							
r	0	1.5	2	2.5	3	3.5	0	1.5
θ								
0	0.1687	0.1708	0.1266	0.1076	0.0525	0.0196	6.85	6.83
45	0.1680	0.1696	0.1719	0.1750	0.1856	0.1931	6.86	6.84
90	0.1665	0.1757	0.1797	0.1825	0.1498	0.0808	6.87	6.79
135	0.1663	0.1738	0.1741	0.1784	0.1877	0.1926	6.87	6.80
180	0.1660	0.1766	0.1718	0.0537	0.0293	0.0137	6.88	6.78
225	0.1681	0.1782	0.1798	0.1749	0.1768	0.1906	6.86	6.76
270	0.1662	0.1829	0.1776	0.1805	0.1441	0.0790	6.87	6.72
315	0.1670	0.1699	0.1769	0.1744	0.1756	0.1856	6.87	6.84

(AT 10 TO 15 SECONDS)

TABLE 4 - SHEET 2

(STATION X = 10)

	$(p_o'/p_o) \times 10$						M					
r	0	1.5	2	2.5	3	3.5	0	1.5	2	2.5	3	3.5
θ												
0	0.1636	0.1664	0.0997	0.0673	0.0675	0.0212	6.90	6.87	-	-	-	-
45	0.1650	0.1697	0.1695	0.1743	0.1823	0.1897	6.89	6.84	6.84	6.80	6.73	6.67
90	0.1656	0.1769	0.1821	0.1806	0.1498	0.0830	6.88	6.78	6.73	6.74	-	-
135	0.1651	0.1798	0.1738	0.1905	0.1918	0.1886	6.88	6.75	6.80	6.66	6.65	6.68
180	0.1656	0.1781	0.1683	0.0512	0.0337	0.0147	6.88	6.76	6.85	-	-	-
250	0.1641	0.1755	0.1748	0.1738	0.1840	0.1862	6.89	6.79	6.79	6.80	6.71	6.70
270	0.1640	0.1783	0.1783	0.1778	0.1438	0.0809	6.89	6.76	6.76	6.77	-	-
315	0.1653	0.1714	0.1745	0.1740	0.1747	0.1858	6.88	6.83	6.80	6.80	6.79	6.70

(AT 60 SECONDS)

WT.2078.C.P.590.K3 - Printed in England

TABLE 4 - SHEET 3

(STATION X = 16)

$(p_o'/p_o) \times 10$							M					
r	0	1	1.5	2.5	3	3.5	0	1	1.5	2.5	3	3.5
θ												
0	0.1684	0.1669	0.1669	0.0806	0.0422	0.0238	6.85	6.87	6.87	-	-	-
45	0.1682	0.1685	0.1703	0.1784	0.1837	0.1892	6.85	6.85	6.84	6.76	6.72	6.67
90	0.1689	0.1712	0.1692	0.1876	0.1591	0.0812	6.85	6.83	6.84	6.68	-	-
135	0.1695	0.1711	0.1718	0.1800	0.1890	0.1617	6.84	6.83	6.82	6.75	6.67	-
180	0.1682	0.1675	0.1649	0.0852	0.0293	0.0155	6.85	6.86	6.89	-	-	-
225	0.1687	0.1695	0.1704	0.1791	0.1871	0.1759	6.85	6.84	6.84	6.76	6.69	6.79
270	0.1689	0.1707	0.1697	0.1932	0.1512	0.0740	6.85	6.83	6.84	6.64	-	-
315	0.1685	0.1698	0.1726	0.1790	0.1809	0.1993	6.85	6.84	6.81	6.76	6.74	6.59

(AT 10 TO 15 SECONDS)

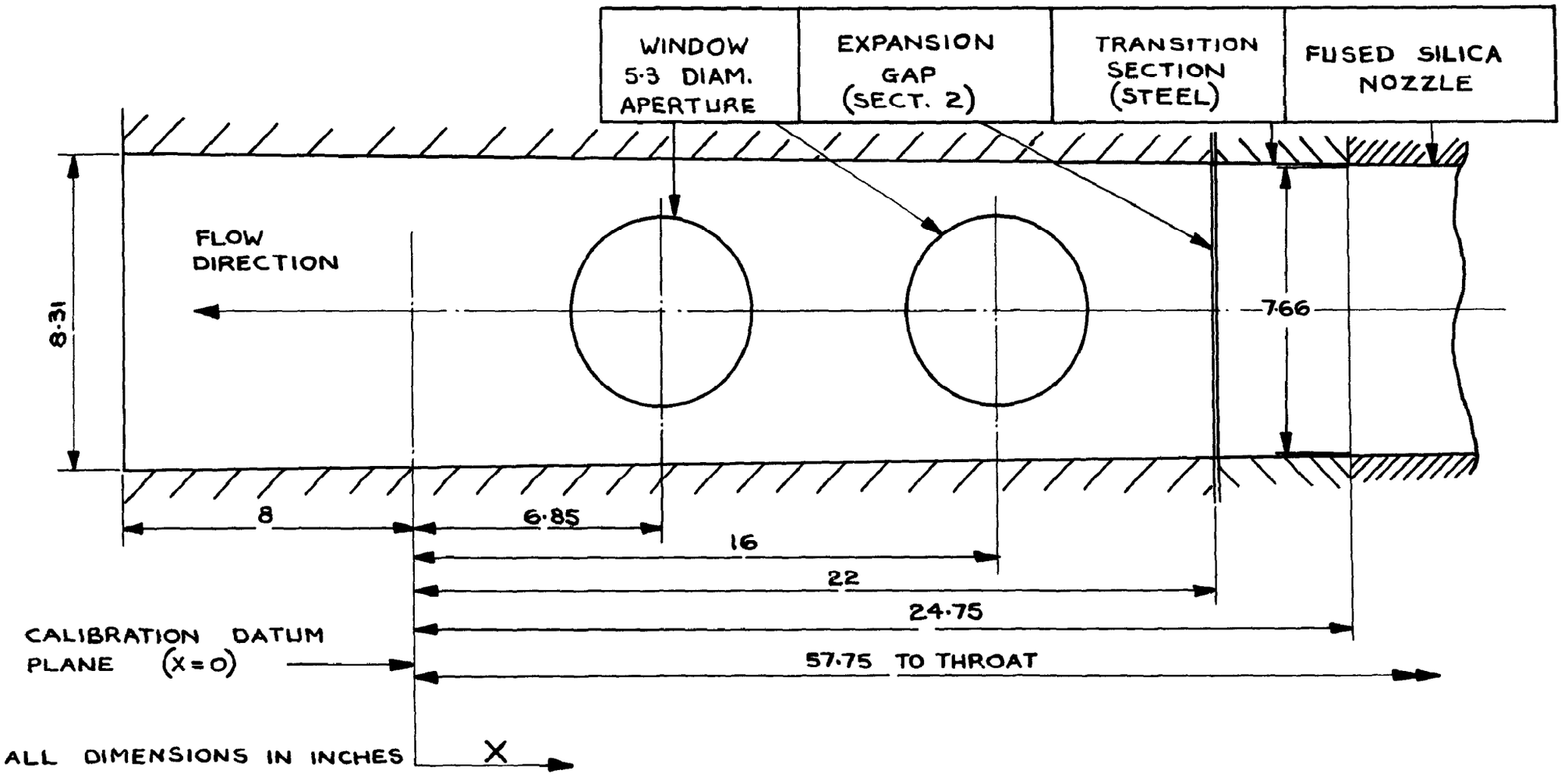

FIG. 1. RELEVANT DETAILS OF WORKING SECTION

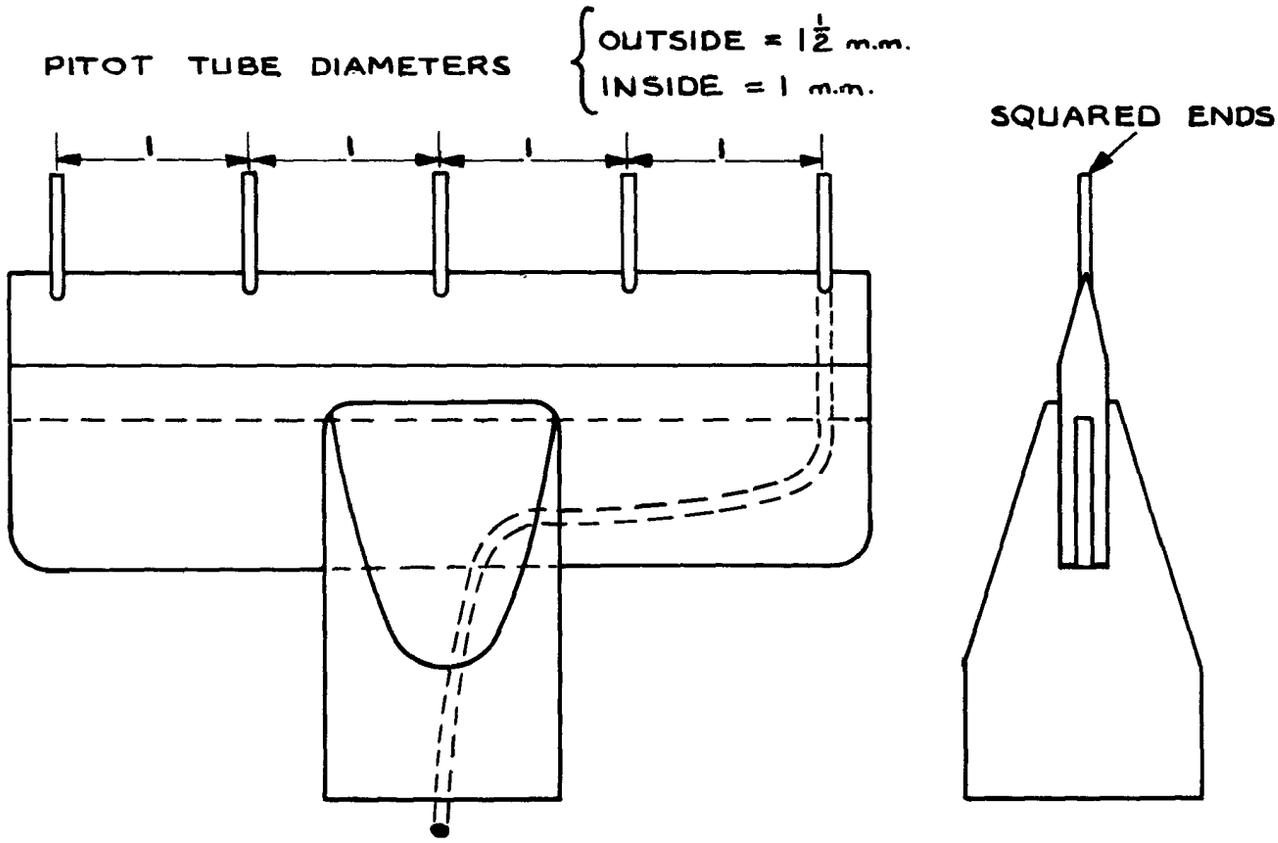

(a) SYMMETRICAL RAKE

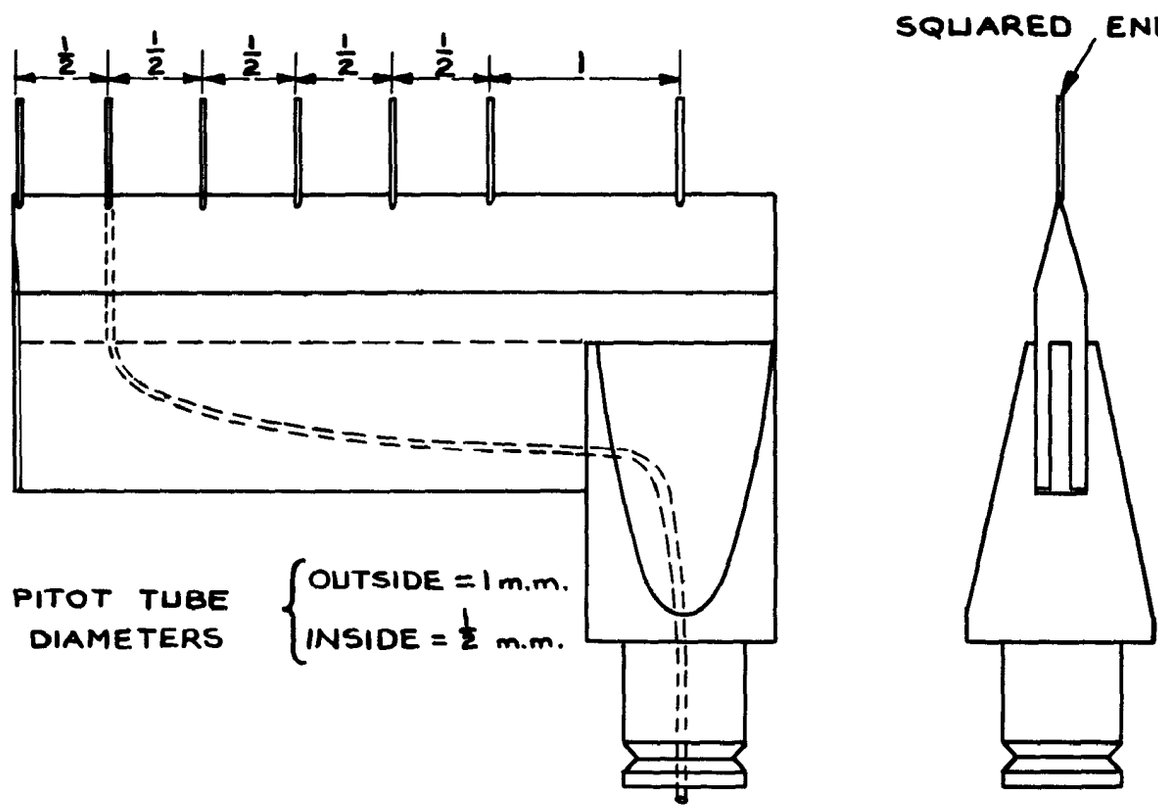

(b) OFFSET RAKE

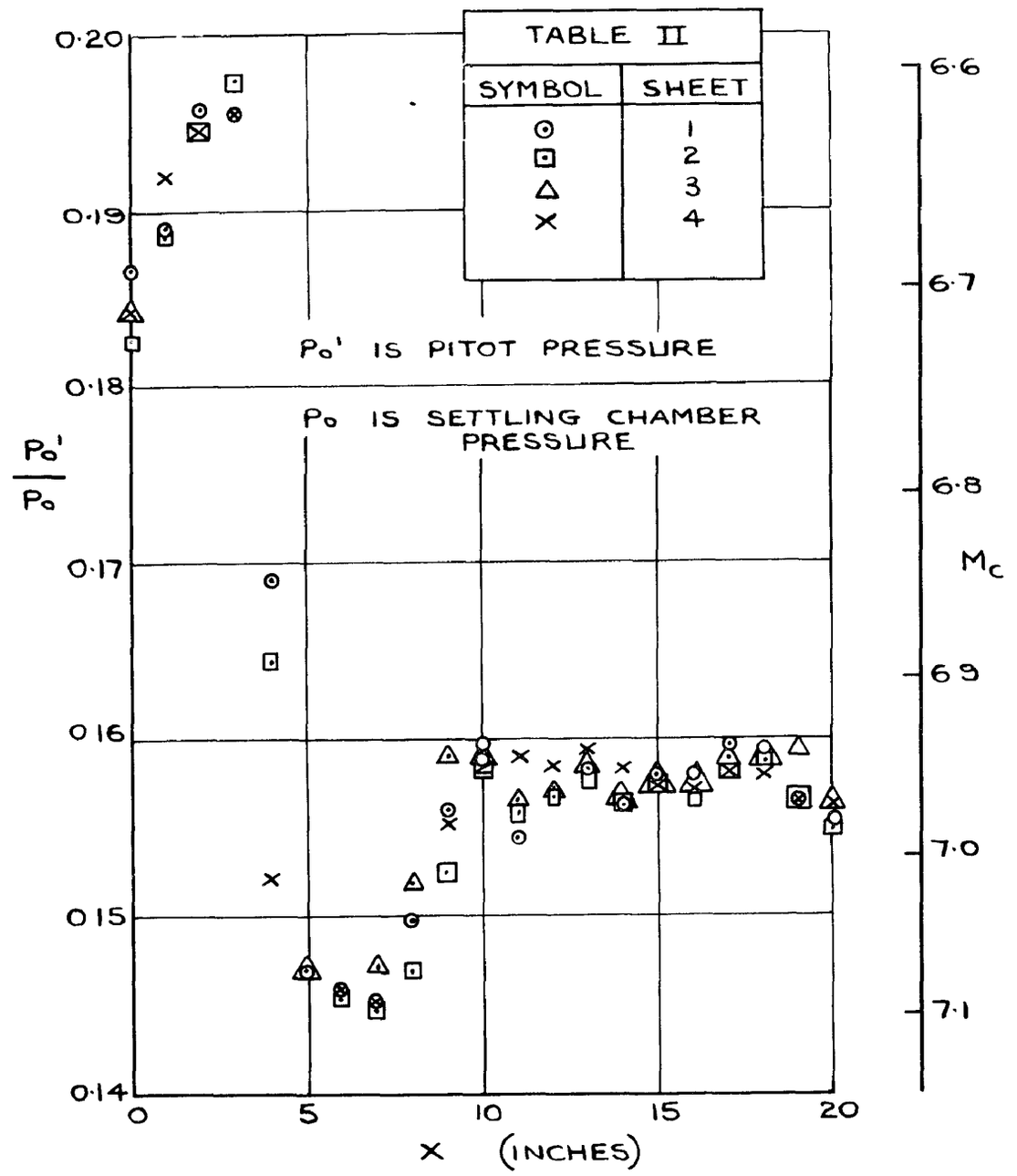

(a) RESULTS OF FOUR TRAVERSES

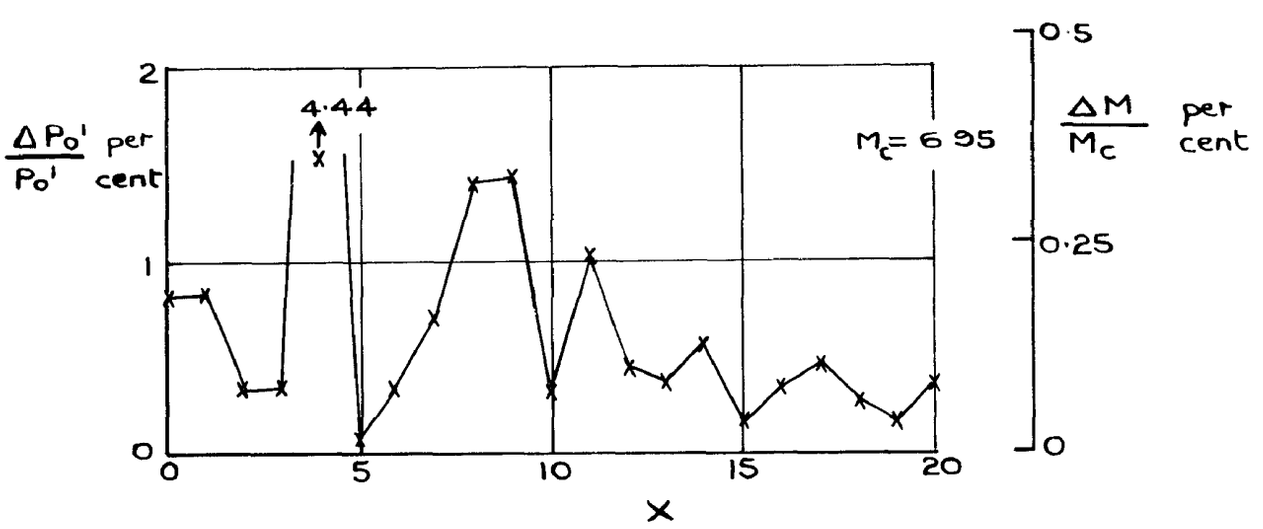

(b) STANDARD DEVIATION

FIG. 3. REPEATABILITY OF CENTRELINE PITOT PRESSURE MEASUREMENTS (1ST. FUSED SILICA NOZZLE)

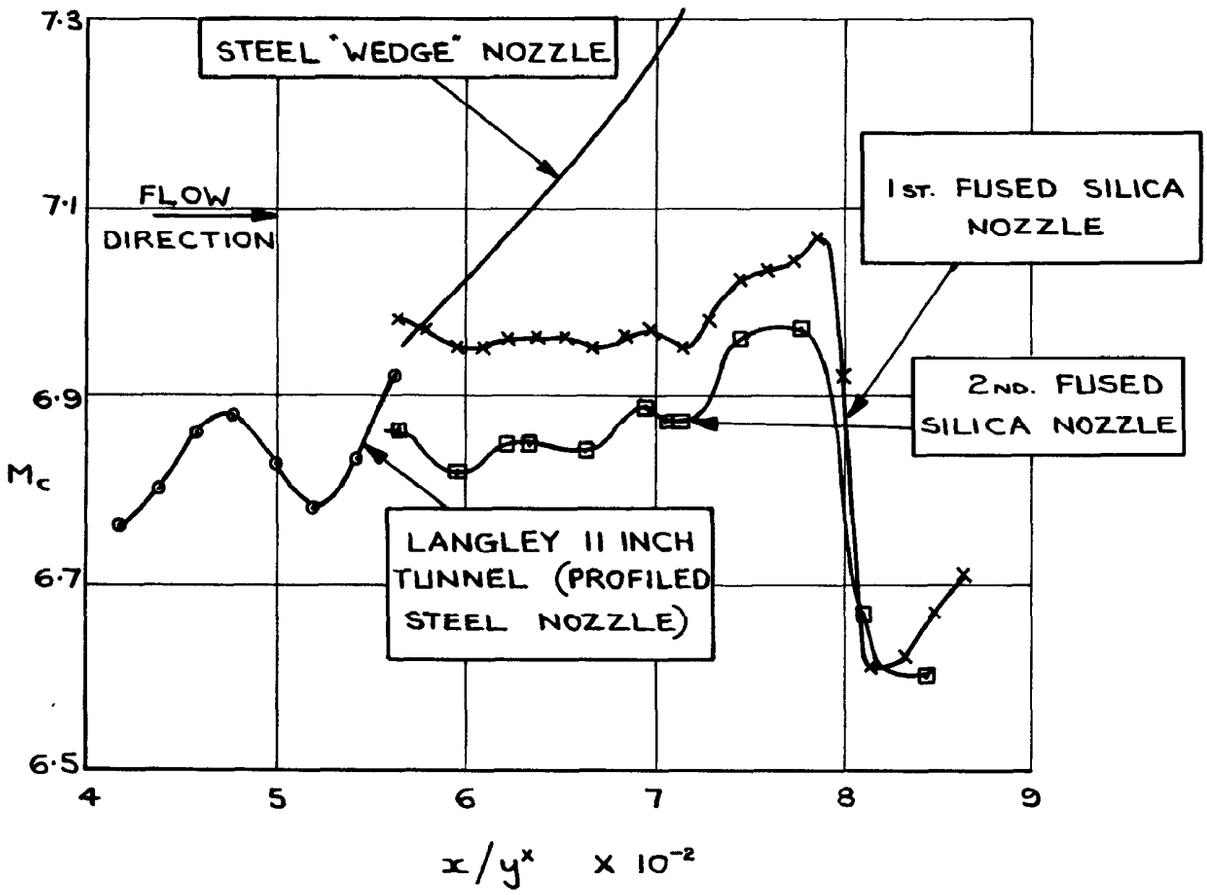

FIG. 4. COMPARISON OF CENTRELINE MACH No. FOR VARIOUS TWO-DIMENSIONAL NOZZLES.

(y^x=THROAT HEIGHT, x=DISTANCE FROM THROAT)

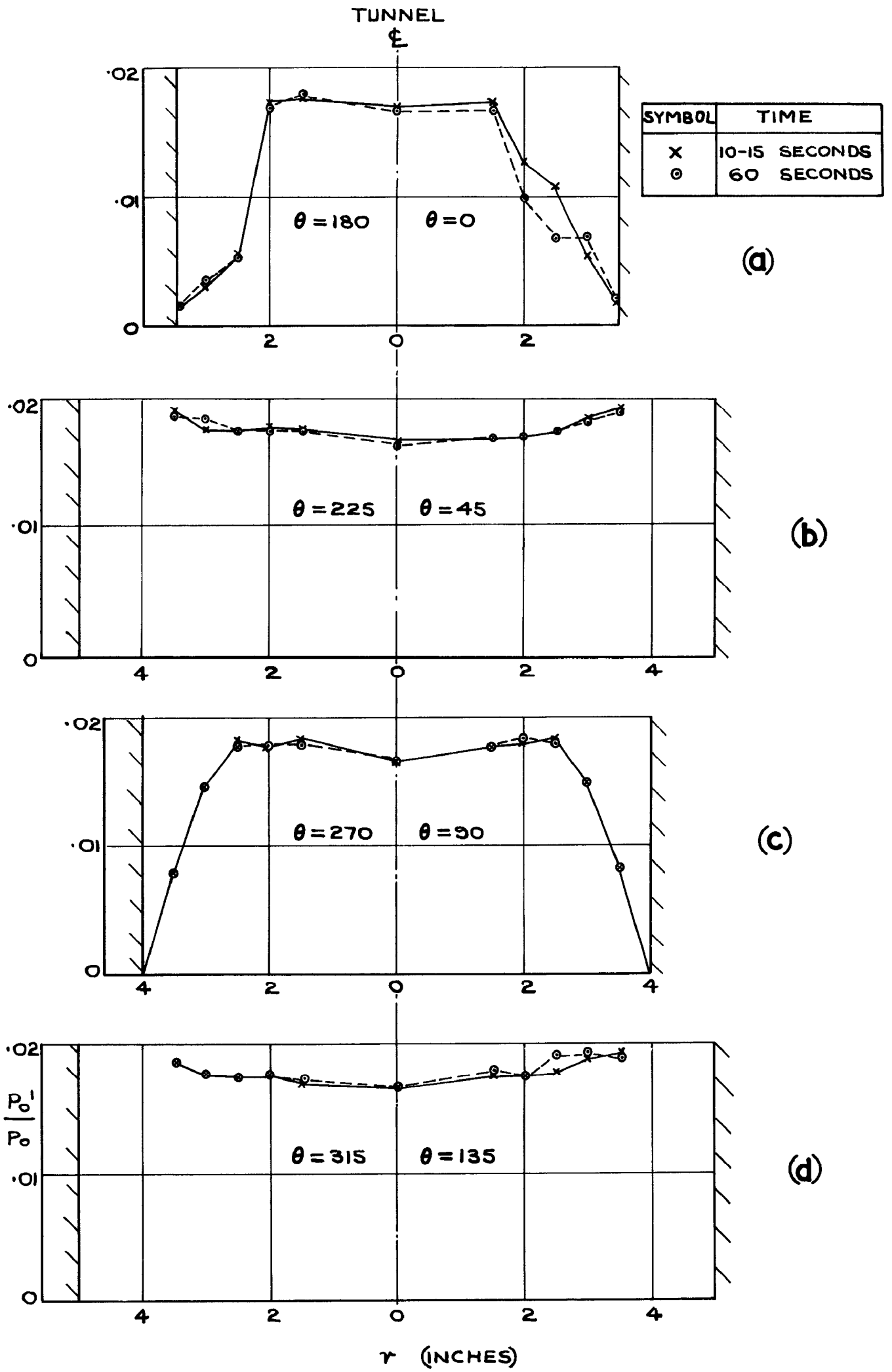

FIG. 5. PROFILES OF PITOT PRESSURE ACROSS A SECTION (X=10, 2nd. FUSED SILICA NOZZLE)

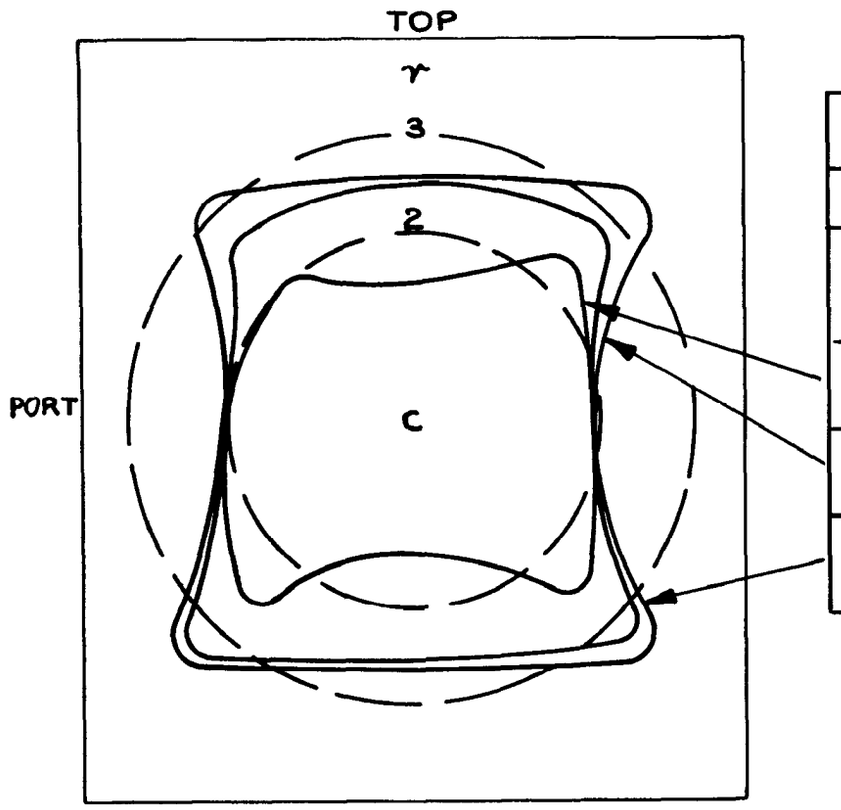

$M_c = 6.87$	
BOUNDARIES	
$\frac{\Delta M}{M_c}$ per cent	M
1	6·80 TO 6·87
2	6·73 TO 6·87
3	6·66 TO 6·87

(a) AT 10 TO 15 SECONDS

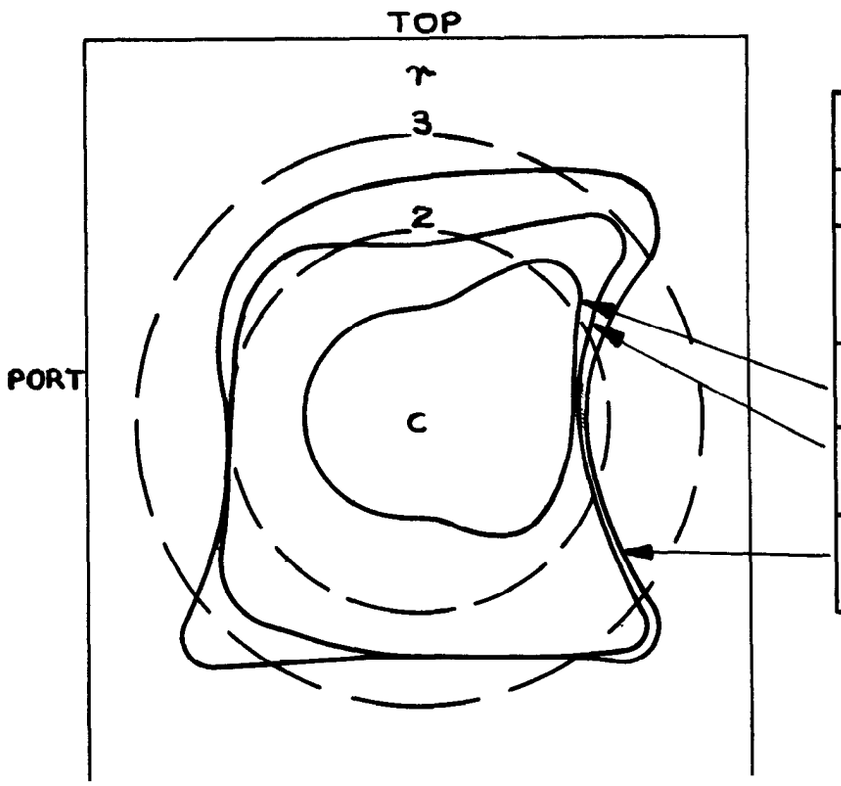

$M_c = 6.89$	
BOUNDARIES	
$\frac{\Delta M}{M_c}$ per cent	M
1	6·82 TO 6·89
2	6·75 TO 6·89
3	6·68 TO 6·89

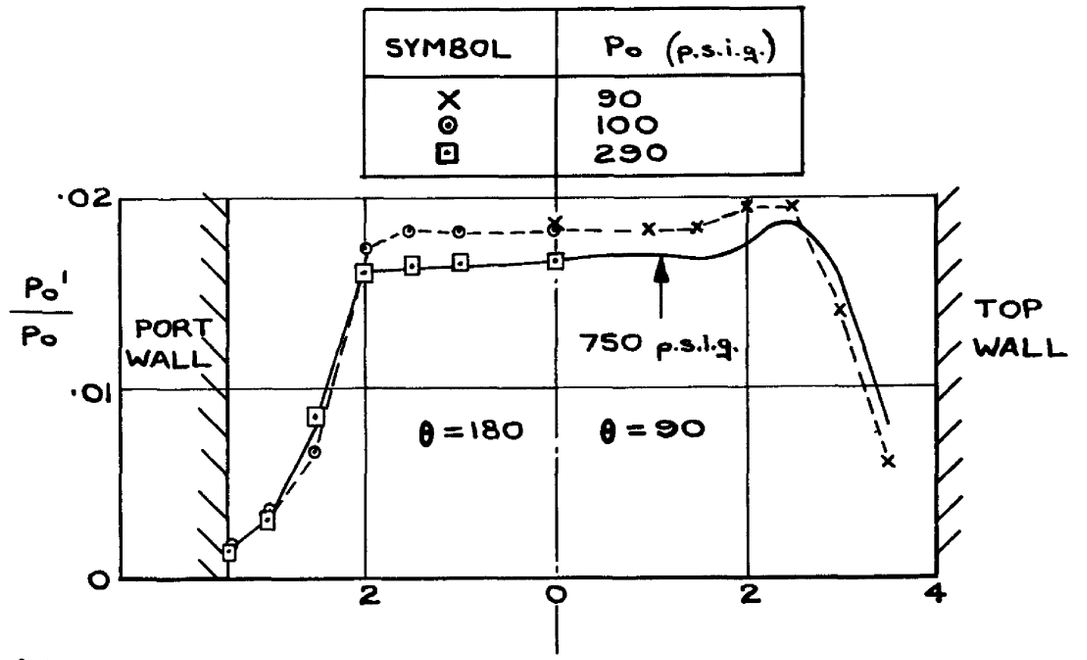

(a) PITOT PRESSURE PROFILES AT LOW STAGNATION PRESSURES (X=16)

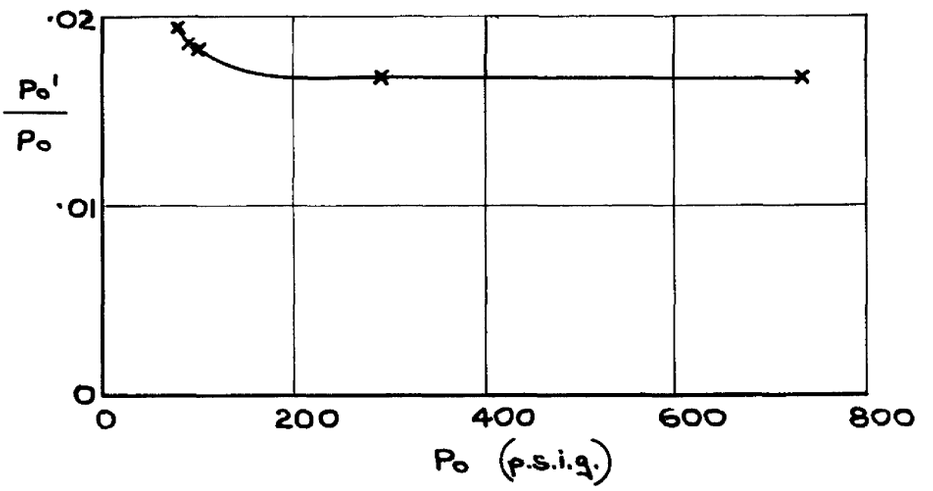

(b) VARIATION OF PITOT PRESSURE WITH STAGNATION PRESSURE (X=16)

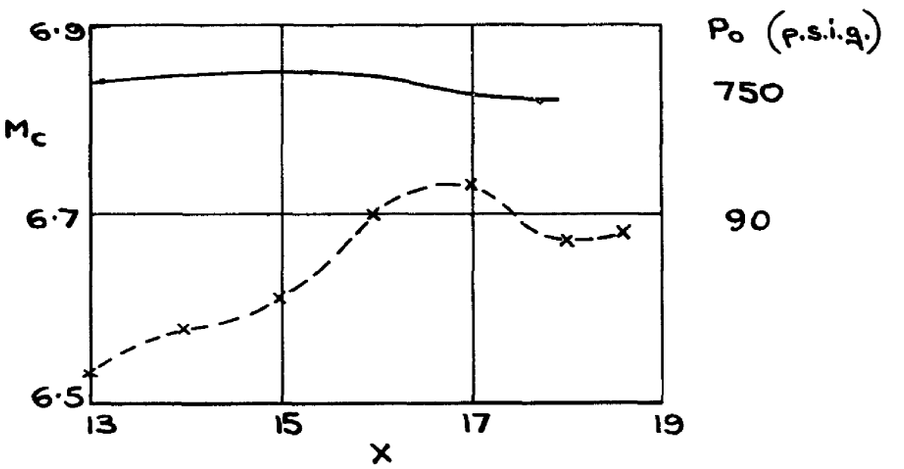

(c) CENTRELINE MACH NUMBER DISTRIBUTION AT LOW STAGNATION PRESSURE.

FIG. 8. CALIBRATION OF FLOW AT LOW STAGNATION PRESSURE.

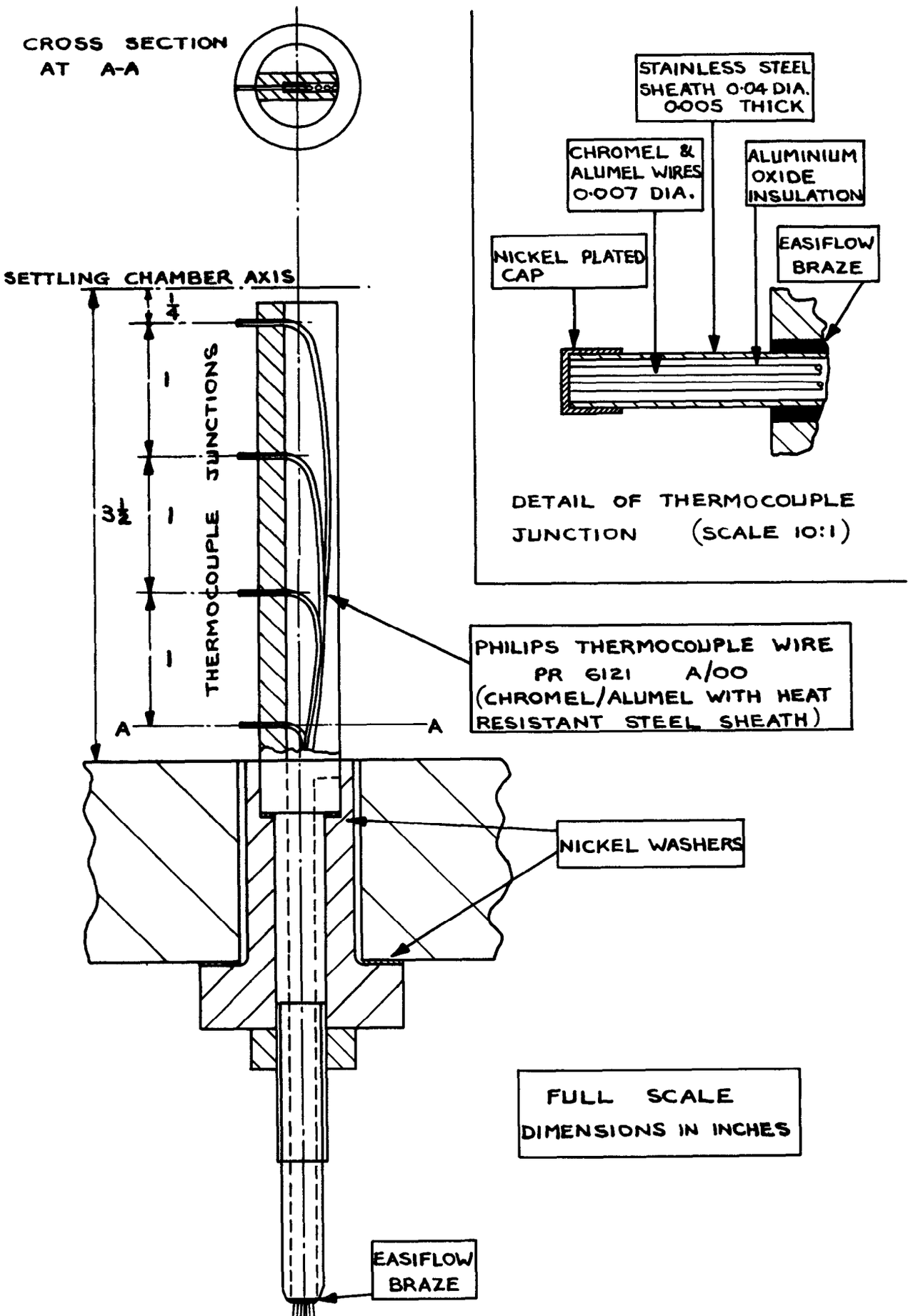

FIG.9(a) SETTLING CHAMBER TOTAL TEMPERATURE PROBE

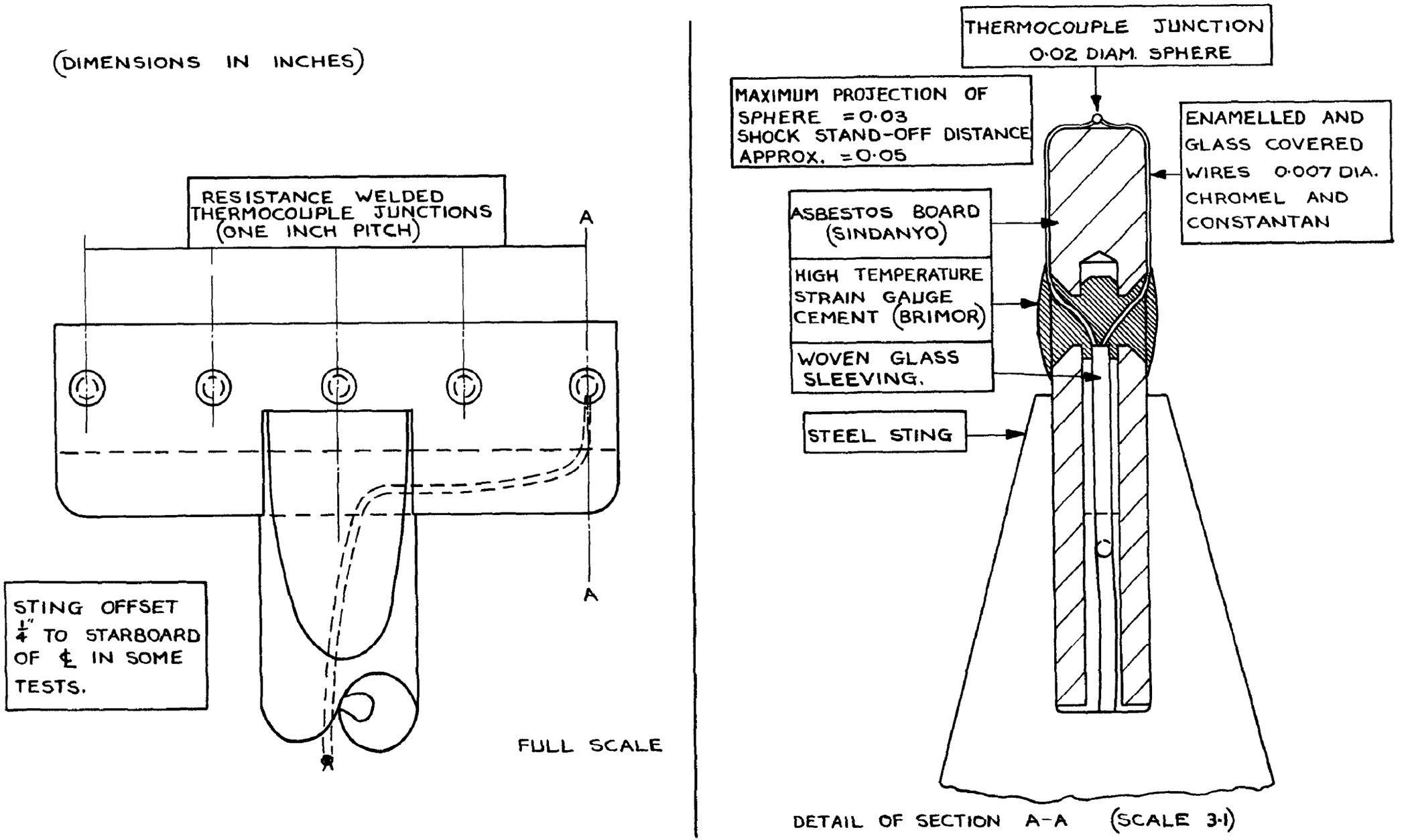

FIG.9(b) WORKING SECTION TOTAL TEMPERATURE PROBE

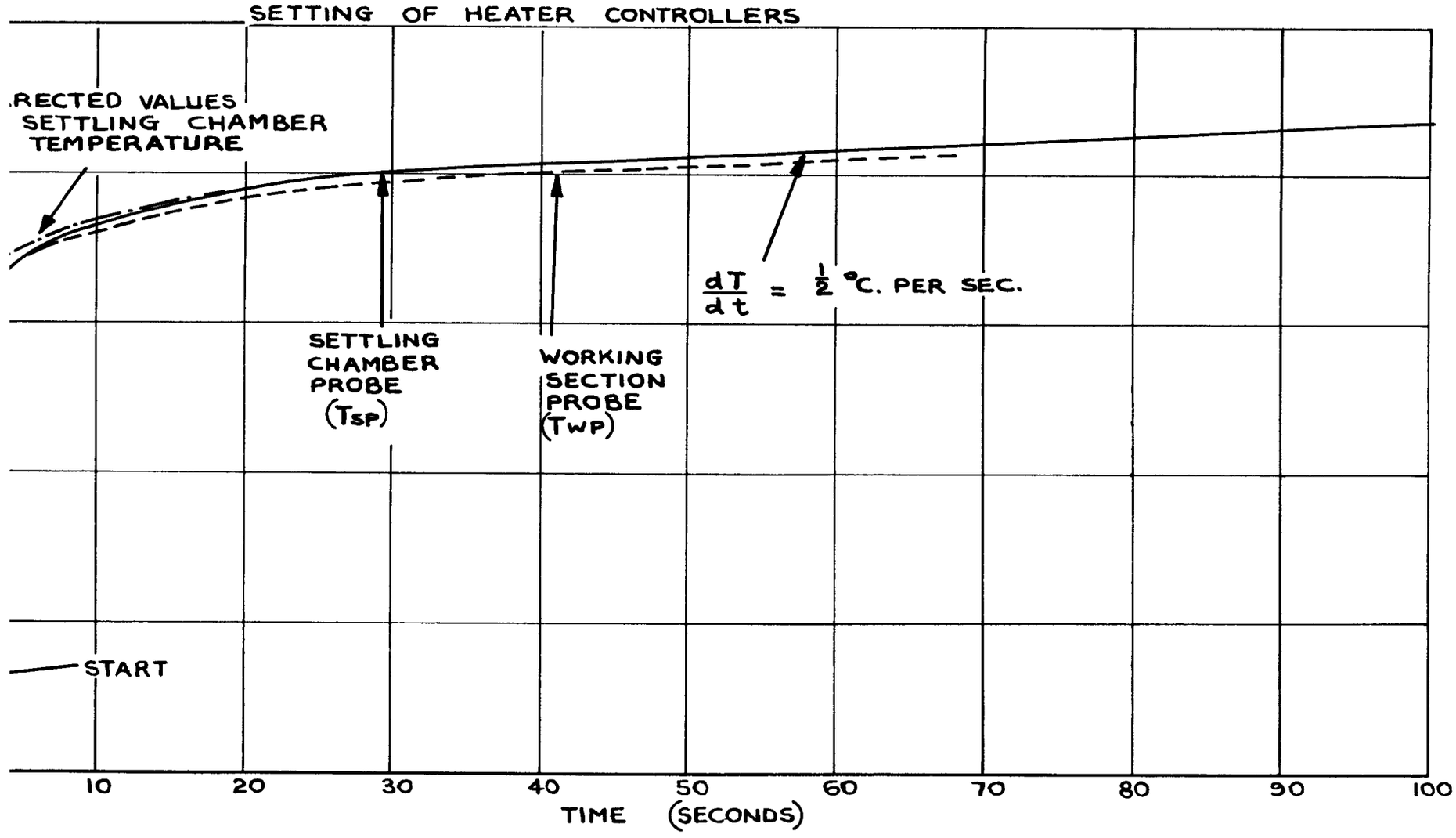

). HISTORY OF AIR TEMPERATURES IN THE SETTLING CHAMBER AND WORKING SECTION

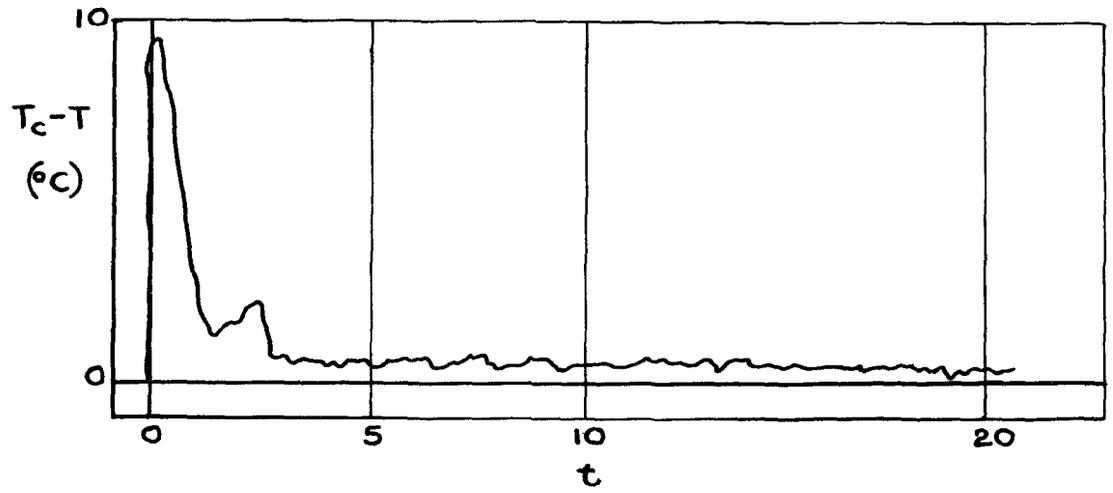

(a) TEMPERATURE DIFFERENCE BETWEEN ADJACENT THERMOCOUPLES ON WORKING SECTION PROBE ($r = 0, \frac{1}{2}$)

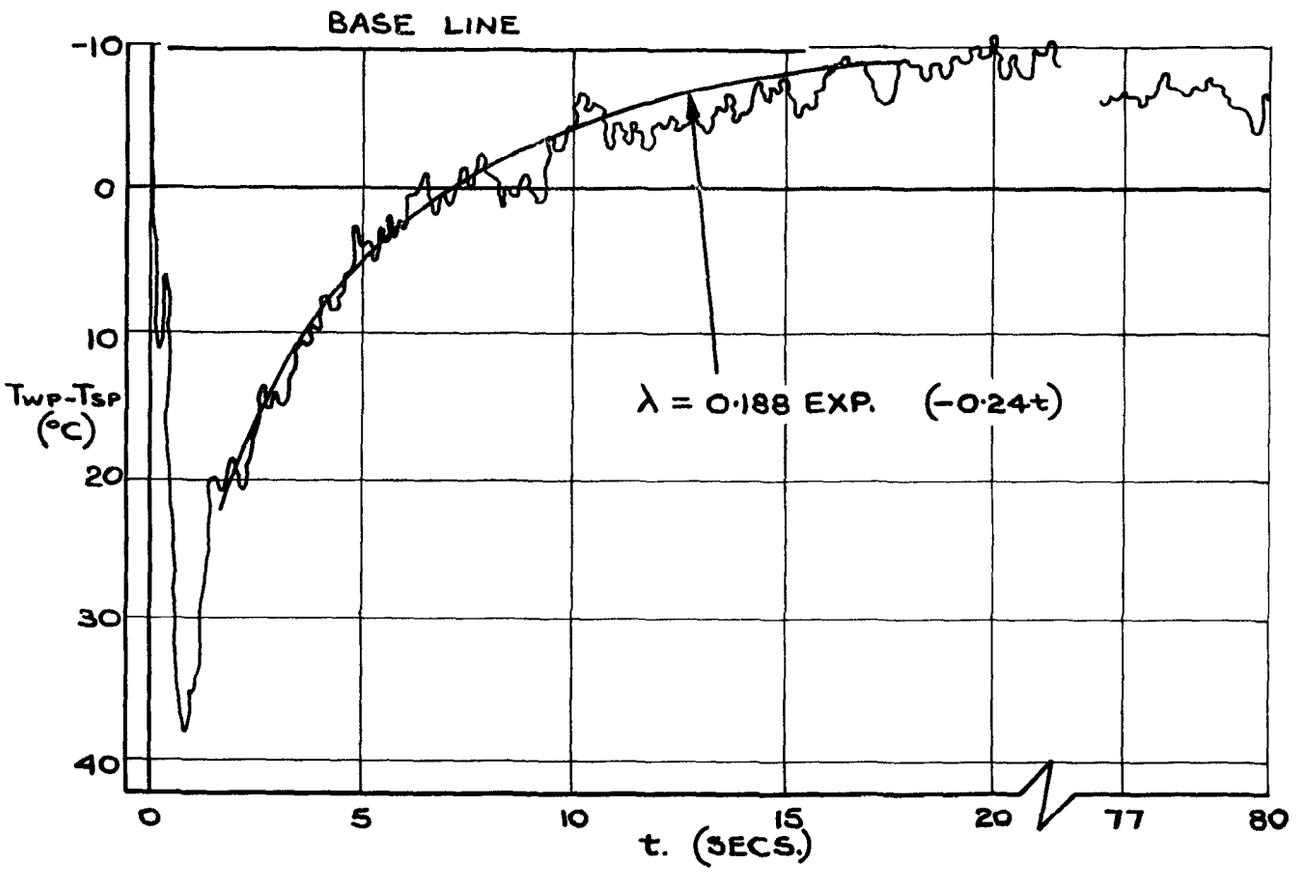

(b) TEMPERATURE DIFFERENCE BETWEEN SETTLING CHAMBER AND WORKING SECTION PROBES.

FIG. 11. OPPOSED THERMOCOUPLE TRACES

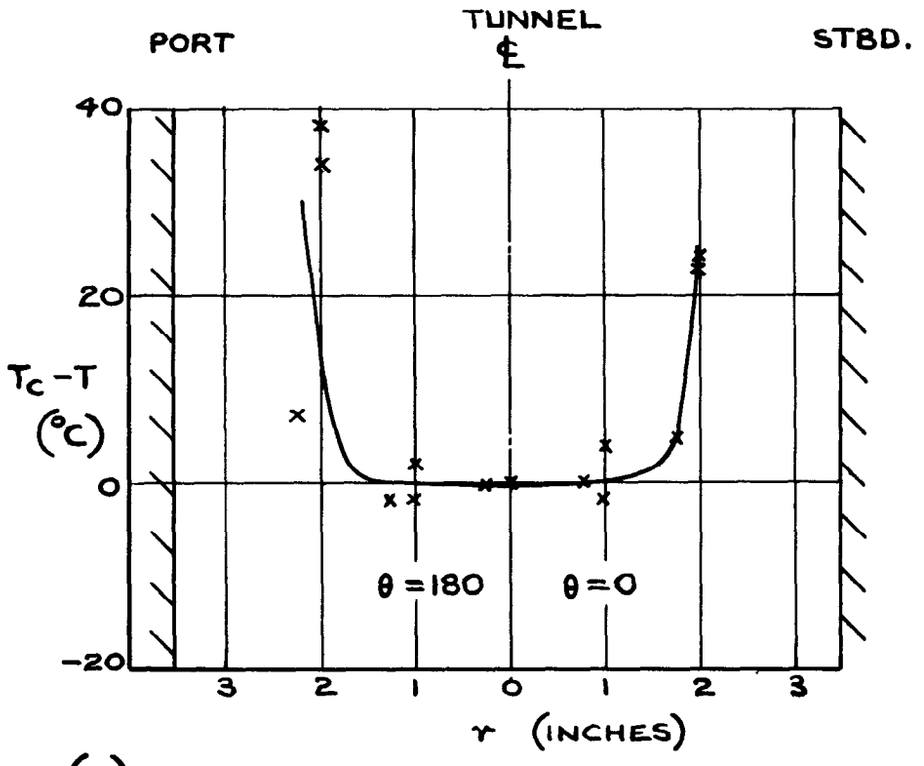

(a) HORIZONTAL

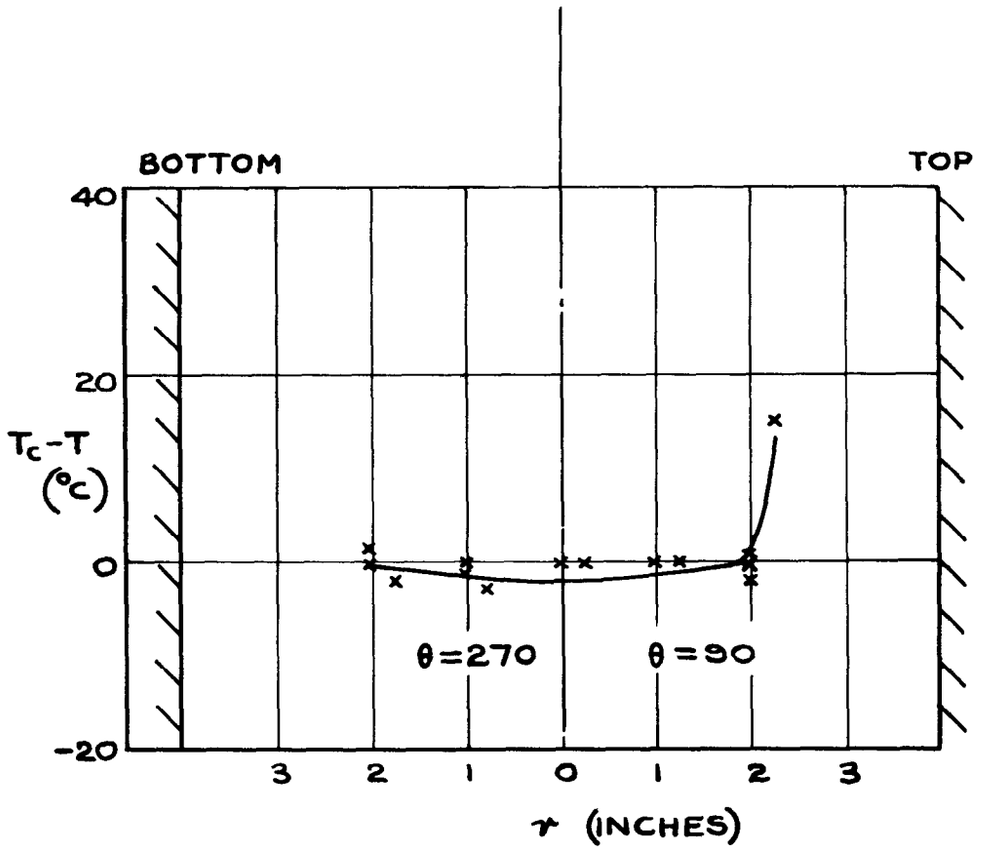

(b) VERTICAL

FIG. 12. PROFILES OF TOTAL TEMPERATURE IN THE WORKING SECTION (T_c = 420 deg. C) (at T = 40 seconds)

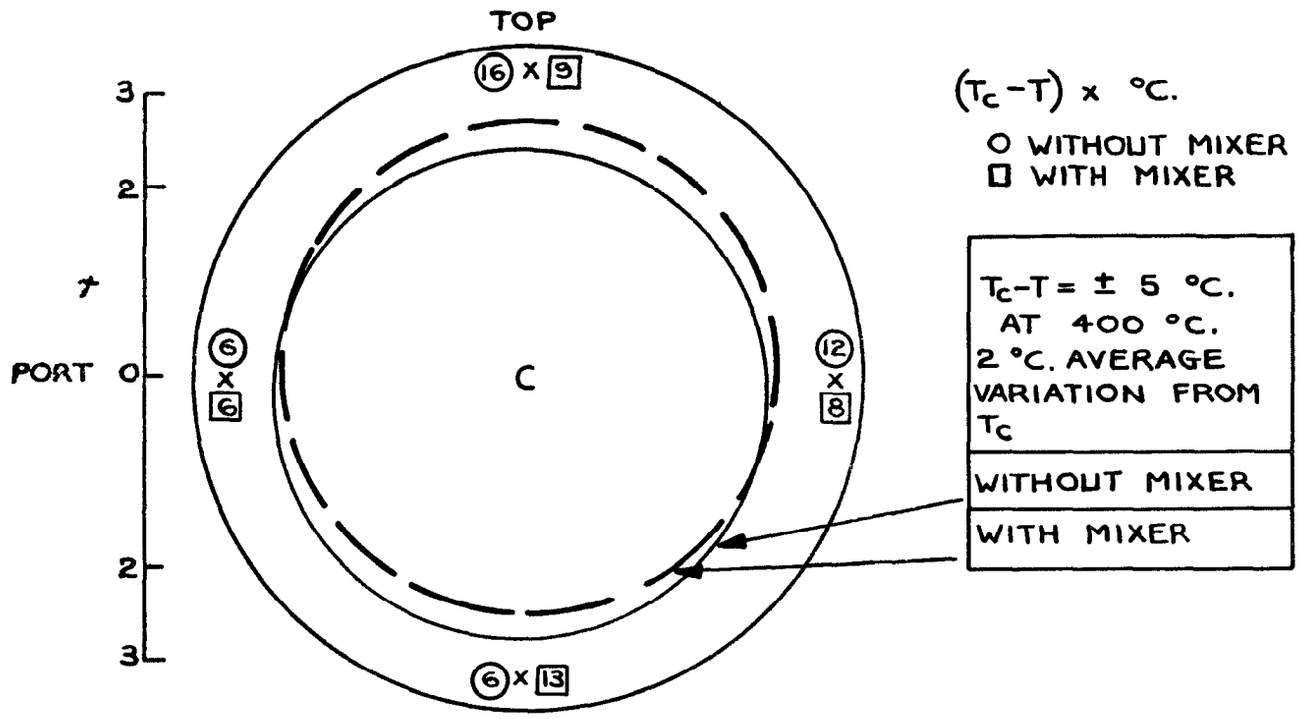

(a) SETTLING CHAMBER

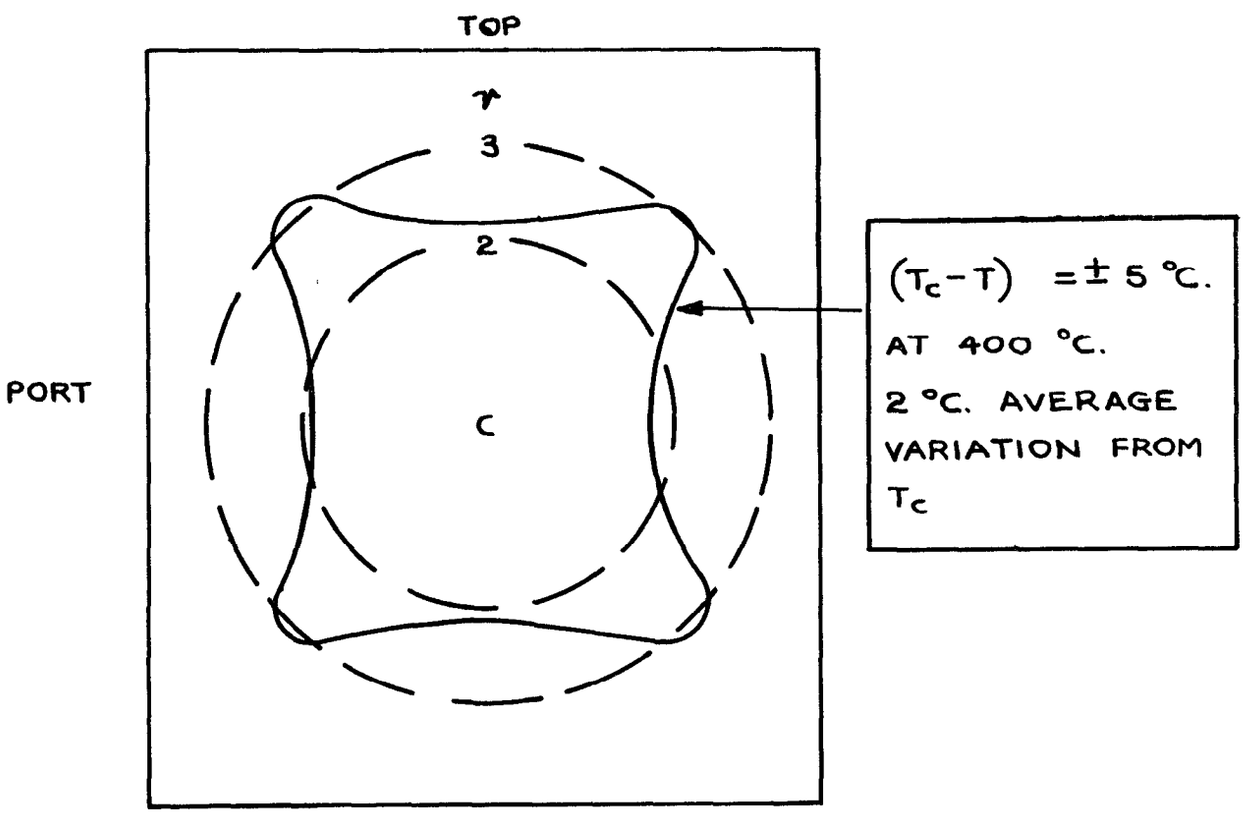

(b) WORKING SECTION (X=10)

FIG. 13. CROSS SECTIONS OF TOTAL TEMPERATURE FIELDS IN THE SETTLING CHAMBER AND WORKING-SECTION ($T_c \approx 400$ °C) (t = 40 seconds)

A.R.C. C.P. No.590

533.6.071:
533.6.011.35

THE 7 IN. x 7 IN. HYPERSONIC WIND TUNNEL AT R.A.E. FARNBOROUGH. PARTS I, II AND III.

Crane, J.F.W., and Crabtree, L.F. August, 1961.

Part I gives some details of the design and lay-out of the plant, together with the calculated performance figures, and the major components of the facility are briefly described. The instrumentation provided for the wind tunnel is described in some detail, including the optical and other methods of flow visualization used.

Part II describes tests on the storage heater, which is cylindrical in form and mounted horizontally, and shows that its performance is adequate for operation at M = 6.8 and probably adequate for flows at M = 8.2 with the existing nozzles.

Part III shows that the fused silica nozzle designed to give M = 7 in the wind tunnel produces a flow field with an average Mach number

(Over)

A.R.C. C.P. No.590

THE 7 IN. x 7 IN. HYPERSONIC W
FARNBOROUGH. PARTS I, II AND
Crane, J.F.W., and Crabtree, L.

Part I gives some detail:
together with the calculated p
of the facility are briefly de
the wind tunnel is described i
other methods of flow visualiz

Part II describes tests
in form and mounted horizontal
adequate for operation at M =
M = 8.2 with the existing nozz

Part III shows that the
M = 7 in the wind tunnel produ

A.R.C. C.P. No.590

THE 7 IN. x 7 IN. HYPERSONIC W
FARNBOROUGH. PARTS I, II AND
Crane, J.F.W., and Crabtree, L.

Part I gives some detail
together with the calculated p
of the facility are briefly de
the wind tunnel is described i
other methods of flow visualiz

Part II describes tests
in form and mounted horizontal
adequate for operation at M = 6
M = 8.2 with the existing nozz

Part III shows that the
M = 7 in the wind tunnel produ

of 6.85 along the centreline of the working section. The Mach number gradually decreases towards the boundary layer, but over a core of approximately four inches there is a decrease of only two per cent below the centreline Mach number.

of 6.85 along the centreline of the working section. The Mach number gradually decreases towards the boundary layer, but over a core of approximately four inches there is a decrease of only two per cent below the centreline Mach number.

of 6.85 along the centreline of the working section. The Mach number gradually decreases towards the boundary layer, but over a core of approximately four inches there is a decrease of only two per cent below the centreline Mach number.

Published by
HER MAJESTY'S STATIONERY OFFICE

To be purchased from
York House, Kingsway, London W.C.2
423 Oxford Street, London W.1
13A Castle Street, Edinburgh 2
109 St. Mary Street, Cardiff
39 King Street, Manchester 2
50 Fairfax Street, Bristol 1
35 Smallbrook, Ringway, Birmingham 5
80 Chichester Street, Belfast 1
or through any bookseller

Printed in England

S.O. CODE No. 23-9012-90